Role of HPIP signaling in cellular adaptation and cell fate regulation in response to metabolic stress: Implications in breast cancer development

A thesis submitted for the degree of
Doctor of Philosophy in Biochemistry

By
Vasudevarao Penugurti
(14LBPH09)

Under the supervision of
Prof. Bramanandam Manavathi Ph.D.,
Department of Biochemistry,
School of Life Sciences,
University of Hyderabad
PO: Central University Campus,
Gachibowli, Hyderabad-500046
Telangana, India

October 2021

Prof. Bramanandam Manavathi Ph.D.,
Department of Biochemistry,
School of Life Sciences,
University of Hyderabad,
Hyderabad - 500046,
Telangana, India

प्रतिष्ठित संस्थान
INSTITUTION OF EMINENCE

CERTIFICATE

This is to certify that the thesis entitled **"Role of HPIP signaling in cellular adaptation and cell fate regulation in response to metabolic stress: Implications in breast cancer development"** submitted to the University of Hyderabad by **Mr. Vasudevarao Penugurti**, bearing the Reg. No **14LBPH09** for the degree of Doctor of Philosophy in Biochemistry is based on the studies carried out by him under my supervision. To the best of my knowledge, this has never been submitted for an award or certificate from any other university or institution, including this institute.

Prof. Bramanandam Manavathi Ph.D.,

Supervisor

Prof. Bramanandam Manavathi, PhD
Department of Biochemistry
School of Life Sciences
University of Hyderabad
Hyderabad-500 046. (TS). INDIA

Head

Department of Biochemistry

HEAD
Dept. of Biochemistry
SCHOOL OF LIFE SCIENCES
UNIVERSITY OF HYDERABAD
HYDERABAD-500 046.

Dean

School of Life Sciences

DEAN
School of Life Sciences
University of Hyderabad
Hyderabad-500 046.

Department of Biochemistry,
School of Life Sciences,
University of Hyderabad,
Hyderabad - 500046,
Telangana, India

प्रतिष्ठित संस्थान
INSTITUTION OF EMINENCE

DECLARATION

I, **Vasudevarao Penugurti**, hereby declare that the work presented in this thesis entitled **"Role of HPIP signaling in cellular adaptation and cell fate regulation in response to metabolic stress: Implications in breast cancer development"** is entirely original and that it was completed at the Department of Biochemistry, School of Life Sciences, University of Hyderabad, Hyderabad, India under the supervision of Professor Bramanandam Manavathi. I also declare that this work has not previously been submitted for the award of a degree or diploma from any other university or institution.

P. Vasudev Rao

Signature of the student

Name: **Vasudevarao Penugurti**

Reg. No: 14LBPH09

Date: 2/11/2021

Place: **University of Hyderabad (UoH), Hyderabad**

Prof. Bramanandam Manavathi Ph.D.,
Department of Biochemistry,
School of Life Sciences,
University of Hyderabad,
Hyderabad - 500046,
Telangana, India

प्रतिष्ठित संस्थान
INSTITUTION OF EMINENCE

CERTIFICATE

This is to certify that the thesis titled **"Role of HPIP signaling in cellular adaptation and cell fate regulation in response to metabolic stress: Implications in breast cancer development"** submitted by **Mr. Vasudevarao Penugurti** bearing Reg. No. **14LBPH09**, in partial fulfillment of the requirements for the Doctor of Philosophy in Biochemistry, is genuine work done by him under my supervision.

This thesis is free of plagiarism and has not previously been submitted in part or whole to this or any other university or institution to award a degree or diploma. Furthermore, prior to submitting the thesis/monograph for adjudication, the student had the following publication(s) and provided proof for them in the form of reprints in the relevant field of his study.

1. **Penugurti V**, Khumukcham SS, Padala C, Dwivedi A, Kamireddy KR, Mukta S, Bhopal T, **Manavathi B**. HPIP protooncogene differentially regulates metabolic adaptation and cell fate in breast cancer cells under glucose stress via AMPK and RNF2 dependent pathways. ***Cancer Lett.*** 2021 Oct 10;518:243-255.

   Aside from his thesis publications, the student was also involved in other publications from the lab.

2. Dwivedi A, Padala C, Kumari A, Khumukcham SS, **Penugurti V**, Ghosh S, Mazumder A, Goffin V, and **Manavathi B**, Hematopoietic PBX-interacting protein is a novel regulator of mammary epithelial cell differentiation, ***FEBS Journal,*** 2021.

3. Khumukcham SS, Samanthapudi VSK, **Penugurti V**, Kumari A, Kesavan PS, Velatooru LR, Kotla SR, Mazumder A, **Manavathi B**. Hematopoietic PBX-interacting protein is a substrate and an inhibitor of the APC/C-Cdc20 complex and regulates mitosis by stabilizing cyclin B1. ***J Biol Chem***. 2019 Jun 28;294(26):10236-10252. (Equal contributions)

4. Bugide S, Gonugunta VK, **Penugurti V**, Malisetty VL, Vadlamudi RK, **Manavathi B**. HPIP promotes epithelial-mesenchymal transition and cisplatin resistance in ovarian cancer cells

through PI3K/AKT pathway activation. ***Cell Oncol (Dordr).*** 2017 Apr;40(2):133-144. (Equal contributions)

5. Malisetty VL, **Penugurti V**, Panta P, Chitta SK, **Manavathi B**. MTA1 expression in human cancers - Clinical and pharmacological significance. ***Biomed Pharmacother.*** 2017 Nov;95:956-964.

6. Samudrala R, Patel S, **Penugurthi V**, **Manavathi B**, Azeem PA, In vitro studies of B2O3–SiO2–Na2O–CaO–ZnO bioactive glass system, ***Journal of Non-Crystalline Solids***, 574 (2021).

7. Mallakuntla MK, **Penugurti V**, **Manavathi B**, Podile AR, Chitooligosaccharides induce apoptosis in human breast cancer cells, ***Carbohydrate Polymer Technologies and Applications*** **2** (2021) 100077.

8. Srinath P, Azeem PA, Venugopal Reddy K**, Penugurti V**, **Manavathi B**. Zirconia-containing wollastonite ceramics derived from biowaste resources for bone tissue engineering. ***Biomed Mater***. 2020 Aug 7;15(5):055025.

9. Palakurthy S, Azeem PA, Venugopal Reddy K, **Penugurti V**, **Manavathi B**. A comparative study on in vitro behavior of calcium silicate ceramics synthesized from biowaste resources. ***J Am Ceram Soc***. 2020; 103: 933– 943.

10. Samudrala R, Azeem PA, **Penugurti V**, **Manavathi B**, In vitro evaluation of niobia added soda lime borosilicate bioactive glasses; ***J. Alloys Compd.*** 2018, 764, 1072-1078.

11. Kumar K, **Penugurti V**, Levi G, Mastai Y, **Manavathi B**, Paik P. Bio-inspired synthesis of a hierarchical self-assembled zinc phosphate nanostructure in the presence of cowpea mosaic virus: in vitro cell cycle, proliferation and prospects for tissue regeneration. ***Biomed Mater***. 2017 Dec 7;13(1):015013.

12. Samudrala R, Abdul Azeem P, **Penugurti V**, **Manavathi B**. Cytocompatibility studies of titania-doped calcium borosilicate bioactive glasses in-vitro. ***Mater Sci Eng C*** Mater Biol Appl. 2017 Aug 1;77:772-779.

The student has attended the following conferences during his Ph.D. program

1. Oral presentation entitled "**HPIP signaling reprograms breast cancer cell metabolism for survival under energy stress**" by **Vasudevarao Penugurti** at conference "Phenotypic heterogeneity as a driver of cancer progression" held on 5-6th January 2019 at Indian Institute of Science, Bengaluru.

2. Presented a poster entitled "**HPIP signaling reprograms breast cancer cell metabolism for survival under energy stress**" by **Vasudevarao Penugurti** and Bramanandam Manavathi at XLII all India cell biology conference, held on 21-23rd December 2018 at BITS Pilani, K K Birla, Goa campus, Goa.

3. Presented a poster entitled "**HPIP signaling critically regulates endosome-dependent focal adhesion disassembly and cell migration through Rab5 activation**" by **Vasudevarao Penugurti**, Saratchandra Khumukhcham, Suresh Bugide, Anita Kumari, P.S. Kesavan, Anju Dwivedi, Vijaya Lakshmi Malisetty, Aprotim Mazumder, and Bramanandam Manavathi at

International Congress of cell biology and APOCB, held on 27-31st January 2018 at CCMB, Hyderabad.

4. Course trained entitled "**Data analytics using R-programming**" held during 17-20th August 2017 at MSME-DI, Bengaluru.

5. Presented a poster entitled "**Loss of HPIP expression correlates with trophoblast differentiation and preeclampsia development**" by Vasudevarao Penugurti, Anju Dwivedi, Anita Kumari, Saratchandra Singh Khumukcham, Oindrilla Dey, Deepak Kumar Kashyap, Vijaya Lakshmi Malisetty, and Bramanandam Manavathi, International Conference on Reproductive Biology and Comparative Endocrinology, held on 09-11th February 2017 at University of Hyderabad, Hyderabad.

6. Participated in an international conference on "**Radiation research: Impact on human, and the environment"** held on 1-4th February 2018 at the University of Hyderabad, Hyderabad.

7. Participated in a workshop entitled "**Animal Models in Cancer**" from October 24-25th, 2017, at the University of Hyderabad.

8. Participated in XL all India cell biology conference held on 17-19th November 2016 at Jiwaji University, Gwalior (MP), India.

9. Participated in a course work entitled "**Immunologicals in animal and human health**" from July 04-16th, 2016, at the University of Hyderabad, Hyderabad.

10. Participated in a workshop entitled "**Cancer drug discovery and development**" from June 22-28th, 2016, at the University of Hyderabad, Hyderabad.

Furthermore, the student has completed the following courses to fulfill the coursework requirement for the Ph.D.

Course Code	Name	Credits	Pass/Fail
BC 801	Analytical Techniques	4	Pass
BC 802	Research ethics, Data Analysis, and Biostatistics	3	Pass
BC 803	Lab Seminar and Record	5	Pass

Supervisor

Prof. Bramanandam Manavathi, PhD
Department of Biochemistry
School of Life Sciences
University of Hyderabad
Hyderabad-500 046. (TS), INDIA

Head

Department of Biochemistry

Dept. of Biochemistry
SCHOOL OF LIFE SCIENCES
UNIVERSITY OF HYDERABAD
HYDERABAD-500 046.

Dean

School of Life Sciences

DEAN
School of Life Sciences
University of Hyderabad
Hyderabad-500 046.

Dedicated to

My mother, Smt. Kondamma Penugurti,

My brother Sri Janardhana Rao Penugurti,

and my wife, Smt. Keerthi Penugurti.

Acknowledgments

❖ First and foremost, I would like to express my heartfelt appreciation to my supervisor, **Prof. Bramanandam Manavathi**, for his continuous encouragement throughout my study with his inspiration, excitement, extensive knowledge, helpful assistance, counsel, and ideas that enabled me to complete this thesis possible. He has been helpful on both a professional and personal level, and I am thankful for that. In the preparation of my thesis, his attention, emotional support, and timely recommendations were valuable. For everything, I am grateful to my boss.

❖ I am always thankful to my doctoral committee members, **Prof. Sharmistha Banerjee** and **Dr. Suresh Yenugu,** for their critical comments and invaluable suggestions on my Ph.D. work.

❖ I would like to thank the current and previous Heads of the Department of Biochemistry, **Prof. Krishnaveni Mishra, Prof. Mrinal Kanti Bhattacharyya,** and **Prof. N. Siva Kumar**, for enabling me to utilize all the department core facilities.

❖ I would like to thank **Prof. Dayananda Siddavattam**, **Prof. KVA Ramaiah**, **Prof. MNV Prasad, Prof. Pallu Reddanna**, and **Prof. Aparna Datta Gupta**, current and past Deans of the School of Life Sciences, for enabling me to utilize all the school core facilities.

❖ I would like to express my gratitude to **Prof. Apparao Podile, Prof. Naresh Babu V Sepuri, Dr. Suresh Yenugu, Prof KVA Ramaiah, Prof. Gutti Ravi Kumar, Dr. Anil Kumar Pasupulati,** and other faculty members for enabling me to utilize their lab facilities.

❖ I am grateful to **Prof. Srikrishna Saripella, Prof. HP Pandey, Prof. RS Dubey, Prof. SP Singh,** and **Dr. RK Singh** of Banaras Hindu University for encouraging and inspiring me to do research.

❖ I am thankful to **Dr. Siva Reddy Kotla** of MD Anderson Cancer Center, Houston, TX, USA, and **Dr. Krishna Gurugubelli** of All India institute of medical science (AIIMS), Amaravati, India, for their insightful comments on my work and helpful advice on my thesis.

❖ I would like to thank **Sri. SB Chary** for his assistance in processing all office-related work and the other non-teaching staff for their quick assistance.

❖ I would like to thank **Dr. Aprotim Mazumder, PS Kesavan, and Sinjini Gosh** for their assistance with confocal and fluorescent microscopy imaging.

❖ I would like to thank **Prof. Dr. Srinivasulu Mukta** and **Prof. Dr. Triveni Bhopal** of **MNJ Institute of Oncology & Regional Cancer Centre-Hyderabad** for providing normal and fresh tumor tissue samples and blocks for conducting clinical research on breast cancer and for their invaluable assistance in analyzing IHC data.

❖ I would like to express my gratitude to **Dr. Nagi Reddy Putluri**, **Dr. Meghashyam Kavuri** of **Baylor College of Medicine-Houston, TX, USA** for their valuable suggestions, and **Dr. Karthik Reddy Kamireddy** of Indian institute of chemical technology (IICT), Hyderabad, India, for his help with metabolomics data analysis.

❖ I am also thankful to my former and present lab members **Dr. Suresh Bugide, Dr. Vijay Narasimha Reddy Gajulapalli, Dr. Oindrilla Dey, Dr. Loka Reddy Velatooru, Dr. Chiranjeevi Padala, Khumukhcham Saratchandra Singh, Anju Dwivedi, Anita Kumari, Abdul Salam PK, Sruchytha Kalali, Yasaswi Gayatri Mishra, Preeti Damala, Siva Reddy Kotla, Samanthapudi Venkata Subramanyam Kumar, Ch. Naresh and G. Venkat Yadav** for making my stay in the lab wonderful.

❖ I have been fortunate to have friends like **Dr. Leela Shiva Ranjani Vutharadi, Dr. Mohan Krishna Mallakuntla, Dr. M. Naresh Kumar, Dr. Kovuru Narasaiah, Dr. Ananda Rao Ravula, Dr. Mohd. Fareed, Dr. Lokanadha Oruganti, Dr. Vengala Rao Yenuganti, Kishore Madhmanchi, Arun Kumar Paripati, Matin Shaik, Koncha Rama Gopal Reddy, Chaitanya, Venkata Rao Badana, Suryanarayana Ravada, Tirupati Gouni, and others** who have always been there for me through my highs and lows.

❖ I would like to thank **Prof. Pallu Reddanna, Prof. Bramanandam Manavathi**, and **Dr. Anil Kumar Pasupulati** for their assistance and care when I was in the hospital.

❖ My heartfelt thanks to **Dr. Pavan Kumar Chigulapalli MBBS, MS.,** for meticulously monitoring my health every month.

❖ I would like to thank the doctors and staff in the University Health Center for caring and providing medicines every month.

❖ I greatly acknowledge CSIR-UGC for JRF and SRF (Sr.2121330530, Ref No: 22/12/2013(ii) EU-V) for my financial support during my Ph.D. tenure.

❖ I also thank all the funding bodies (CSIR-UGC, DBT, CREBB, DST, FIST, UPE, PURSE, MoE, and STARS/STARS-1) for their financial assistance to Prof. BM, Department of Biochemistry and School Life Sciences, UoH.

❖ I would like to express my gratitude to my brother, **Sri. Penugurti Janardhana Rao**, for his financial and personal assistance from my childhood. I won't be able to hold this important position without his help. I am also grateful to my mother, **Smt. Penugurti Kondamma**, for her unconditional love and care. I am always thankful to my brother **Sri. Penugurti Venu Gopal Rao** for his guidance, assistance, and support throughout my life. I want to express my gratitude to my wife, **Smt. Penugurti Keerthi**, for her unwavering love and support. She stood with me through all my difficulties, diversions, and frustration. She offered me support and assistance, helped me avoid many drawbacks. Finally, I am grateful to all my in-laws, especially **Uriti Yadav**, **Uriti Simhachalam, Bagadi Appanna**, and **Uriti Suryanarayana,** for their encouragement and financial support after my marriage.

❖ I would like to thank the most important person in my life, Sri. **Gandem Rama Rao** always encouraged me to pursue higher education, including a Ph.D. degree. His assistance is priceless, and he assisted me in various ways, including financial and emotional support. I am incredibly grateful to him.

❖ Finally, I thank God Almighty for his blessings throughout my life.

Vasudevarao Penugurti

Table of contents

List of Figures

Figure…….……..…….Page No

List of Tables

ACRONYMS

7AAD	7-Aminoactinomycin D
ACC	Acetyl Co-A carboxylase
ADP	Adenosine diphosphate
AI	Aromatase inhibitors
AICAR	5' Aminoimidazole-4-carboxamide ribonucleotide
AKT	Protein kinase B
AMP	Adenosine monophosphate
AMPK	5' AMP-activated protein kinase
AO	Acridine orange
ATG (s)	Autophagy related gene (s)
ATP	Adenosine triphosphate
BC	Breast cancer
BRCA1&2	Breast cancer type 1&2 susceptibility genes
BSA	Bovine serum albumin
CAFs	Cancer-associated fibroblasts
CaMKK1	Calcium/Calmodulin dependent protein kinase kinase 1
CC	Compound C AKA Dorsomorphin
CBS	Cystathionine β-synthase
cDNA	Complementary DNA
CHX	Cycloheximide
CSF-1	Colony-stimulating factor 1
CTC	Circulating tumor cells
DAPI	4', 6-diamidino-2-phenylindole
DCIS	Ductal carcinoma *in situ*
DMEM	Dulbecco's modified Eagle's medium

DMSO	Dimethyl sulfoxide
dNTP	Deoxyribonucleotide triphosphate
ECL	Enhanced chemiluminescence
ECM	Extracellular matrix
EDTA	Ethylene diamine tetraacetic acid
EGFR	Epidermal growth factor receptor
EMT	Epithelial-mesenchymal transition
EtBr	Ethidium Bromide
ER	Estrogen Receptor
ErbB2	Avian erythroblastosis oncogene B2
ERK	Extracellular signal-regulated kinase
FOXO3a	Forkhead box O3
FRE	FOXO3a response element
GAPDH	Glyceraldehyde-3-phosphate dehydrogenase
GATA1	GATA-binding factor 1
GDH	Glutamate dehydrogenase (GLDH)
GFP	Green fluorescent protein
GLS	Glutaminase
GOT 1/2	Glutamic-oxaloacetic transaminase ½
GS	Glucose stress
GSK-3β	Glycogen synthase kinase-3β
GST	Glutathione S-Transferase
HEK 293T	Human embryonic kidney cells
HER2	Human epidermal growth factor receptor 2
HIF-1α	Hypoxia inducible factor-1α
HLA-G	Human leukocyte antigen-G

HPIP	Hematopoietic PBX-interacting protein
IDC	Invasive ductal carcinomas
IgG	Immunoglobulin
IDC	Invasive ductal carcinoma
ILS	Invasive lobular carcinoma
IPTG	Isopropyl β-D-thiogalactopyranoside
kDa	Kilo Dalton
αKGDH	Alpha-ketoglutarate dehydrogenase
LCIS	Lobular carcinoma *in situ*
LKB1	Liver kinase B1
M	Molar
MAPK	Mitogen-activated protein kinase
MBC	Metastatic breast cancer
MCT 1	Monocarboxylate transporter 1
MDH	Malate dehydrogenase
MDSCs	Myeloid-derived suppressor cells
MEK	MAPK/ERK kinase
$MgCl_2$	Magnesium chloride
MMP	Matrix metalloproteinase
MTT	3-(4,5-dimethylthiazol-2-yl)-2,5-diphenyltetrazolium bromide
MYC	BHLH Transcription Factor
NaCl	Sodium chloride
NAF	Sodium Fluoride
NRF 1	Nuclear respiratory factor 1
OD	Optical density
OXPHOS	Oxidative phosphorylation

PAGE	Polyacrylamide gel electrophoresis
PARP	Poly (ADP-ribose) polymerase
PBS	Phosphate-buffered saline
PBX1	Pre-B-cell leukemia homeobox protein 1
PCR	Polymerase chain reaction
PDL-1	Programmed death-ligand 1
PGC 1α	Peroxisome proliferator-activated receptor-γ coactivator 1α
PI	Protease inhibitors
PI3K	Phosphatidyl inositol 3-kinase
PMSF	Phenyl methyl sulfonyl fluoride
RNF2	Ring Finger Protein 2
PR	Progesterone receptor
RPM	Rotations per minute
RPMI	Roswell Park Memorial Institute medium
SDS	Sodium dodecyl sulfate
SDH	Succinate dehydrogenase
SERM	Selective estrogen receptor modulators
SLC1A5	Solute Carrier Family 1 Member 5 (ASCT2)
TAM	Tumor-associated macrophages
Taq	*Thermophilus aquaticus*
TBST	Tris-buffered saline Tween-20
TCA cycle	Tricarboxylic acid cycle
TFAM	Transcription Factor A, Mitochondrial
TME	Tumor microenvironment
TNBC	Triple-negative breast cancer
TSG	Tumor suppressor genes

Chapter-I

1. General introduction

1.1. Cancer

In general, cancer is defined as uncontrolled cell growth. Besides this, cancer is represented by various hallmarks, including self-sufficiency in growth signals, anti-apoptosis, evading immune surveillance, increased angiogenesis, and metastasis (1). Cancer cells may disseminate from the primary tumor, enter the bloodstream, survive immune assault, and successfully develop a secondary tumor via a process called metastasis. Depending on their aggressiveness, tumors can be classified as benign or malignant. A benign tumor is not dangerous and does not exhibit signs of metastasis, whereas malignant tumors are those that have spread to distant organs and begun to proliferate and form secondary tumors. Cancer may initiate in any organ and at any location. Cancers are categorized based on the origin of the tissue, such as breast, liver, pancreatic, endometrial cancer, and so on.

1.2. Breast cancer (BC)

BC is the most prevalent type of cancer in women, and it begins in the mammary gland. Because of their various genetic subtypes and heterogeneity, BCs are the most complicated cancers.

1.2.1. Structure of mammary gland

The mammary gland is a composite, dilated sweat gland that mainly comprises of blood arteries, lobules, and ducts. In the hollow chamber known as alveoli, milk-secreting cuboidal cells and surrounding epithelial cells are found. All these alveoli are linked together to create a clump known as a lobule. The lactiferous duct connects these lobules and opens into the nipple (Figure 1). Extracellular matrix (ECM) is a complex connective tissue found in the mammary gland consisting of fibroblasts, stromal cells, adipocytes, and other related myoepithelial basement membranes. Connective tissue is required to maintain the morphology of the lactiferous duct, basic mammary gland structure, and overall organ development.

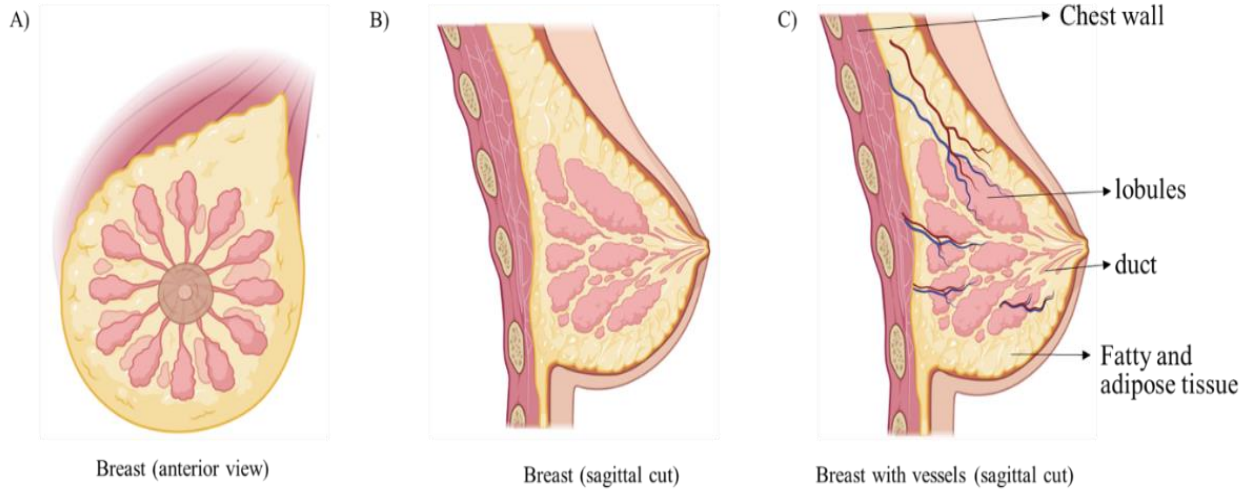

Figure 1: Structure of mammary gland: The arrangement of the lobules, ducts, and veins in the mammary gland. **A)** Frontal image of the breast. **B)** Sagittal breast cut. **C)** Breast with vessels (sagittal cut). (Ref: drawn using Biorender software)

1.2.2. Classification of BC

Based on histology

According to histology and invasiveness, BC is classified into four significant subtypes (2).

(A) Carcinoma in the ducts

Carcinoma in the ducts may be invasive or non-invasive. The non-invasive carcinoma is ductal carcinoma *in situ* (DCIS). This form of BC is non-invasive before being diagnosed. Because altered cells do not metastasize, it is termed as non-invasive. Cancer begins in the lining of the milk-producing ducts and does not extend to the surrounding tissues. DCIS affects 60,000 people each year, accounting for 25% of all newly diagnosed cancers in the United States. According to the Indian Council of Medical Research (ICMR), the incidence of DCIS-detected cancers in India is very low, although the total number of BC cases is significantly higher. This may be due to lack of early diagnosis, and most cancers are detected at an advanced stage. If undetected at an early stage, DCIS becomes invasive over a period and is termed invasive ductal carcinoma (IDC) (Figure 2).

(B) Invasive type of ductal carcinoma (IDC)

It is the most common form of BC, accounting for 80% of all occurrences. It begins in the ducts and makes its way through the lymphatic and circulatory systems to distant organs. IDC accounts for approximately 8 out of every 10 cases of BC. According to the American Cancer Society, it is the most prevalent type of BC in the United States, with an estimated 0.18 million cancer cases per year (Figure 2).

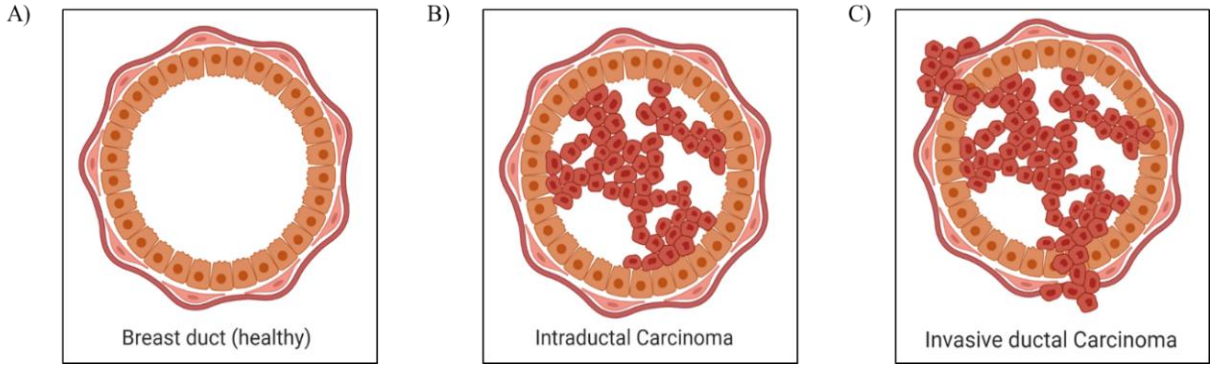

Figure 2: Various types of breast ductal carcinoma. A) Arrangement of a healthy breast duct. **B)** Non-invasive carcinoma in the ducts. **C)** Carcinoma at the metastatic stage in the ducts (IDC) (Ref: drawn using Biorender software)

(C) Carcinoma in the lobules

It may be invasive or non-invasive. The non-invasive cancer is called lobular carcinoma *in situ* (LCIS), and it begins in the milk-producing tissues of the breast. In general, it is not a carcinoma as the other subtypes, but it may be referred to as neoplasia since it is non-invasive and not dangerous. It is not detectable with standard mammography but may be detected with a tissue biopsy. It has a greater chance of developing BC and will become invasive at a later stage (Figure 3).

(D) Invasive lobular carcinoma (ILC)

It originated in the mammary milk-producing glands (lobules) and may spread to other body areas. It is less frequent and affects one out of every ten BC patients (Figure 3).

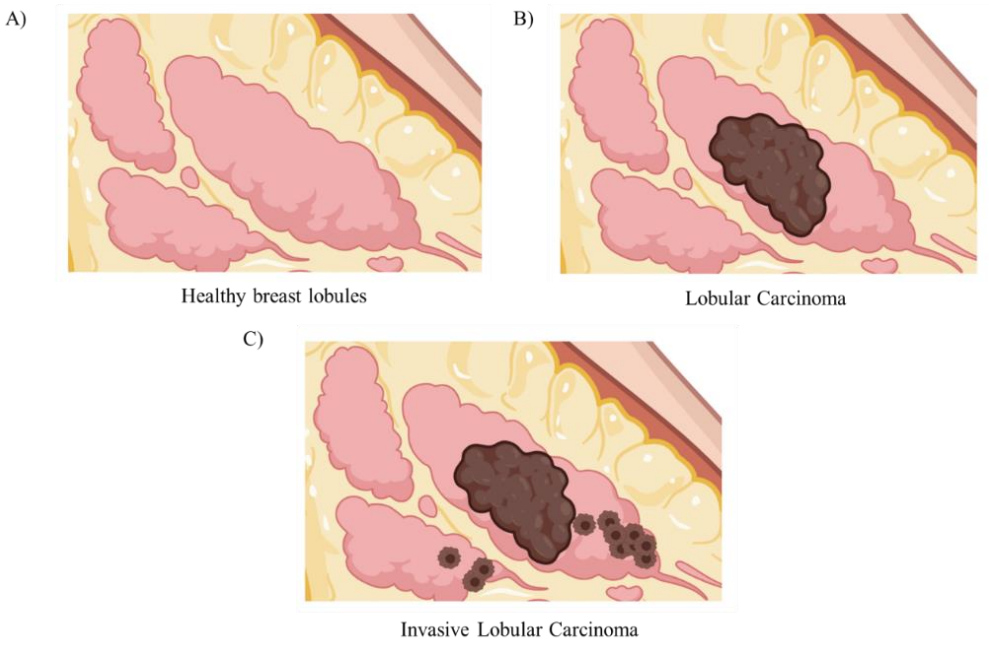

Figure 3: Different types of lobular carcinoma. A) Arrangement of normal lobules. B) Carcinoma in the breast lobules. **C)** Carcinoma at the metastatic stage in the lobules. (Ref: drawn using Biorender software)

Classification based on the receptor expression

Based on the expression profile of various receptors such as estrogen receptor (ER), progesterone receptor (PR), and human epidermal growth factor receptor 2 (HER2), BCs are categorized as luminal (A and B), HER2+, or TNBC (Figure 4) (3, 4).

Luminal subtype A is the most prevalent form of BC, which expresses ER, has a stronger PR expression profile, and relatively low HER2 expression. Because of the existence of ER and PR, it may be treated with hormone or endocrine therapy (3, 4). It accounts for approximately 50-55% of total BCs.

Luminal subtype B expresses ER but has a reduced PR expression profile and is positive or negative for HER2. It accounts for 20-30% of total BCs.

HER2+ breast carcinomas express HER2 receptor but lack the ER and PR. HER2+ tumors are usually aggressive and have a high recurrence rate. It is responsible for 12-20% of all BCs.

Triple-negative breast cancer (TNBC) accounts for 15-20% of all BCs and is distinguished by the lack of ER, PR, and HER2 receptor expression. These cancers are very aggressive, have high-grade tumors, and often contain mutations in the p53 and BRCA 1&2 genes. Because of the lack of receptors, hormone therapy does not affect these tumors (4).

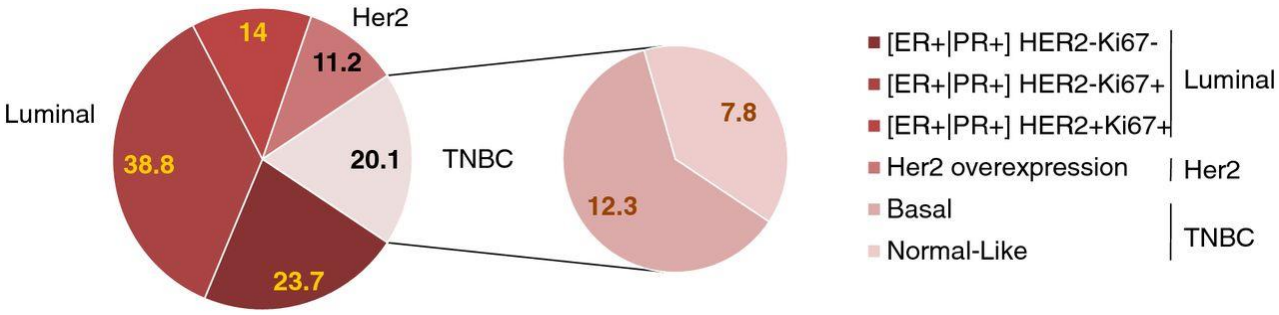

Figure 4: BC categorization based on receptor expression: Luminol type (A and B); $HER2^{+}$ type; TNBC type (Ref- Gajulapalli VN *et al.* **Biosci Rep**, 2016)

Various other types of BC

In addition to the subtypes listed above, BCs were further classified as inflammatory (1-3%), medullary (3-5%), metaplastic (MpBC, 0.2-5%), mucinous, tubular, and papillary.

1.2.3. Risk factors for BC

An older age, a family history of BC, genes inherited from the parents, late marriage, late pregnancy, and never breastfeeding are all the possible risk factors for BC. Mutations in *BRCA1* and *BRCA2* may increase the chance of developing BC (5).

1.2.4. Screening of BC and possible treatment

Timely detection is the most efficient method of preventing BC. Cancer screening comprises monthly self-examinations starting at the age of 20, clinical breast exams every three years starting at the age of 20, and yearly mammograms beginning at the age of 40. A lump, alteration in the breast, dimpling, and a red scaly patch are signs of BC. It is often diagnosed in its advanced stages (stage 3 or 4), complicating treatment in developing nations such as India. BC

patients get a variety of treatment possibilities, including surgery, radiation, chemotherapy, and targeted treatments such as hormone therapy. Anthracyclines, taxanes, and platinum agents are among the most recent chemotherapeutic agents used to treat BC (6, 7). Another type of drug, aromatase inhibitors (AIs), which decrease blood estrogen levels, shows promising results in BC treatment (7, 8). Selective estrogen receptor modulators (SERMs) have been shown to bind to the ERα/β and activate the signaling against the estrogen. Tamoxifen is a well-known estrogen receptor antagonist/SERM that is useful in treating BC (9).

1.3. Cancer and breast cancer facts across the world and in India

Cancer is the deadliest disease after cardiovascular disease, and it is the second-largest cause of mortality globally. Breast cancer is the fifth leading cause of cancer-related fatalities in both sexes (Table 1) (10). Despite fewer new cases (one-third of western countries), India has a greater mortality rate than western countries, attributed to a lack of awareness and delayed illness detection (11, 12). Surprisingly, urbanized areas have a higher prevalence of BC than rural areas due to lifestyle changes, food habits, late childbearing, increased alcohol use, and increasing contraceptive usage. Unfortunately, the prevalence of BC is higher in India at a younger age (30-50) than in western countries (50-70), and tumors in children and adolescents are more aggressive, necessitating earlier diagnosis and improved treatment.

	Diagnosed in 2020-worldwide/India (millions)	**Projected cases by 2040-worldwide/India (millions)**
Cancer	19.3/1.32	30.2/2.09
Breast cancer	2.26/0.178	3.19/0.272
	Deaths in 2020-worldwide/India (millions)	**Projected deaths by 2040-worldwide/India (millions)**
Cancer	9.96/0.85	16.3/1.38
Breast cancer	0.68/0.09	1.04/0.147

Table 1: Cancer and breast cancer statistics across the world and in India

2. Review of literature

2.1. Cancer and its microenvironment

Cancer is characterized by uncontrolled cell growth, resistance to apoptosis, and metastasis to other body regions. Hanahan *et al.,* proposed six unique characteristic features to comprehend the complexity of cancer (1). These may be acquired throughout the many stages of human tumor growth. They include maintaining a higher proliferative rate, escaping the growth inhibitors, reducing cell death, aiding replicative immortality, increasing angiogenesis, and promoting invasion and metastasis (1). Cancer has gained various features due to its complexity and heterogeneity, including altering cellular energy metabolism and aggressively avoiding immune cell assault. In the emerging hallmarks of cancer, Pavlov *et al.* included altered tumor metabolism as one of them (13).

2.1.1. Tumor microenvironment (TME)

The tumor ecosystem consists of a varied population of cancer cells and stroma that create a distinct microenvironment. It also contains immune cells, adipose cells, and cancer-associated fibroblasts (CAFs) in addition to cancer cells (Figure 5). The progression of a tumor depends on the microenvironment and its interaction with tumor cells. The interaction of microenvironment with tumor cells dictates cellular fate, including proliferation, metastasis, apoptosis, or elimination (14). For instance, tumor-associated macrophages (TAM) are generated in response to tumorigenesis, and their primary role is to inhibit the development of the tumor. On the other hand, TAM promotes tumor cell invasion through a paracrine signaling loop involving the colony-stimulating factor (CSF-1), which is derived from tumors, and epidermal growth factor (EGF) derived from macrophages (14, 15). Myeloid-derived suppressor cells (MDSC) originate from the myeloid lineage that behaves as tumor suppressor cells. They are another kind of immune cell that helps cancer cells evade the immune system

and are reliant on the microenvironment (16). CAFs are distinct from normal fibroblasts in the TME. When CAFs are associated with cancer cells, they cause intraepithelial neoplasia, while normal fibroblasts cannot form tumors. Additionally, they induce a mesenchymal-like phenotype and facilitate metastasis. This shows the complexity of fibroblast activity in developing cancer cell proliferation and metastasis (17). In addition to the specific cell types involved in carcinogenesis, the ECM may promote disease progression. Likewise, extracellular TME composition is a significant predictor of clinical outcomes. Tumors with increased levels of protease inhibitors in their ECM have a better prognosis, while tumors with higher integrins and matrix metalloproteinases (MMPs) have a worse prognosis and are more likely to relapse (18, 19). Based on this analysis, it is possible to believe that the TME is central environment in cancer progresson and metastasis.

At various stages of the disease, solid tumors exhibit different microenvironments. They began with a single transformed cell and then multiplied by autocrine signaling to synthesize multiple growth factors that are required for angiogenesis. Tumor regions are those that are close to blood vessels and receive an abundance of nutrients and oxygen. In contrast, hypoxic areas are those that are far from blood vessels and receive a deficiency of nutrients and oxygen (20). In this scenario, the metabolic and signaling pathways show variations from hypoxic to normoxia, with more rewired metabolic pathways observed in hypoxic regions for proliferation and survival. Under conditions of hypoxia and other stresses, cancer cells upregulate certain transcriptional factors like hypoxia-inducible factor 1-alpha (HIF-1α), the primary metabolic adaptive mechanism before angiogenesis (21). Cancer cells exposed to metabolic stress exhibit altered cell growth and survival pathways such as glycolysis and oxidative phosphorylation (OXPHOS), and for metastatic destinations, both glycolysis and OXPHOS pathways are prominent (22). The tumor microenvironment exhibits heterogeneity in the population, signaling molecules, downregulation of tumor suppressor genes (TSGs), upregulation of

oncogenes, and expression of various metabolic pathway enzymes. For example, monocarboxylate transporter 1 (MCT1) is abundant in cancer cells but is absent or extremely low in tumor-associated macrophages in the same environment (23). In order to manage cell survival, tumor cells have several altered pathways such as increased glycolysis, TCA cycle for anaplerosis, and glutaminolysis for the supply of glutamine to nucleic acid synthesis than normal cells (24). Cancer cells exhibit not only metabolic differences but also variations in other phenotypes such as immune escape. Most cancer cells, for example, exhibit substantially reduced amounts of major histocompatibility complex-I compared to normal cells (25). This suggests that the TME is an essential regulator of cancer development and migration.

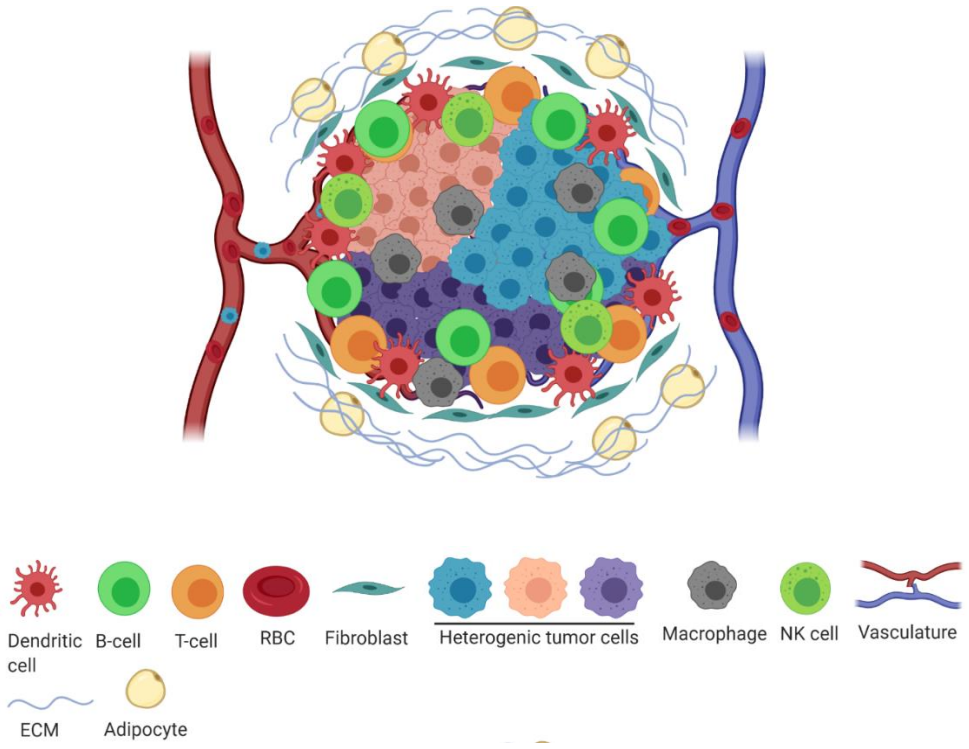

Figure 5: Tumor microenvironment showing the varied population of immune cells, fibroblast, heterogeneous tumor cells, ECM, and other signaling molecules.

2.1.2. Metabolic stress

Due to rapid cell proliferation and poor angiogenesis, solid tumors lack essential elements such as glucose and oxygen, resulting in metabolic stress. To cope with metabolic stress, cancer

cells develop a variety of adaptations. For instance, when oxygen levels in solid tumors are low (0.3-2 percent), cells use the HIF-1α pathway to promote cell survival by transcriptionally upregulating glycolytic, glutaminolysis, and glucose transporters (26). These elevated metabolic pathways deplete the glucose levels in mammalian cells, inducing the onset of glucose stress (0.4-0.6 mM). Under metabolic stress, cancer cells rewire their metabolic pathways with alternative pathways such as glutaminolysis and lipolysis (27). Glucose is a rich carbon source, and glutamine is the rich nitrogen source for rapidly dividing cells (13). These nutrients are the necessary materials for synthesizing the macromolecules of the cell. In normal cells, glucose is used systematically via glycolysis, the TCA cycle, and OXPHOS. On the other hand, rapidly proliferating cells utilize glucose through glycolysis though in the presence of oxygen, a process known as the Warburg effect (28). Increased glycolysis results in the formation of a variety of glycolysis intermediates. They are used in rapidly dividing cells to produce nucleic acids, lipids, proteins, and other macromolecules. Glutamine is another essential energy nutrient in the rapidly dividing cells, and it is utilized in the TCA cycle by entering as an anaplerotic substance. Cancer cells prefer glutamine as an alternate carbon source under conditions of glucose stress. For this pathway to operate in cancer cells under nutrient-depleted conditions, they need to suppress the TSGs while activating oncogenic pathways (29). Tumors that succumb to nutritional deficiency upregulate transcription factors such as MYC and kinases such as AMPK, the metabolic sensor of cancer cell survival. Cancer cells utilize these transcription factors and kinases to control metabolic pathways like glycolysis, glutamine metabolism, TCA cycle, and OXPHOS (29). For example, MYC transcriptionally upregulates the glutamine metabolizing enzymes like glutaminase (GLS), glutamate dehydrogenase (GDH), glutamic-oxaloacetic transaminase 1/2 (GOT 1/2), and α-ketoglutarate dehydrogenase (αKGDH) (30). MYC is also important in glutamine metabolism and up-regulation of glutamine transporters such as SLC1A5, which is required for glutamine import in cancer cells under glucose deprivation conditions (31). AMPK is also identified to

control various pathways, including glycolysis, TCA cycle, and glutaminolysis, both under metabolic stress as well as in normal conditions, suggesting a role in tumorigenesis (32). To summarise, cancer cells reorganize metabolic pathways in response to metabolic stress as part of their survival adaptation.

2.1.3. Survival strategies by cancer cells under metabolic stress

A) Metastasis as one of the survival mechanisms

Most birds and animals migrate from one location to another for various reasons. To escape from an unfavorable climate, to enable them to discover the abundance of food available throughout the year, to lay their eggs, or give birth to newborn animals in a safe and hygienic environment. Similarly, cancer cells may migrate from their original site to other sites for various reasons, including evading immune attacks in which cancer-specific antigens are neutralized by immune cells, overcoming metabolic stress such as nutrient deficiency and hypoxia, and forming secondary colonies at distant sites with more favorable conditions. One of the critical aspects of cancer progression is metastasis, which depends on the invasive phenotype. When cancer cells are deprived of nutrients due to an inadequate blood supply, subjected to an immune assault, or exposed to other variables in their environment, they prefer to move to distant parts of the body to replenish and multiply (33). Most cells avoid being attacked by the immune system during metastasis by masking or mutating the necessary signaling (34). Cancer cells have been shown to develop a phenotype that can protect or hide them from the immune system when subjected to evolutionary pressure. Steinert *et al.*, demonstrated that circulating tumor cells (CTC) exhibited a distinct non-immunogenic phenotype by overexpressing the cluster of differentiation 47 (CD47) (35). This protein inhibits the cytotoxic and phagocytic activity of activated immune cells and has a significant downregulation of calreticulin (35, 36). Increased expression of programmed death-ligand 1 (PDL1) on the membrane of various cancer cells causes epithelial-mesenchymal transition

(EMT) as well as stem cell-like features in cancer cells, indicating that the intrinsic mechanism of PD-L1 promotes cancer progression and metastasis (37, 38). Furthermore, human leukocyte antigen G (HLA-G) expression was significantly related to tumor immune evasion, invasion, and disease progression. It inhibits immune cell cytolysis, proliferation, suppresses cytokine production, induces immune cell death, and stimulates myeloid-derived suppressor cells (MDSCs) (39). These lines of evidence indicate that the expression of many markers during EMT and metastasis leads to immune escape, enabling cancer cells to survive.

B) Autophagy as an adaptive mechanism of cell survival

Autophagy is a catabolic process that degrades damaged cellular components into small molecules with the help of lysosomes. The autophagy process is aided by around thirty autophagy-associated (ATG) proteins (40). Autophagy serves as the primary source of amino acids, fatty acids, and nucleotides for cells that are unable to get sufficient nutrients from the external environment to support adenosine triphosphate (ATP) synthesis and biogenesis (41). Autophagy has dual functions in cancer, as it both stimulates and inhibits tumor formation, depending on the level of autophagy in cells. Autophagy and its related mechanism in cancer cell survival in metabolic stress have received significant interest. Conditions in the TME, such as unavailability of glucose or hypoxia, activate autophagy in cancer cells to ensure cell survival. According to recent research, depletion of ATGs cause cancer cells to become more sensitive to hypoxia-induced cell death (42). In another study, Beclin 1 depletion leads to cell death under conditions of metabolic stress (43). Under metabolic stress and genotoxic stress, autophagy improves cell survival by inhibiting p62-mediated p38 activation, which may enable tumor growth (44). According to recent studies on the role of autophagy in metastatic evolution, autophagy promotes the development of numerous ladders across the metastatic cascade (45, 46). Autophagy is enhanced in RAS-transformed cancer cells, increasing their growth, carcinogenesis, proliferation, and metastasis (47-49). Defects in mitochondrial

metabolism, as well as the consequent sensitivity to stress, are considered to be essential components in RAS-driven cancers. These findings imply that malignancies associated with RAS may be "autophagy-dependent" (49-51). CAFs trigger autophagy to enhance survival in some cancers. As a result, combining anti-cancer drugs with autophagy inhibitors has a synergistic effect on cancer treatment (52). Additionally, several drugs have been discovered that are effective in treating cancer by targeting autophagy, demonstrating that autophagy is a factor in carcinogenesis (52, 53). These discoveries laid the groundwork for a more in-depth examination of autophagy to better understand how carcinogenesis and autophagy addiction are selected for and operated in cancer cells.

C) Mitochondrial biogenesis

Mitochondrial biogenesis is the phenomenon by which cells increase the number of mitochondria (54). Various mechanisms stimulate mitochondrial biogenesis in response to cellular stress or external stimuli such as aerobic exercise (55). The functions of mitochondrial biogenesis in cancer are manifested via several factors, including metabolism, tissue composition, microenvironment, tumor phase, and heterogeneity. Cancer cells often use an enormous quantity of ATP in order to grow and spread. This inherent property of malignant cells necessitates a competent adaptation that will keep them alive in the presence of metabolic stresses such as hypoxia, an unfavorable pH, and so on. Since the primary purpose of mitochondria is to generate additional ATP, cancer cells utilize specific proteins such as MYC or PGC-1α to initiate this biogenesis, allowing the cancer cells to proliferate even in stressful conditions (56). Cancer cells use a variety of mechanisms to activate tumor promoter genes and deactivate TSGs (57). When glucose levels are low, for example, cancer cells activate AMPK, which enhances the production of PGC1α and mitochondrial transcription factor A (TFAM), promoting cellular energy levels through the increase in mitochondrial number in cancer cells (58, 59). An increase in mitochondrial biogenesis is observed not only in acute

stress but also in chronic stress. Chronic energy restriction activates AMPK, which upsurges the expression of nuclear respiratory factor-1 and stimulates mitochondrial biogenesis (60). These data indicate that cancer cells may survive under metabolic stress circumstances via the stimulation of mitochondrial biogenesis.

D) Metabolic reprogramming

Otto Warburg identified abnormal glucose metabolism as a distinguishing feature of cancer cells almost a century ago (61). He discovered that growing tumor cells convert most of their glucose to lactate even when oxygen is available and speculated that this was related to mitochondrial metabolic inefficiency since the aerobic glycolysis pathway is inefficient (28, 61). However, further study showed that mitochondrial metabolism is not defective in terms of its ability for OXPHOS but rather reprogrammed to meet the requirements of tumor cells (62). At first, metabolic rewiring was thought to occur in response to proliferation and survival. Actively proliferating cells exhibit increased transcription and translation, reducing the ATP: ADP ratio. Reduced ATP altered the allosteric properties of metabolic enzymes. However, in response to growth factor signaling, metabolic pathways reprogramme in order to meet the increased macromolecule synthesis associated with cell growth and proliferation (62). Increased glycolysis, glutaminolysis, amino acid and lipid metabolism, activation of the pentose phosphate pathway (PPP), and macromolecule synthesis are all examples of typically altered pathways in tumor cells (29, 63). These results prompted considerable study into cancer-related metabolic changes, metabolic reprogramming emerging as a characteristic feature of cancer.

(i) Glycolysis

Glucose is catabolized to pyruvate in normal cells by a series of biochemical reactions catalyzed by various enzymes. In the presence of oxygen, pyruvate is transformed to acetyl Co-

A and enters the mitochondria to drive the TCA cycle in normal cells. The NADH and $FADH_2$ produced as a result of this process are subsequently utilized to enhance OXPHOS and improve energy output while the normal cells catabolize pyruvate to lactate under anaerobic circumstances (64). However, even in the presence of oxygen, pyruvate to lactate conversion is the most common pathway in cancer cells, a process known as the Warburg effect. Pyruvate is the end product of glycolysis, and it provides a rich supply source for the pathway that transforms pyruvate into lactate. In cancer cells, glycolysis is preferred over OXPHOS, despite generating less ATP (63). As a result, the glycolysis pathway is more active in cancer cells, and the rate of glucose absorption must be raised to compensate for tumor cells' inadequate energy generation and satisfy their metabolic requirements for growth and proliferation. Cancer cells activate oncogenes while suppressing tumor suppressor genes in order to promote glucose metabolic reprogramming. HIF-1α is one such oncogene, and it is the primary regulator of glucose metabolism during hypoxic stress. HIF-1α regulates aerobic glycolysis by elevating the transcription of glucose transporters and glycolytic genes (65, 66). MYC is another significant proto-oncogene that induces the transition from anaerobic to aerobic glycolysis in tumor cells. Regardless of hypoxia, MYC increases the expression of a most glycolytic genes, glucose transporters and glutamine import and metabolism related genes (67, 68).

Additionally, oncogenic AKT activation enhances glucose uptake and aerobic glycolysis in transformed cells (69-71). EGFR mutation enhances PI3K/AKT/mTOR activation in lung cancer cell lines, maintaining GLUT1 membrane localization and de novo pyrimidine synthesis (72). On the other hand, TP53 inhibits glycolysis in several ways. TP53 has been found to decrease GLUT1 and GLUT4 transcription, and a cancer-associated p53 mutation has been demonstrated to reverse these inhibitory effects (73). Furthermore, TP53 reduced hypoxia-induced glycolysis by increasing Ras-related glycolysis inhibitor and calcium channel regulator (RRAD) expression, reducing GLUT1 translocation to the plasma membrane and total aerobic

glycolysis (74). Another study discovered that deleting TP53 enhanced aerobic glycolysis and GLUT3 synthesis via activating the IKK-NF-B pathway (75). These pieces of evidence demonstrate that glycolysis is a critical pathway for cell survival under metabolic stress and is cancer cells' most common metabolic adaptation.

(ii) Glutaminolysis

Glutamine is found in higher levels in blood and muscles, and it supports cell growth in both normal and cancerous conditions; however, cancer cells are more addicted to glutamine (76). Glutaminolysis is a metabolic process in which glutamine is converted to glutamate and further converted to α-ketoglutarate, which is then utilized to produce amino acids, cholesterol lipids, and other essential metabolites (77). In glutamine-dependent cancer cells, mitochondrial glutaminase (GLS) converts glutamine to glutamate, which is then metabolized to α-ketoglutarate by glutamate dehydrogenase (GDH) (77). During GDH flux, a reduced form of NADH or NADPH is produced, coupled with ammonium and a cofactor. Rather than continuing the process of OXPHOS and ATP synthesis, ketoglutarate serves as an anaplerotic substrate. For example, malate, a TCA intermediate, may be exported from the mitochondria to the cytoplasm via malic enzyme 1 (ME1) to generate pyruvate and NADPH. Citrate is another critical molecule that links mitochondrial metabolism to lipid synthesis. Citrate generated during the TCA cycle is promptly exported to the cytoplasm, or α-ketoglutarate is transported to the cytoplasm and converted to citrate and NADPH by isocitrate dehydrogenase (IDH).

Furthermore, glutamine is the primary nitrogen source for the production of purines and pyrimidines. MYC is often involved in glutaminolysis. MYC promotes the transcription of several high-affinity glutamine transporters, including SLC1A5/ASCT2 and SLC38A5/SN2 (78). GLS expression was elevated in MYC-induced liver tumors (79, 80). Additionally, MYC enhanced the expression of lactate dehydrogenase A (LDH-A), rerouting glucose-derived

pyruvate to lactate. MYC-mediated mitochondrial reprogramming resulted in glutamine addiction in cancer cells, which was required to maintain mitochondrial integrity and TCA function (79, 81). Multiple shreds of evidence indicate that glutaminolysis is essential for cell survival under metabolic stress and is the most prominent metabolic response of cancer cells. According to the findings shown above, cancer cells use any of these mechanisms for proliferation and survival under metabolic stress (Figure 6).

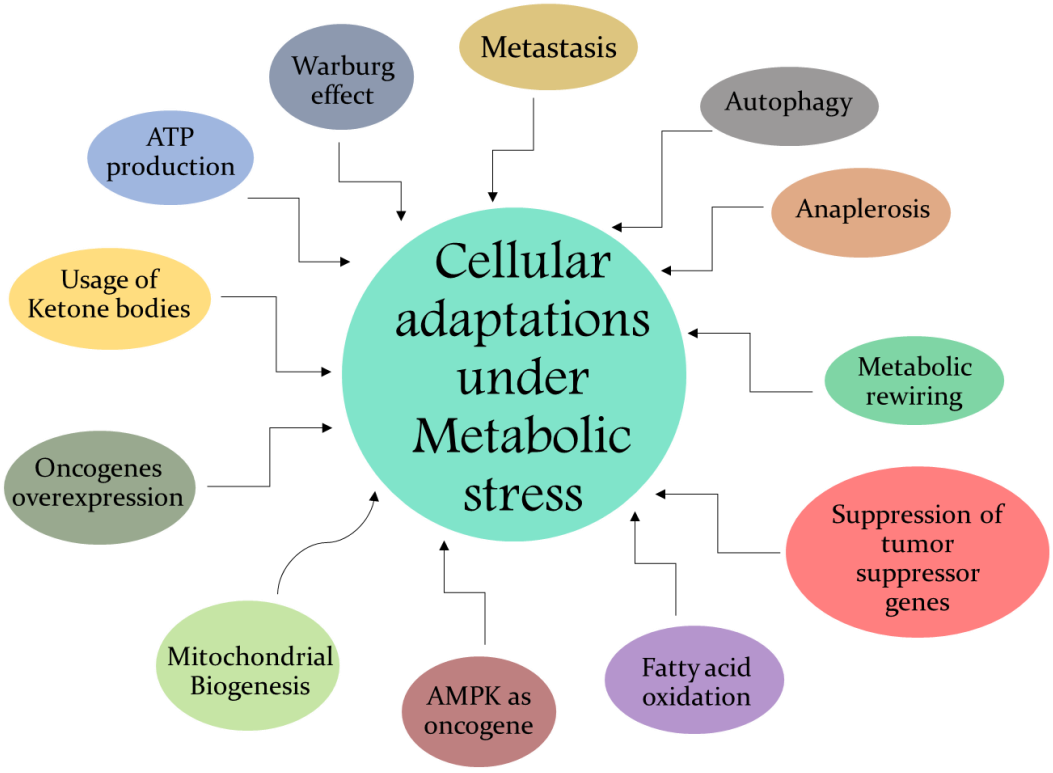

Figure 6: Cancer cells utilize various cellular adaptive mechanisms under metabolic stress for their survival and proliferation.

E) AMPK acts as a contextual oncogene in promoting cell survival under metabolic stress

Structure of AMPK

AMPK is a highly conserved, heterotrimeric protein made up of three subunits, namely α, β, and γ, each of which has various isoforms produced by distinct genes. The α forms a catalytic monomer, whereas β and γ serve as regulatory subunits. Humans have two isoforms of the

catalytic subunit-α, namely subunit α1 encoded by *PRKAA1* and subunit α2 encoded by *PRKAA2*. Similarly, the regulatory subunit-β has two isoforms β1 and β2, which are encoded by *PRKAB1* and *PRKAB2* genes, respectively, and the subunit-γ has three isoforms 1, 2, and 3, which are encoded by *PRKAG1*, *PRKAG2*, and *PRKAG3*, respectively. Twelve different functional AMPK complexes can be formed by the amalgamation of any three different isoforms mentioned but comprising one each from α, β, and γ subunits (Figure 7).

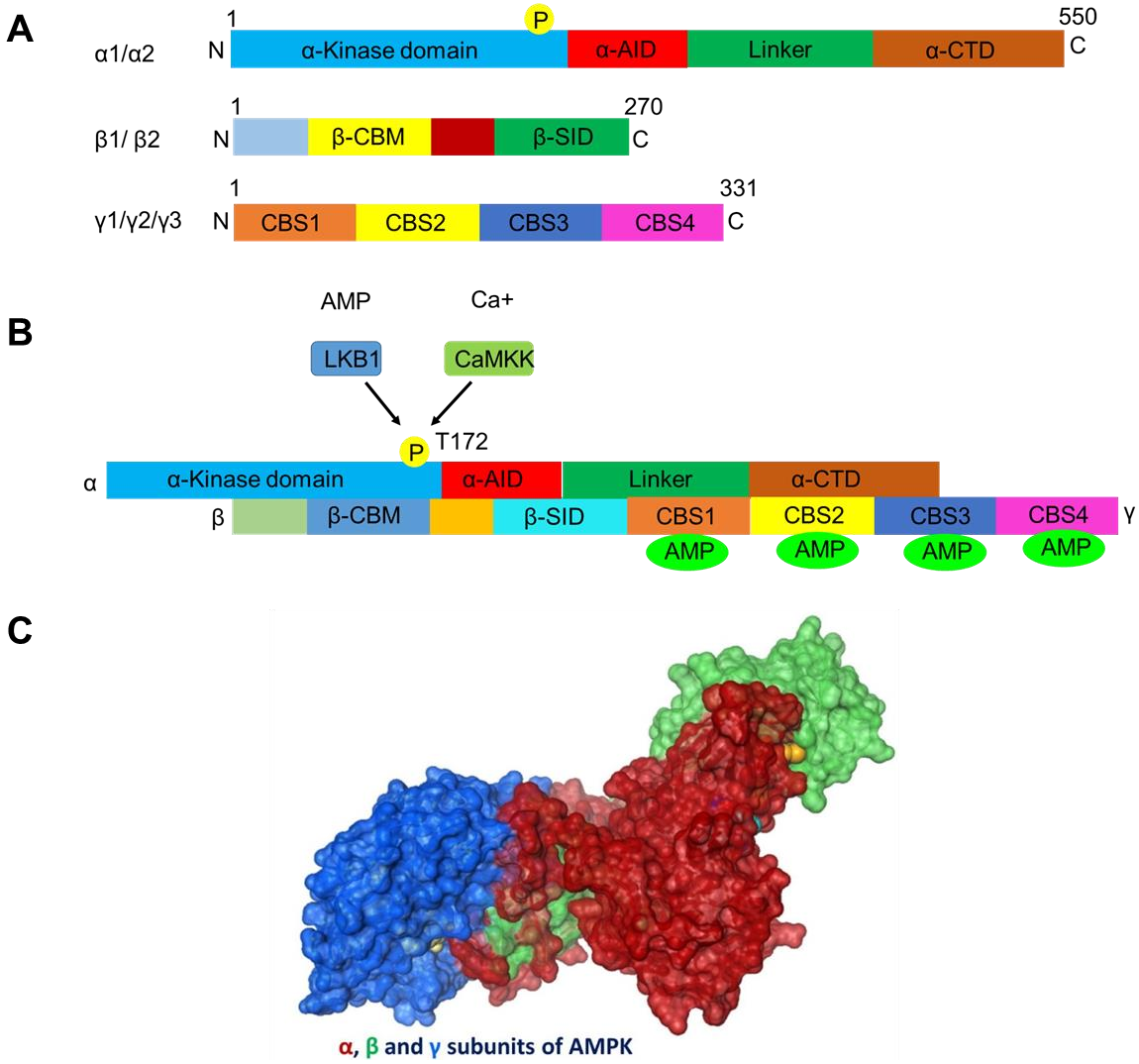

Figure 7: **A)** AMPK is made up of a catalytic protein subunit (α) and two regulatory protein subunits (β and γ). **B)** Under low energy conditions, AMP binds to the CBS domain present in the γ subunit, inducing conformational changes in the catalytic domain of the subunit-α, which is then phosphorylated at T172 by upstream kinases such as LKB1 and CaMKK. **C)** Crystal structure of AMPK (Ref: K.O. Cameron, and R.G. Kurumbail, Bioorganic & Medicinal Chemistry Letters, 2016).

AMPK activation mechanisms

AMPK is a serine/threonine kinase that functions as a metabolic detector, activated when low cellular ATP levels. Many metabolic stresses induce AMPK activation, including amino acid deficiency, oxygen or glucose insufficiency, ECM loss, strenuous exercise, and mitochondrial damage (82-86). When the ATP: AMP ratio is low, AMP binds to the CBS domain present in the γ-subunit. This binding leads to a conformational shift in the heterotrimeric protein complex and exposes the catalytic domain in the subunit-α. Kinases present upstream of the AMPK, such as Liver kinase B1 (LKB1), calcium/calmodulin-dependent protein kinase kinase 1 (CaMKK1), or TGF1 activated kinase (TAK1), phosphorylate AMPK at T172, resulting in AMPK activation. Once AMP or ADP binds to the AMPK γ subunit, protein phosphatase 2C (PP2A), PP2A, and PPM1E cannot deactivate the AMPK resulting in prolonged AMPK activation (87). Sirtuin-1, a NAD-dependent deacetylase, deacetylates LKB1, and this deacetylation increases LKB1 activation, suggesting a link between the two different energy-sensing regulators, AMPK and Sirtuin-1 (88, 89). Another study shows that myristoylation of the AMPK β subunit is required for AMPK activation (90).

Numerous pharmacological compounds, including AICAR and metformin, have been shown to activate AMPK. An exciting study by Zong et al. (2019) unveiled that different levels of nutritional stress activate different pools of AMPK in a hierarchal and spatiotemporal manner in the cells, leading to varied phosphorylation substrates that could have important physiological implications (91). Nutrient and non-nutrient components of one's diet, such as α linoleic acid, monounsaturated fatty acids, berberine, curcumin, etc., can also regulate AMPK activation (92). Various direct and indirect activators of AMPK have potential therapeutical significance. Their mode of action with respect to the structure of AMPK has been previously described (93). In recent studies, for instance, a PAN-AMPK activator, O304, has been shown to suppress the dephosphorylation of AMPK, thereby increasing its activity. O304 has shown

promising effects in both animals and phase IIa clinical trials in type II diabetes patients treated with metformin (94). AMPK activation has also been shown to have roles in bone metabolism and its consequent roles in osteoporosis, also known as diabetes mellitus induced bone fragility (95). Osteocalcin that is secreted by osteoblasts is known to be possibly involved in glucose metabolism (96). It has been shown that metformin, an AMPK activator, stimulates osteocalcin expression in osteoblasts, implicating AMPK activation as a prospective for osteoporosis treatment (95). Metformin's cardioprotective roles via AMPK activation have also been recently explored (97). Table 2 describes all of the activators that either directly or indirectly activate AMPK.

Name	Mechanism	Target	Reference
AICAR	Acts as AMP analog	Binds with CBS domain of AMPKγ subunit	(98)
Benzimidazole		AMPKβ subunit	(99)
Berberine	Increases AMP	Complex I of Electron transport chain (ETC)	(100)
Compound 13		AMPKα subunit	(101)
Cryptotashinone	Increases AMP		(102)
Curcumin	Increases AMP	Complex V of ETC	(103)
Epigallocatechin 3-gallate	Increases AMP	Complex V of ETC	(104)
Genistein	Increases AMP	Complex V of ETC	(105)
Ginsenoside Rb1	Increases AMP		(106)
Metformin	Increases AMP P	Complex I of ETC	(95)
MT63-78		AMPKβ subunit	(107)
Pioglitazone	Increases AMP	Complex I of ETC	(108)
PT1		AMPKγ subunit	(109)
Quercetin	Increases AMP	Complex V of ETC	(110)
Resveratrol	Increases AMP	Complex V of ETC	(111)
Rosiglitazone	Increases AMP	Complex I of ETC	(112)
Salicylate		AMPKβ subunit	(113)
A769662		AMPKβ subunit	(114)
Troglitazone	Increases AMP	Complex I of ETC	(115)
α-Lipoic acid	Increases AMP		(116)
Magnolol	Translocates LKB1 to the cytoplasm	Targets LKB1	(102)

Table 2: List of AMPK activators and their mechanism of action in various cellular functions

Role of AMPK in metabolic transformation in various cancers

AMPK is a stress response kinase that can function as either friend or foe in a context-dependent manner. In response to metabolic stress, AMPK activation increases energy-producing pathways while decreasing energy-consuming pathways, thus establishing energy homeostasis (117). In order to maintain energy production under glucose deprivation, AMPK promotes mitochondrial biogenesis through the AMPK-p38-PGC-1α axis. Interestingly, it functions as a tumor promoter in response to various stresses, such as hypoxia or glucose deprivation, and allows cancer cells to adapt metabolically to ensure growth and survival. Data from both *in vitro* and *in vivo* studies have shown a significant connection between AMPK activation and cancer progression. The LKB1-AMPK signaling pathway, for example, has been shown to regulate glucose starvation-induced oxidative stress in cancers, inducing matrix metalloproteinase-9 (MMP-9) expression, which, apart from its roles in tumor invasion and metastasis, also aids in angiogenesis (118). AMPK also helps tumor cells to deal with an energy crisis and hence promote tumorigenesis by modulating nucleotide synthesis by phosphorylation-dependent conversion of phosphoribosyl pyrophosphate synthetase (PRPS) 1/2 hexamer to monomer, a protein that catalyzes the first reaction in nucleotide synthesis (119). AMPK has also been shown to be a potential therapeutic target for pre-B acute lymphoblastic leukemia and glioblastoma (120, 121). In glioblastoma cells, it was found that under glucose deprivation, AMPK aids in the transport of AMPK-mediated acetyl-CoA synthetase 2 (ACSS2) into the nucleus, where it leads to H3 acetylation and promotion of autophagy and tumorigenesis (122). Furthermore, AMPK overexpression or activation in various cancers has been reported. The accumulating body of data supports AMPK's carcinogenic actions in different cancers, and as a result, AMPK is considered a possible therapeutic target in cancer (123). Here, we discuss AMPK activation and its possible role in the progression of various cancers.

Lung cancer:

Lung cancer is the most diagnosed type of cancer (11.4 percent of all cases) and the leading cause of cancer mortality worldwide (18% of all cancer deaths) (GLOBOCAN, 2020) (10). The severity of lung cancer is determined by its aggressiveness and the milieu around the tumor. AMPK promotes mitochondrial biogenesis during glucose deprivation in lung cancer cells through the AMPK-p38-PGC-1 axis (58). The pathway involving AMPK and pyruvate kinase M (PKM1) is shown to be essential for cell survival under hypoglycemia conditions. Depletion of PKM1 increases cell death even in the presence of AMPK, suggesting that the AMPK-PKM1 axis is required for cell survival (124). Under glucose-limited conditions, AMPK was also known to regulate the expression of phosphofructokinase (PFK), another glycolytic enzyme (59). It is essential for maintaining NAPDH levels during glucose deprivation and matrix detachment growth, as well as anchorage-independent growth by inhibiting fatty acid synthesis and increasing fatty acid oxidation (125). While LKB1-AMPK signaling maintains energy and oxidative stress homeostasis, it also has the potential to promote cancer progression and metastasis under metabolic stress conditions through MMP-9 induction (118). As a serine/threonine kinase, AMPK also contributes to cell survival by phosphorylating certain proteins involved in glycolysis and glycogen synthesis. For example, AMPK promotes the expression of phosphoglucomutase 1 (PGM1), a glycogen metabolizing enzyme, via phosphorylating histone deacetylase 8 (HDAC8) in lung cancer cells subjected to glucose stress (126). These findings indicate that AMPK acts as a tumor promoter in lung cancer under metabolic stress.

Breast Cancer (BC):

BC is the most severe type of cancer in women and is heterogeneous due to expression of various types of receptors. Due to this variability, more sophisticated strategies were present in cancer cells to overcome the nutritional stress. Typically, tumor cells exploit metabolic

transformation by operating the Warburg effect, a process in which cancer cells prefer glucose over oxygen, as previously explained. Breast cancer cells have enhanced glycolysis, thus targeting glycolysis with 2-DG has a favorable impact, but AMPK, a conditional oncogene that rescues cancer cells through the CREB/PGC-1/ERR pathway, has a different effect. As a result, the combination of glycolysis and AMPK inhibitors has a synergistic impact on killing breast cancer cells (127). Cancer cells require more glucose under normal and metabolic stress conditions due to their higher glycolytic rate. Consequently, cancer cells rewire their pathways, resulting in increased expression of glucose transporters such as GLUT1 and GLUT4 and glutamine transporters such as SLC1A5 (128). Cancer cells also respond to stress by increasing the activity of carnitine palmitoyltransferase 1C (CPT1C), an enzyme required for fatty acid (FA) oxidation and ATP generation (129). Aside from metabolic roles, AMPK is important in post-translational modifications like phosphorylation and ubiquitination. When cells are subjected to glucose stress, checkpoint kinase 1 (CHK1) is ubiquitinated following phosphorylation by AMPK as part of an adaptative process to ensure cell survival (130). Alternatively, AMPK activates AKT in response to metabolic stress by phosphorylating S-phase kinase-associated protein 2 (SKP2) at S256, activating its ubiquitination activity and subsequently degrading AKT (131). Apart from metabolic stress, cancer cells often experience anoikis, an apoptotic process that occurs when cells spread and migrate to different body parts. Cancer cells adopt specific pathways, such as AMPK upregulation or activation by upstream kinases. AMPK promotes anchorage-independent growth or anoikis resistance in breast cancer cells by phosphorylating a novel substrate, PEA15 at S116 (132). Besides from its role in cell survival and proliferation, AMPK is also implicated in breast cancer cell invasion and migration. When AMPK is activated, the expression and nuclear localization of TWIST, a transcription factor involved in EMT, is enhanced. As a result, the EMT and metastasis activity of breast cancer cells is increased (133). These lines of data suggest that when breast cancer tumors are under metabolic stress, AMPK functions as a tumor promoter.

Prostate Cancer:

According to research conducted by H.U. Park et al., AMPK was shown to be active in 40% of prostate cancer tissues. The role of AMPK in cell survival under energy-depleted circumstances was found in the same research utilizing AMPK inhibition (Compound C) or AMPK depletion (using gene-specific siRNAs). This resulted in the cells being more susceptible to apoptosis in energy-depleted conditions, indicating that it functions in cell survival (134). Glucose deprivation enhances AMPK mediated androgen synthesis in PCa cells. Because of an increase in GLUT1 expression, which is followed by an increase in glutathione levels, androgen-sensitive PCa cells become even more resistant to glucose depletion-induced cell death (135). When cells are starved for glucose, they rearrange their metabolic pathways and adopt specific additional survival strategies. PTEN-deficient prostate cancer cells, for example, activate the AMPK pathway to grow in low-nutrient conditions by scavenging necrotic debris and extracellular protein through macropinocytosis (136). Based on the evidence presented above, AMPK seems to function as a tumor promoter in prostate cancers when the tumor is exposed to metabolic stress.

Hepatocellular carcinoma (HCC):

HCC is the fifth most common kind of cancer, with a high recurrence rate and a poor prognosis. The disease's development is influenced by many mechanisms, including the AMPK pathway. It has been shown that the Hepatitis B virus (HBV) X protein (HBx) activates AMPK and ACC phosphorylation through a calcium-dependent CaMKK1 pathway, which is needed for the activation of fatty acid oxidation in HCC and is known to enhance cell survival under metabolic stress (137). AMPK phosphorylates one of the components of the mTORC2 complex, causing the mTORC2-AKT axis to be activated and, as a result, increasing the survival of liver cancer cells under metabolic stress (138). Interestingly, it has been shown that when glucose is restricted in HCC, AMPK arrests cells in the G0/G1 phase, eventually leading to apoptosis.

PKC initially favors this but subsequently inhibits AMPK activation, resulting in the alleviation of apoptosis (139).

Renal Carcinoma

Metformin, formerly used to treat Type 2 diabetes, has anti-cancer properties, but its function in cell proliferation is controversial. Recently, it was reported that metformin-mediated AMPK activation increases renal cancer cell proliferation during glucose deprivation through its interaction with pyruvate kinase M2 (PKM2), suggesting that metformin-mediated AMPK activation has pro-tumor activity (140). In another research, AMPK is activated in response to increased calcium levels in cells owing to increased autophagy, which destroys the p53 and eventually increases clear cell renal carcinoma proliferation (ccRCC) (141). Another study found that down-regulation of HSP60 impairs the function of the respiratory complex I, resulting in excessive ROS production and AMPK activation, which increases the Warburg effect in ccRCC cells and promotes cell proliferation and metastasis (142).

Various other cancers:

Elevated levels of AMPK α alpha were also observed in colorectal cancer patients who had poor prognoses (143). Activating the AMPK/mTOR pathway by NMIIA (non-muscle myosin IIA) or enolase (ENO1) was reported in colorectal cancer (144, 145). In gastric cancer, MACC1-AS1 is reported to activate the AMPK/Lin28 pathway to confer cell survival in response to metabolic stress (146). AMPK also supports the survival of MYC-positive melanoma cells, but it does so via suppressing oxidative stress (147). In human medulloblastoma and glioblastoma multiforme, AMPK increases cell survival in response to acute stress by activating eukaryotic elongation factor 2 kinase (eEF2K), limiting translation elongation and eEF2K expression, which correlates with increased overall survival (148). The LSR/LKB1/AMPK pathway also plays an essential role in ovarian cancer cell survival and tumor formation (149). According to these lines of evidence, AMPK activation or expression

is increased in a variety of cancers, and its expression regulates cancer growth in both normal and metabolic stress conditions.

Targeting of AMPK in cancers

Because AMPK is essential for cell survival under metabolic stress, combining anti-metabolic drugs with AMPK inhibitors or genetically depleting AMPK is often considered an effective therapy. Despite compound C(CC)/Dorshomorphin is known to inhibit AMPK effectively, it can also inhibit other kinases. For example, CC can also inhibits bone morphogenetic protein (BMP) receptor type I (150) and activin-like kinase receptors 2, 3, and 6 (ALK2, ALK3, and ALK6) (151). It urges the need to discover new therapeutic agents that selectively target AMPK. In addition to small molecule inhibitors, AMPK can be targeted by siRNA, shRNA, or gRNAs, which selectively deplete AMPK. According to recent research, gRNAs (guide RNAs) may be utilized to target AMPK activation and cancer. Saito et al., reported that a combination of AMPK depletion utilizing gene-specific gRNA and metabolic stress inhibitors substantially suppresses AML growth by inducing oxidative stress and DNA damage (152). Several studies have shown that AMPK acts as an oncogene context-dependent and can be targeted using small molecular inhibitors. Osimertinib is a potential treatment for colorectal cancer (CRC); however, it has several side effects. It stimulates the LKB1-AMPK pathway, which is responsible for drug resistance in CRC. As a result, treating CRC with Osimertinib in combination with LKB1-AMPK inhibitors has the potential therapeutic effect (153). By phosphorylating a variety of substrates, including PFK and PFKFB3, AMPK promotes glycolysis. Because PFKFB3 is an allosteric glycolysis activator that is phosphorylated by AMPK, a combination of AMPK inhibitors and glycolysis inhibitors may be beneficial in treating cancers (154). Autophagy is also necessary for tumor cell survival in the face of metabolic stress. As a consequence, targeting autophagy is another approach in cancer treatment, although chemoresistance is a significant obstacle once again. Chemotherapy

resistance is the most frequent obstacle in cancer treatment. AMPK and several other pathways are known to mediate chemoresistance. Increased glycolysis, seen in several cancers, requires AMPK activation. Telmisartan, a novel AMPK phosphorylation inhibitor, suppresses autophagy flux, ultimately generates ROS, and stimulates TRAIL expression in lung cancer (155). All these lines of evidence suggest that targeting AMPK using a single agent or in a combination of drugs that induces resistance through an AMPK mediated pathway has a potential benefit in cancer treatment.

2.2. Hematopoietic PBX interacting protein (HPIP)

Pre-B-cell leukemia homeobox interacting protein 1 (PBXIP1), also known as hematopoietic PBX interacting protein (HPIP), is a transcriptional repressor that interacts with PBX1 (156). The HPIP gene is located on chromosome 1 (q21.3) and encodes a protein that consists of 731 amino acids with no homology to other proteins (Figure 9). HPIP has an estimated molecular weight of 80 kDa, although it appears on SDS-PAGE to be about 100 kDa, perhaps due to post-translational modifications. HPIP interacts with members of the PBX family, such as PBX2 and PBX3, to prevent PBX-HOX complexes from binding to DNA, thus suppressing E2A-PBX transcription (156). HPIP is mainly found in the cytoplasm, although it has been detected in the nucleus. HPIP contains a functional nuclear export signal and two nuclear localization signals that direct HPIP to the nucleus and impede PBX1 driven transcription (Figure 8) (157). HPIP and PBX1 are more highly articulated in early progenitor cells than in matured cells (156), indicating a function for HPIP in early hematopoiesis. According to a recent study, HPIP controls erythroid differentiation and progenitor cell proliferation via regulating PI3K/AKT/GSK3β signaling (158). The erythroid family-explicit transcription factor *GATA1* binds to the HPIP promoter in K562, a leukemia cell line, and drives its transcription (158). In germ cells, HPIP also exhibits repressive function as it impedes the functional interaction of ERβ with TEX11 (159). In breast cancer cells, it interacts with microtubules and suppresses

ERα transcription functions (160). According to new findings, HPIP is a novel p53 protein transcriptional target that is phosphorylated by TBK1 and degraded by MDM2 in breast cancer cells (161). In breast cancer cells, HPIP has been shown to form a signaling complex with microtubules, estrogen receptor alpha (ERα), p85 subunit of PI3K, and Src kinase, leading to AKT activation and ERK1/2 pathways in response to estrogen (160). The activated AKT and ERK1/2 also affected ER phosphorylation and estrogen-receptor gene expression (162). Furthermore, adenocarcinomas in mice were promoted by increased HPIP expression in breast cancer cells, demonstrating the oncogenic nature of HPIP (160). Accumulating data suggests that HPIP regulates cellular processes such as cell migration, invasion, EMT, proliferation, differentiation, and cell survival by regulating several signaling pathways (Figure 9) (158, 160, 163-173).

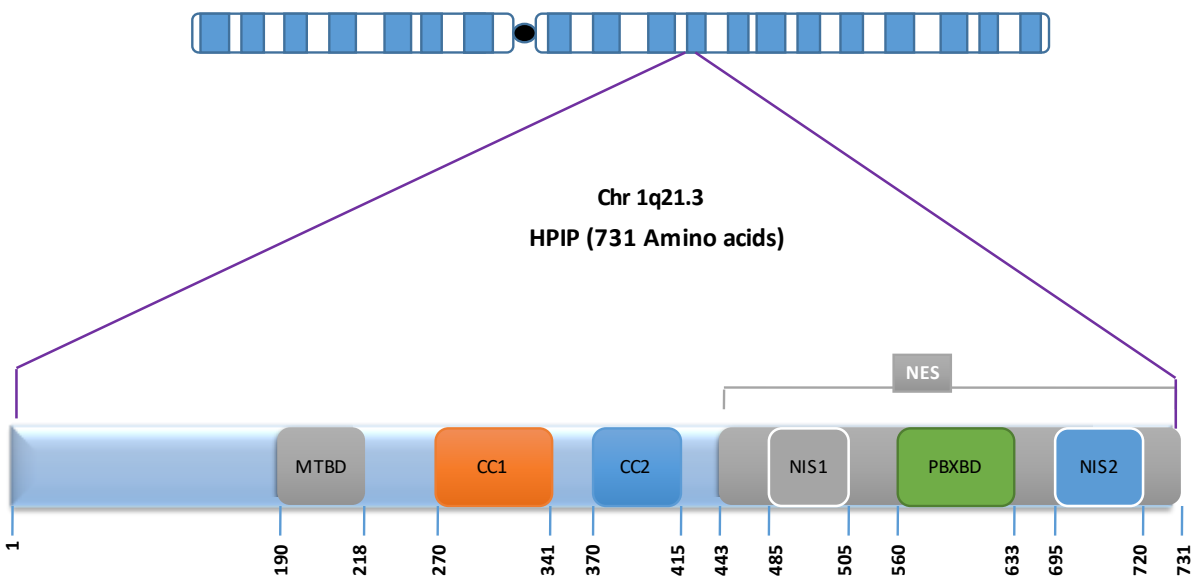

Figure 8: Chromosomal localization and physical map of HPIP. The distinct domains of HPIP (MTBD, CC1, CC2, NIS, NES, and PBXBD) are shown. MTBD- Microtubule binding domain; CC1&2, Coiled-coil domains 1&2; NIS, nuclear import signal; NES-nuclear export signal, PBXBD-PBX binding domain.

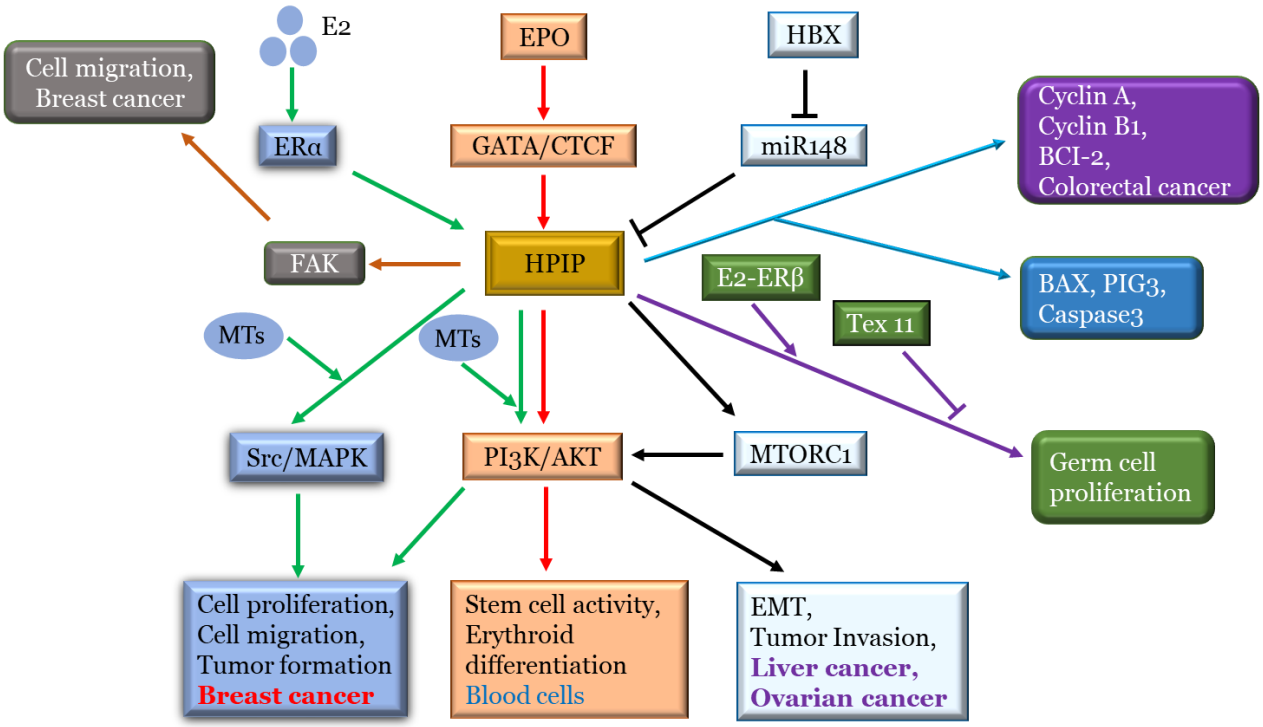

Figure 9: **HPIP signaling in various physiological processes:** HPIP networks with numerous signaling proteins, including microtubules, ERα, ERβ, TEX11, and controls diverse biological functions.

HPIP overexpression has been reported in many cancers, including breast cancer (BC), hepatocellular carcinoma (HCC), colorectal cancer (CRC), astrocytoma, spinal glioblastoma, thyroid carcinoma, leiomyosarcomas, gastric, non-small cell lung cancer (NSCLC), oral, cervical, liver, endometrial cancer, pancreatic cancer and ovarian cancers (160, 164, 166, 168, 170, 172-180). Based on these processes linked with HPIP-mediated cellular activities and its role in tumor development, HPIP is considered as a potential therapeutic target for cancer treatment.

HPIP signaling in various cellular functions and cancers:

Src/MAPK and PI3K/AKT pathways:

HPIP was identified as an ERα-interacting protein that activates growth-regulating kinases such as MAPK and AKT, resulting in the development of BC (160, 162). Inhibiting MDM2

causes p53-dependent activation of HPIP signaling through the AKT pathway, which increases BC progression (161). TGF1β regulates EMT induction through HPIP expression. Thereby, HPIP promotes EMT in ovarian cancer cells by activating PI3K/AKT pathway, which results in increased migration and invasion (171). HPIP has been reported to show an intriguing character in this malignancy, namely that it induces EMT and cell proliferation through PI3K/AKT pathway activation and GSK3β pathway inhibition (169). Reduced miR-148a expression in hepatoma cells increases HPIP expression, resulting in AKT and ERK activation, and subsequent mTOR activation through the AKT/ERK/FOXO4/ATF5 pathway leads to hepatocellular carcinoma (HCC) progression (163). CSR1 levels are substantially reduced in HCC patients, resulting in increased expression of HPIP and activation of the PI3K/AKT pathway, which promotes HCC development (181). HPIP regulates CRC cell proliferation, migration, and EMT through the MAPK/ERK1/2 and PI3K/AKT pathways (170). HPIP increases HNSCC cell proliferation, migration, and invasion via activating the PI3K/AKT signaling pathway (177).

FAK pathway activation:

HPIP interacts with FAK to regulate focal adhesion dynamics in IDC of the breast leads to enhanced cell migration. The same study reported that HPIP activates Calpain 2 through the MAPK pathway, subsequent Talin proteolysis, a regulatory step in focal disassembly and cellular migration (182).

HPIP functions in other diseases

Osteoarthritis (OA) is the most prevalent age-related and post-traumatic degenerative joint disease in the world. HPIP expression was substantially increased in OA cartilage. It promotes the growth of chondrocyte cells. In mice, a lack of HPIP reduced the formation of articular cartilage and protected against the development of OA. An intra-articular injection of an adeno-

associated virus (AAV) containing HPIP-shRNA reduced OA articular cartilage dilapidation after damage. HPIP interacts with LEF1 to drive the transcription of Wnt signaling genes. Because HPIP has been shown to enhance LEF1 transcriptional activity and acetylate H3K56ac in the context of Wnt signaling targeting gene promoters, it is thought that HPIP may be a viable therapeutic target for patients with osteoarthritis (183).

HPIP and cell cycle regulation:

The functions of HPIP in cancer cell proliferation and cell cycle regulation also has been identified. As a microtubule-binding protein, it interacts with numerous cell cycle regulatory proteins, including cyclins and cyclin-dependent kinases (CDK), to control cell cycle progression at various stages, including the G1/S and G2/M transitions. HPIP is upregulated in liver cancer and promotes HCC proliferation by triggering the G2/M transition, according to a recent study (174). The same group discovered that HPIP is required for the anchorage-independent growth of HCC cells. They identified that the 531-631 amino acid region of HPIP is essential for activating G2/M transition and inhibition of GADD45, a negative regulator of G2/M transition (174). In colorectal cancer cells, HPIP activates the G1/S and G2/M transitions, leading to increased levels of Cyclin A, Cyclin D1, and Cyclin B1, which ultimately leads to an increase in cell proliferation, invasion, and apoptosis (170). The same group discovered that HPIP stimulates the MAPK/ERK1/2 and PI3K/AKT pathways, essential drivers of cell growth (170). Another research led by Manavathi group revealed HPIP as the primary regulatory component of APC/C-CDC20 mediated cell cycle regulation. HPIP promotes the G2/M transition of the cell cycle by transiently stabilizing cyclin B1 and inhibiting APC/C-CDC20-mediated degradation, enabling early mitotic entry. HPIP depletion caused chromosomal abnormalities as well as defects in cytokinesis in HeLa cells (184). Together, these findings imply that HPIP is a critical regulator of cell cycle progression.

HPIP and EMT

The epithelial-mesenchymal transition (EMT) is essential for many processes such as metastasis, wound healing, and embryogenesis. Various interactions between cells and ECM occur during EMT, resulting in the separation of epithelial cells from one another and from the basement membrane and subsequent activation of a new transcriptional cascade to promote the mesenchymal fate (185). Metastasis is one of the most common causes of cancer-related mortality, and EMT has been shown to induce carcinogenesis as well as metastatic features. EMT was recognized as a critical marker of metastasis and carcinogenesis due to these characteristics (186). When HPIP was depleted using gene-specific siRNAs, TGF-1β mediated EMT was decreased in lung cancer cells, whereas HPIP overexpression promotes cell migration and invasion through enhancing TGF-1β mediated EMT. HPIP regulates Smad2 activity mechanistically via controlling TGF1β-mediated Smad2 phosphorylation; hence, HPIP may be a potential target in EMT-mediated lung cancer progression (171, 173). Highly metastatic ovarian cancer showed that HPIP regulates EMT through the PI3K/AKT/GSK-3 axis (169). In another study, HPIP knockdown reduces EMT in spinal glioblastoma, which resulted in decreased metastasis and invasion. This showed HPIP's possible involvement in glioblastoma EMT promotion (167). HPIP knockdown reduced cell proliferation, migration, and EMT in thyroid cancer by impeding the PI3K/AKT pathway, while HPIP overexpression promotes EMT through the PI3K/AKT pathway activation (172). HPIP was shown to be necessary for regulating colorectal cancer proliferation, metastasis, and EMT via activating PI3K/AKT and MAPK/ERK1/2 pathways (170). In a recent study, researchers identified a small molecular inhibitor that suppresses the actions of HPIP by targeting its downstream targets, which include many critical kinases involved in cancer growth and progression. They discovered that TXX-1-10 can regulate HPIP mediated functions and the genes involved in DNA replication, cell cycle, apoptosis, cell adhesion, cell migration, and invasion. It also

controls the expression of genes involved in cell proliferation and extracellular matrix organization (165). This study concludes that TXX-1-10 is a new and potential candidate drug for cancer treatment by limiting the HPIP mediated EMT.

2.3. Ring Finger Protein 2 (RNF2) and its cellular functions

Ring finger protein-2 (RNF2, DING, RING1B, or RING2) is an E3 ubiquitin ligase that monoubiquitinates histone H2A at lysine 119 (H2AK119ub) (187-189). The RNF2 gene is located on the chromosome at 1q25.3, and the coding region is made up of nine exons that encode a total of 336 amino acid-containing protein (190, 191). RNF2 is present in polycomb group (PcG) complex protein that serves as an epigenetic regulator and may trigger several physiological processes. Numerous studies have demonstrated that RNF2 overexpression contributes to the pathological development of different cancers and influences their clinical features. Increased RNF2 expression, for example, has been linked to the development and progression of HCC, melanoma, BC, pancreatic, prostate, bladder, gastric, and urothelial carcinoma (190, 192-195). RNF2 expression is also linked to radioresistance and chemoresistance in some malignancies, including lung and ovarian cancer.

Chapter II

3. Background

There is an enormous need for metabolic energy in rapidly proliferating cells, such as cancer cells, to produce different biomolecules. Cancer cells often rewire metabolic pathways to meet their specific requirements in order to do this (13, 20, 196). Cancer cells depend on glycolysis to generate energy since glucose is the primary energy and carbon source for rapidly proliferating cells; nevertheless, under glucose stress, glutamine is used as an anaplerotic substance for ATP synthesis and to maintain redox homeostasis, ensuring cell survival (13, 30, 197). Cancer cells use specific pathways or other mechanisms to ensure their survival under metabolic stress. They may enhance anaplerosis, the Warburg effect, the use of ketone bodies or non-glucose sources such as glutamine, lactate, and the rewiring of metabolic pathways. Specific tumor types activate certain kinases like AMPK for their survival, restricting energy-consuming pathways like fatty acid synthesis and enhancing energy-generating pathways, including fatty acid oxidation (β-oxidation). In some other cancers, mitochondrial biogenesis generates energy, enhancing cell survival, where metastasis and autophagy are other adaptive mechanisms in escaping the cancer cells from immune attack (198). Typically, reduced expression of tumor suppressor genes and increased oncogenic gene expression is observed in cancer cells during metabolic stress as a part of cellular adaptation (198). For example, oncogenes, such as protein kinase B (AKT), MYC, and RAS, are overexpressed under metabolic stress to support cancer cell survival (199).

The balance of energy generation and consumption must determine cell survival and tumor development under metabolic stress (200). As a result, tumor cells develop adaptations for survival under such conditions by inhibiting energy-consuming pathways and increasing energy-producing pathways (29). One example is the expression of AMP-activated protein kinase (AMPK), a metabolic sensor activated in cells in response to a low ATP: AMP ratio (134, 201). For example, AMPK-mediated pyruvate kinase M1 expression is essential for cell

survival under hypoglycemic conditions (124) and modulates the expression of phosphofructokinase, another glycolytic enzyme, under glucose stress (58). AMPK establishes energy homeostasis under glucose stress by promoting mitochondrial biogenesis and oxidative phosphorylation via the peroxisome proliferator-activated receptor-gamma coactivator 1-alpha (PGC-1α) pathway (58). AMPK also enhances the nicotinamide adenine dinucleotide phosphate (NADPH) pool by inhibiting the acetyl-CoA carboxylase 1 (ACC1) and ACC2 enzymes that utilize NADPH in fatty acid synthesis while promoting fatty acid oxidation, thus establishing metabolic homeostasis (125). Similarly, AMPK instigates cells to utilize non-glucose sources to provide energy under glucose-limiting conditions, thereby maintaining energy homeostasis and cell survival (58, 59). However, the molecular mechanisms underlying this process remain elusive.

Hematopoietic PBX1-interacting protein (HPIP) is a scaffolding protein that interacts with various signaling proteins, including the estrogen receptor (ER), phosphoinositide 3-kinase (PI3K), Src, and TANK binding kinase 1 (160-162). HPIP participates in various cellular functions, such as cell proliferation, differentiation, and migration (169-171, 173, 202) and, by acting as a G2/M enhancer, promotes cell proliferation (166, 184). In hematopoietic cells, HPIP promotes erythroid differentiation via the PI3K/AKT/GATA binding protein 1 (GATA1) pathway (158) and promotes cell motility by regulating focal adhesion turnover in breast cancer (BC) cells (182). Recent studies have also suggested its role in osteoarthritis (183). HPIP is a proto-oncogene that regulates the epithelial-mesenchymal transition, anchorage-independent growth, and cell invasion in various cancer cells (169-171, 173, 202). Furthermore, HPIP overexpression has been reported in several cancers, including BC. Dwivedi et al. have established that HPIP is required for mammary gland development. They discovered that HPIP expression is induced in lactation and pregnancy stages of mouse mammary gland development. Prolactin (PRL) is a lactogenic hormone that stimulates HPIP expression through

STAT5-mediated transcription. The PI3K/AKT pathway is activated by this induced HPIP, which enhances β-casein production and mammary gland development (203).

4. Rationale and Hypothesis

Despite both AMPK and HPIP being overexpressed in several cancers, including BC (117, 166), an anomaly exists between them with respect to their functions. Often AMPK acts as a contextual oncogene, while HPIP is predominantly a protooncogene that regulates cell cycle progression, cell migration, and differentiation. However, the role of HPIP in metabolic stress conditions is largely unknown. In this study, we explored the potential role of HPIP in metabolic stress using BC as a model system.

5. Objectives

1. To elucidate the role of HPIP in breast cancer (BC) cell survival under acute or chronic glucose stress

2. To analyze the expression levels of HPIP and AMPK in a subset of breast tumors

6. Materials and Methods

6.1. Cell culture

MCF7, ZR-75-1, T-47D, MDA-MB-231, MDA-MB-453, MDA-MB-468, BT-549, SKBR3, BT-474 and HEK 293T cells were purchased from National Center for Cell Science (NCCS), Pune, India. Cell lines were cultured in high-glucose DMEM (4.5 g/l glucose and 0.584 g/l glutamine, Invitrogen# 11965092) supplemented with 10% (v/v) FBS (Invitrogen), 100 U/mL penicillin and 100 µg/mL streptomycin (Thermo scientific, USA) at 37 °C with 5% humidified CO_2.

AN3CA, HEC-1-A, and Ishikawa cells were obtained from the American type of culture collection (ATCC), USA. After receiving the cells, AN3CA cells were maintained in minimal

essential medium (MEM) (Gibco, Waltham, Massachusetts, USA, Cat# 11095080), whereas HEC-1-A cells were maintained in McCoy's 5a medium (Gibco, Cat# 16600108). Ishikawa cells were maintained in Dulbecco's Modified Eagle Medium/Nutrient Mixture F-12 (DMEM: F12) (Gibco, Cat# 11320033). All the cell lines were adapted to grow in high glucose-containing DMEM (Gibco, Cat#11965092) with 10% Fetal Bovine Serum (FBS) (Gibco, Cat#10270106) and 1% Antibiotic-Antimycotic (Gibco, Cat#15240062) for our experimental purposes. Cell lines were maintained in 5% CO_2 in a humidified chamber.

6.2. Induction of metabolite stress

To induce various metabolite stress such as glucose, glutamine, pyruvate stress, cells were washed twice with PBS and then incubated in DMEM with a minimal amount of glucose (0.45 g/l glucose, Invitrogen) or glutamine (0.5 mM) or pyruvate (0.25 mM) or combined stress (0.45 g/l glucose, 0.5 mM glutamine, 0.25 mM pyruvate) supplemented with 10% dialyzed FBS (Invitrogen) with 100 U/mL penicillin and 100 μg/mL streptomycin (Thermo scientific, USA) at 37 °C with 5% humidified CO_2.

6.3. Plasmid constructs and transfection

Plasmids encoding HPIP were used from our previous study (158, 160). For the ectopic expression of FOXO3a, we used FLAG-FOXO3a, which was a gift from Michael Greenberg (Addgene plasmid #8360; http://n2t.net/addgene:8360; RRID: Addgene_8360) (204). RNF2 and MYC coding sequences were subcloned into pEGFP-C1 vector, and the primers used to subclone these constructs were listed in Table 3. Scrambled control shRNA (pGIPz vector) (short hairpin RNA), FOXO3a gene-specific shRNAs (pGIPz-shFOXO3a#5 and 18), HPIP gene-specific shRNAs (pGIPz-HPIP#17, 21, and 22), scrambled siRNA, and HPIP gene-specific siRNAs were purchased from Dharmacon-GE Healthcare (Lafayette, Colorado, USA). RNF2 and MYC gene-specific shRNAs were purchased from shRNA resource center, Indian

Institute of Science, India. According to the manufacturer's protocols, plasmids and shRNAs were transfected in mammalian cells using Lipofectamine 2000 (Invitrogen, USA) either in 60- or 100-mm cell culture dishes.

6.4. Generation of stable clones

SKBR3 or MCF7 cells stably expressing either shCtrl or shHPIP#22 or shFOXO3a#5 were generated by transfecting either pGIPz-shCtrl or pGIPz-shHPIP#22 or pGIPz-shFOXO3a#5 plasmids, respectively, using Lipofectamine 2000 (Invitrogen, USA) according to manufacturer instructions and described in our previous reports (158). FLAG-HPIP or T7-HPIP were described previously (169) and were transfected into shFOXO3a cells for HPIP ectopic expression.

Stable knockdown of RNF2 and MYC was done using pLKO-shRNF2, and pLKO-shMYC was achieved by lentiviral transduction of SKBR3 or MCF7 cells lentivirus produced in HEK 293T as described previously (158) followed by selection with puromycin (500-2000 ng/mL).

6.5. Ethical approval for patient sample collection and animal study

Fresh BC and its adjacent tissues were collected from patients, with informed consent, recruited from the Mehdi Nawaj Jung (MNJ) Institute of Oncology & Regional Cancer Center, Hyderabad, India, for immunoblotting and quantitative reverse transcription-polymerase chain reaction (qRT-PCR) analysis after acquiring ethics board approval from the MNJ Institute of Oncology & Regional Cancer Centre and the University of Hyderabad, Hyderabad, India (IEC No- UH/IEC/2016/190). BC and adjacent tissue blocks were also collected for immunohistochemistry (IHC).

NCr Nude mice (CrTac:NCr-Foxn1^{nu}) were purchased from Vivo BioTech Ltd., Hyderabad. All the animal experiments performed in this study are with the approval of the Institutional Animal Ethics Committee (IAEC), University of Hyderabad (UoH) (IAEC No-

UH/IAEC/BM/2017-II/P3). Animals were maintained at Easy Flow AHU equipment (Techiniplast, Italy), and experiments were executed by following IAEC guidelines at the University of Hyderabad (UoH).

6.6. Quantitative real time-polymerase chain reaction (qRT-PCR)

Cells were treated as indicated, and then total RNA was isolated using TRIzol reagent (Invitrogen, USA, Cat#15596026) following manufacture instructions. Based on manufacturer protocols, approximately 1-2 µg of total RNA was converted into cDNA using iScript cDNA synthesis kit (Bio-Rad, CA, USA, cat#1708890). Initially, all the primers were standardized for the amplification of the desired gene by using *Taq* master mix (Emerald master mix, Takara, Japan, cat#RR320A), and then qRT-PCR was performed by using the cDNA, which was diluted to 1:3 as a template and SYBR green master mix (TB Green Premix Ex Taq II (Tli RNase H Plus), Takara, Japan, cat#RR820B) and with primers listed in Table 3 and further analysis were done using GraphPad Prism.

	RT PCR primers (polarity 5'-3')
HPIP-FP	ATGGGTCTTCTGCTGGACAA
HPIP-RP	CAGGCTCTGAAGCTCTTCCTT
β-actin FP	AGCCATGTACGTAGCCATCC
β-actin RP	CTCTCAGCTGTGGTGGTGAA
FOXO3a-FP	GACAGAGAAGGTACAAGGG
FOXO3a-RP	GACTTTACCCTGGTCTCAG
RNF2-FP	TGATCACTTATCCAAGTATC
RNF2-RP	AAAGGCTCATTTGTGCTC
SLC1A5-FP	AAGGGCCCCACGTCCCACC
SLC1A5-RP	CCCAGGACCAGACGTTCCT
cMYC-FP	TTCTCTCCGTCCTCGGATTCTC
cMYC-RP	GAAGGTGATCCAGACTCTGACCT
GDH-FP	GGTCATCGAAGGCTACCG
GDH-RP	GCCCTTTTTTGCTAGCTCCAT
GOT1-FP	AGCTGTGCTTCTCGTCTTGC
GOT1-RP	CTGCATCCCAGTAGCGATA
GLS-FP	GTGGTGATCAAAGGGTAAAG
GLS-RP	GCTTCCAGCAAAAATTTAACA

	ChIP primers (polarity 5'-3')
FRE1-FP	GACACTTAGGGCTGAAGGAGGCCA
FRE1-RP	TCCAGTCCAGCCCCCTGACATTTG
FRE2-FP	CCCAGCCTCACTTCCCTTTTCC
FRE2-RP	GCTATGGTCCTGCACCCGGTT
FRE3-FP	CTGGCTTGGGAGAAGAGGTGT
FRE3-RP	AGCTTGGGCTGAAGTCCCTGT
FNS-FP (non-specific region)	GGAATAAGGAAAAGGGAAGGCG
FNS-RP (non-specific region)	AAAAAACAGCTAAAGGGGGAGC
cMRE-GLS-FP	CTAAGTACTTTCCCATTGTCC
cMRE-GLS-RP	CCTTTGGCATGTTACAGCCTT
cMNS-GLS-FP (non-specific region)	AAACTCTGTGGATCTACTCC
cMNS-GLS-RP (non-specific region)	TGGAATACGGGTTCTCTAAG
cMRE-SLC1A5-FP	TGTTAACCTCCCAAACGGCCA
cMRE-SLC1A5-RP	GCCAACATGGTGAAACCCGTC
cMNS-SLC1A5-FP(non-specific region)	ATTATTAATCTGCCTTCTATGGG
cMNS-SLC1A5-RP(non-specific region)	CTGAGCCCGTTTAGCG
	Sub cloning primers (polarity 5'-3')
pEGFPC1-RNF2-FP	ATCGGCCTCGAGGCATGTCTCAGGCTGTGCAGACA
pEGFPC1-RNF2-RP	GCGCGCGGATCCTCATTTGTGCTCCTTTGTAGG
pEGFPC1-MYC-FP	ATGCCTCGAGGCCTGGATTTTTTTCGG
pEGFPC1-MYC-FP	GCATGGATCCTTACGCACAAGAGTTCC
	Site directed mutagenesis (polarity 5'-3')
pEGFPC1-RNF2(H69Y)-FP	GAGTGTTTATATCGTTTTTGTGCA
pEGFPC1-RNF2(H69Y)-RP	TGCACAAAAACGATATAAACACTC

Table 3: List of primers used in this study for qRT PCR and subcloning

6.7. Immunoblotting

SKBR3, MCF7, HEK293T, and other cells were treated as indicated in each experiment. After harvesting, cells were lysed in either in NP-40 buffer (50 mM Tris-HCl, pH 8.0, 150 mM NaCl, 1% NP-40 with protease and phosphatase inhibitors (Roche, USA)) or Radio Immune Precipitation Assay buffer (RIPA) (50 mM Tris-HCl, pH 8.0, 150 mM NaCl, 1% NP-40, 0.5% sodium deoxycholate, 0.1% sodium dodecyl sulfate with protease and phosphatase inhibitors)

and then subjected to 8-15% SDS-PAGE followed by western blotting analysis using the antibodies listed in Table 4.

6.8. 3-(4,5-dimethylthiazol-2-yl)-2,5-diphenyl tetrazolium bromide (MTT) Assay

Approximately 5×10^3 cells were seeded in 96 well plates after counting using a hemocytometer and then allowed to adhere overnight. The next day treatment was done as indicated and then allowed to grow for various time points. At each time point, 20 µl of 5 mg/ml concentrated MTT (ThermoScientific, cat#M6494) was added to each well and incubated for 3-4 hr at 37 ºC for the formation of formazan crystals, and then these crystals were dissolved in Dimethyl sulfoxide (DMSO) (Ameresco, cat#97061-250). After that, absorbance was measured at 570 nm with a reference filter 655 nm using ELISA plate reader (Synergy HTX multimode reader, Biotek-India).

Name of Antibody	Company Name	Catalog	WB dilutions	IHC dilutions	IP dilutions	ChIP dilutions
HPIP	Bethyl laboratories	A301-628A	1:2000	1:100	1:250	1:250
RNF2	Abcam	Ab101273	1:2000	1:500	1:250	
pFOXO3a (S413)	Cell signaling Technology (CST)	8174S	1:1000			
FOXO3a	CST	12829S	1:1000			
pAMPK (T172)	CST	2535S	1:1000			
AMPK	CST	5831S	1:1000			
pACC (S79)	CST	11818S	1:1000	1:800		
ACC	CST	3676S	1:1000			
GDH1	SCBT	SC-515542	1:500			
SLC1A5	Abcam	Ab187692	1:1000			
β-Tubulin	Sigma Aldrich	SAB4200715	1:2000			
β- Actin	Sigma Aldrich	A3854	1:25000			
GAPDH	CST	2118S	1:1000			
FLAG	CST	14793S	1:1000			
α-Tubulin	CST	3873S	1:2500			
PI3K(p85)	CST	4292S	1:1000			
pAKT(S473)	CST	4060T	1:1000			
AKT	CST	4691T	1:1000			
c-MYC	CST	18583S	1:1000		1:250	1:250
PBXIP1(HPIP)	Abcam	Ab176591	1:1000			
PARP	CST	9542T	1:1000			
Caspase-3	CST	14220T	1:1000			

GFP-Tag	Sigma Aldrich	G1544	1:4000			
T7-Tag	Merck Millipore	69522	1:5000		1:500	
HA-Tag	Sigma Aldrich	SAB4300603	1:500			
His tag	SCBT	SC-8036	1:500			
Lamin B1	SCBT	SC-374015	1:500			
Total Ubiquitin	Sigma Aldrich	U5379	1:100			
PBXIP1(HPIP)	Sigma Aldrich	HPA006949	1:2500	1:200		
Normal IgG-Mouse	SCBT	SC-20254			1:500	1:500
Normal IgG-Rabbit	SCBT	SC-2023			1:500	1:500
Rabbit IgG-HRP	SCBT	sc-2357	1:5000			
Mouse IgG-HRP	SCBT	sc-516102	1:5000			

Table 4: List of antibodies used in this study for immunoblotting, immunoprecipitation, and immunohistochemistry

6.9. Co-Immunoprecipitation (CO-IP) analysis

Co-Immunoprecipitation (Co-IP) was performed as described previously (182). For Co-IP, protein extracts from cells were prepared in NTEN buffer (100 mM NaCl, 20 mM Tris, pH 8.0, 1 mM EDTA, 0.5% Nonidet P-40 with 1X protease and phosphatase inhibitors). After estimating the total protein concentration from the cell lysates by using RC-DC reagents (Bio-Rad, USA, cat#5000121), approximately 1 mg of the protein was incubated with primary antibodies overnight at 4 ℃ followed by snaring the protein-antibody complexes with protein A/G PLUS-Agarose beads (Santa Cruz Biotechnology, USA, Cat#sc-2003) by incubation for 1 hr. After thorough washings, protein complexes were subjected to western blotting using respective antibodies listed in Table 4.

6.10. Chromatin immunoprecipitation assay (ChIP) and Double ChIP

We used biological software TFBIND (205) or PROMO-ALGGEN (206, 207) to predict binding sites of FOXO3a, HPIP, and MYC onto the promoter regions of *HPIP, SLC1A5,* and *GLS.* Generally, the Forkhead-containing proteins consist of the consensus motif

(TTGTTTAC), the most enriched motif (208). Chromatin immunoprecipitation analyses were performed based on our earlier protocols (158). Briefly, cells were subjected to isolation of total chromatin and further immunoprecipitated with respective antibodies, DNA was extracted, and then they were subjected to qRT-PCR analysis with indicated primers mentioned in Table 3. Double ChIP was performed based on earlier reports (209). Briefly, ChIP was performed initially with a single antibody and then eluted the protein-chromatin complexes, and to this, a second antibody was added and then eluted the protein-DNA complexes, digested the proteins using proteinase K and then purified, further used in the qRT-PCR analysis.

6.11. ATP measurement assay

Approximately 5×10^5 cells were plated in 6 well culture dishes and allowed to adhere overnight. The next day, the medium was replaced with glucose starvation medium (DMEM with 2mM glucose, 10% Dialyzed FBS). After another 12 hours, cells were lysed in lysis buffer (10 mM Tris-HCl, pH 7.5, 100 mM NaCl, 1mM EDTA, and 0.01% Triton X -100) centrifuged at 12000g for 15 min at 4 ºC. The lysates were used for ATP determination in each sample using an ATP determination kit (Invitrogen, USA, cat# A22066).

6.12. Colony formation assay

Stably transfected cells were incubated in glucose stress medium for 12 hr. Cells were then trypsinized and then counted using a hemocytometer, an equal number of SKBR3 cells ($0.5x10^3$) were seeded in 6 well plates. After 12 hr of seeding, cells were washed twice with phosphate-buffered saline and then incubated in complete medium and further grown for 14-21 days, stained with 0.5% crystal violet solution, and then colony counting was done using a bright field microscope at 4X magnification, and further analysis was done using GraphPad Prism.

6.13. Soft agar assay

Stably transfected cells were incubated in 2 mM glucose medium for 12 hr. Cells were then trypsinized and then counted using a hemocytometer, an equal number of SKBR3 cells ($10x10^3$) were seeded in 6 well plates with two-layered agarose. These cells were further grown for 14-21 days and stained with 0.05% crystal violet solution, and then colony counting was done using a bright field microscope, and further analysis was done using GraphPad Prism.

6.14. Metabolic flux analysis

An equal number of SKBR3 cells ($3x10^6$) were seeded into 10-cm dishes. After 12 hr of incubation at 37 °C, cells were transfected either with siCtrl or siHPIP (siGenome siRNA, Horizon, USA, Cat#M-015428-01-0010). Post transfection (48 hr), cells were washed twice with PBS and then further washed with glucose-free DMEM containing 10% dialyzed FBS, 4 mM glutamine, and penicillin-streptomycin. After overnight starvation (12 hr), 4 mM $^{13}C_5$-Glutamine (Cambridge Isotope Laboratories, catalog # CLM- 1822-H) containing medium was added, and cells were incubated for another 6 hr to measure the TCA metabolites. The dishes were then washed with PBS, followed by snap-frozen in liquid nitrogen. The frozen plates were then used for extraction of metabolites and LC-MS/MS analysis.

6.15. Isotope labeling by targeted mass spectrometry (MS)

Cells were scraped from snap-frozen dishes into a 0.5 ml mixture of water/methanol (1:1), sonicated for 1 min (two 30 sec pulses), and mixed with 450 µl ice-cold chloroform. The resulting homogenate was then mixed with 150 µl ice-cold water and vortexed again for 2 min. The homogenate was incubated at –20 °C for 30 min and centrifuged at 4 °C for 10 min to partition the aqueous and organic layers. The aqueous and organic layers were combined and dried at 37 °C for 45 min in an automatic environmental speed vaccume system (Thermo Fisher Scientific). The extract was reconstituted in a 500 µl solution of ice-cold methanol/water (1:1) and filtered through a 3 kDa molecular filter (Amicon Ultracel) at 4 °C for 120 min to remove

proteins. The filtrate was dried at 37 °C for 45 min in a speed vacuum and stored at –80 °C until MS/MS analysis. Before MS/MS analysis, the dried extract was resuspended in a 100 µl solution of methanol/water (1:1) containing 0.1% formic acid and then analyzed using multiple reaction monitoring (MRM). 10 µL of each sample was injected and analyzed using a 6495 QQQ triple quadrupole mass spectrometer (Agilent Technologies) coupled to a 1290 series HPLC system via selected reaction monitoring (SRM). Metabolites were targeted in negative ion modes: the electrospray source ionization (ESI) voltage was –3,500 V in negative ion mode. Approximately 9 to 12 data points were acquired per detected metabolite. To target the TCA flux, the samples were loaded to the mass spectrometer via normal-phase chromatography using a Luna amino column (3 µm, 100A 2× 150 mm). The mobile phase containing water (solvent A), with solvent A modified by the addition of 5 mM ammonium acetate (pH 9.9) and 100% acetonitrile (ACN) (solvent B). The binary pump flow rate was 0.2 ml/min with a gradient spanning 80% B to 2% A over 20 min followed by 2% solvent B to 80% solvent A for a 5 min period followed by 80% B for 13 min period. The flow rate was gradually increased during the separation from 0.2 mL/min (0–20 mins), 0.3 mL/min (20.1–25 min), 0.35 mL/min (25–30 min), 0.4 mL/min (30–37.99 min) and finally set at 0.2 mL/min (5 min).

6.16. Cycloheximide pulse-chase experiment

In 60 mm dishes, an equal number of stably knockdown SKBR3 cells (1×10^6) were seeded and allowed to adhere overnight. The following day, cells were treated with cycloheximide (30 µg/mL) in a glucose stress medium (2 mM glucose) for various time periods. Cells were trypsinized, centrifuged, and the cell pellet was washed with PBS at each time point. These cells were lysed using RIPA buffer for 20 min on a ROTOSPIN at 4 °C, followed by 10 min centrifugation at 13000 rpm. Total protein was determined using RC-DC reagents, and an equal quantity of protein was resolved on 10-15% SDS PAGE before immunoblotting with HPIP

RNF2 and β-actin. ImageJ software was used to quantify signal intensities (210), and protein half-life ($t_{1/2}$) was determined as described previously (184, 211, 212).

6.17. Immunohistochemistry (IHC)

Formalin-fixed, paraffin-embedded blocks of human BC and surrounding tissues procured from the MNJ Institute of Oncology and regional cancer center were cut into 4 µm-thick sections. Following deparaffinization and rehydration, sections were incubated for 20–40 minutes at 100 °C in 10 mM sodium citrate buffer (pH 6.0) or 10 mM Tris-ethylenediaminetetraacetic acid buffer (pH 9.0) for antigen retrieval. The mouse/rabbit polydetector DAB HRP brown kit (BioSB, BSB-023) was used to stain all sections, and hematoxylin was used to counterstain them. Sections were evaluated based on previous studies and examined for the proportion of stained cells (182) staining intensity was scored from 0 to 1 (lowest) to 3 (highest), with 0 indicating no immunoreactivity and 1-3 indicating HPIP, pACC (S79), or RNF2 immunoreactivity.

6.18. Fractionation assay

Fractionations were carried out in accordance with the procedures outlined in previous studies (213). In brief, cells were cultured in 2 mM glucose-containing medium for 12 hr before being trypsinized, centrifuged, and resuspended in Buffer A. These resuspended cells were homogenized and centrifuged to collect the cytoplasmic fractions (Cyt) in the supernatant. The pellet was washed and resuspended in Buffers S1 and S2 for the nucleus fractions (Nuc). The nuclear fractions were lysed in RIPA buffer. The total protein was determined, and immunoblotting was performed using the HPIP, MYC, Lamin B1, β-actin antibodies, and their details were described in Table 4.

6.19. AO-PI and AO-EtBr assay

The methods described in earlier reports were used for the acridine orange-propidium iodide (AO-PI) and acridine orange-ethidium bromide (AO-EtBr) staining assays (214). Cells were trypsinized and then treated with AO-PI for 5 minutes at room temperature. A cell counter was used to count the cells (Luna FL, cell counter, Logos Biosystems, South Korea). For the AO-EtBr assay, cells were seeded in 6 well plates, cultured in 2 mM glucose for various time intervals, then incubated with AO-EtBr for 15 minutes at room temperature, followed by imaging with a fluorescence microscope, and then red, and green fluorescent cells were counted and represented in bar graphs (early and late apoptotic cells). GraphPad Prism was used to generate the graph and for the analyses.

6.20. APC-Annexin V assay (FACS analysis)

The APC Annexin V assay was carried out exactly as reported earlier (184). In brief, cells were cultured in 2 mM glucose medium for various time periods before being harvested by trypsinizing and centrifugation. Cells were then treated for 15 minutes with APC Annexin V and 7-AAD before being examined by FACS using LSR Fortessa (BD biosciences, USA).

6.21. Ubiquitination assay

The ubiquitination assay was carried out precisely as described previously (184). Cells were cultured in 2 mM glucose for 12 hours (acute stress) or 48 hours (chronic stress). Cells were treated with MG132 (a proteasomal inhibitor, 30 μM) for 4 hours before harvesting at each time point. After that, cells were collected and lysed in NTEN buffer containing protease, phosphatase, and deubiquitinating enzyme inhibitors (N-Ethylmaleimide, 20 mM). Co-IP was performed using the HPIP antibody, followed by immunoblotting with the ubiquitin antibody and additional antibodies listed in Table 4.

6.22. In-vivo tumor growth

To induce tumor development in mouse xenografts, 4-5 week old female mice were injected subcutaneously with 1×10^6 SKBR3 cells (shCtrl or shHPIP) in 100 µL of sterile media with matrigel (1:1). Tumor volumes were assessed every three days after tumor development (10-15 days after injected cells). Animals were dissected, and tumor samples were collected after 30-35 days. They were immediately examined for GFP intensity (Stable cells have a pGIPz vector backbone, which produces GFP fluorescence) and weighed the tumors for tumor weight. To estimate the tumor volume (mm^3), we used the following formula: Tumor volume= (length x $width^2$)/2, where length represents the largest tumor diameter and width indicates the perpendicular tumor diameter. Tissues were separated for different histopathological investigations.

6.23. Breast cancer patients' data analysis and sources

For the survival of the patients, we studied the expression of HPIP/AMPK using cBioPortal (https://www.cbioportal.org/), a cancer genomics data set. In cBioPortal, high or low mRNA expression of a gene is determined by standard deviations. The Kaplan Meier survival curve for co-gene expression was plotted using invasive breast carcinoma (TGCA, Cell 2015) as (high expression, HPIP: EXP>0.6, PRKAA1: EXP>0.6) vs. (low expression, HPIP: EXP<0.6, PRKAA1: EXP<0.6). This was also used to analyze the correlation between HPIP and AMPK with the survival of the patients (215, 216). Oncomine (www.oncomine.org) (The University of Michigan, MI, USA) database was used to analyze the expression of AMPK and HPIP in human breast cancers. We analyzed different data sets of Oncomine for the expression profile of these genes (217). Gene expression profiling interactive analysis (GEPIA) data set was used to analyze the correlative expression between HPIP and AMPK (218). We exported all the data from each data set and then analyzed it using GraphPad prism software.

6.24. Statistical analysis

Differences among the groups were analyzed using two-way analysis of variance (ANOVA), one-way ANOVA, or a *t*-test (paired or unpaired) depending on the number of groups analyzed, and multiple comparisons were performed using Sidak's multiple comparisons test. Differences were considered significant at $p < 0.05$.

7. Results

7.1. HPIP is a metabolic stress response gene

To examine the role of HPIP signaling in response to glucose deprivation, HPIP levels in SKBR3 cells, a $HER2^+$ BC cell line, cultured either in 2 mM glucose (GS), 0.5 mM glutamine (QS), 0.25 mM sodium pyruvate (SS), or combined stress (2 mM glucose, 0.5 mM glutamine, 0.25 mM sodium pyruvate, GQSS) for 12 hr were measured. A significant increase in HPIP transcript levels and protein was observed and accompanied by enhanced phosphorylation of AMPK and its substrate, ACC (Fig. 10A and B). Similar results were also observed in another BC cell line, MCF7, which was ER^+ (Fig. 10C). Next, a dose-dependent increase in HPIP was observed at both the transcript and protein levels upon treatment, with glucose concentrations ranging from 25 mM (high glucose) to 2 mM (low glucose) (Fig. 10D and E). Similar results were observed for MCF7 cells but not in MDA-MB231 cells (triple-negative breast cancer cell line) (Fig. 10F and 10G). Furthermore, a time-dependent induction of HPIP expression in SKBR3 cells showed progressively elevated expression from 0–12 hr and then declined by 24 hr, which correlated with AMPK activation (Fig. 10H). Together, these results indicated an inherent association between HPIP and glucose levels and that the AMPK pathway most likely controlled HPIP expression.

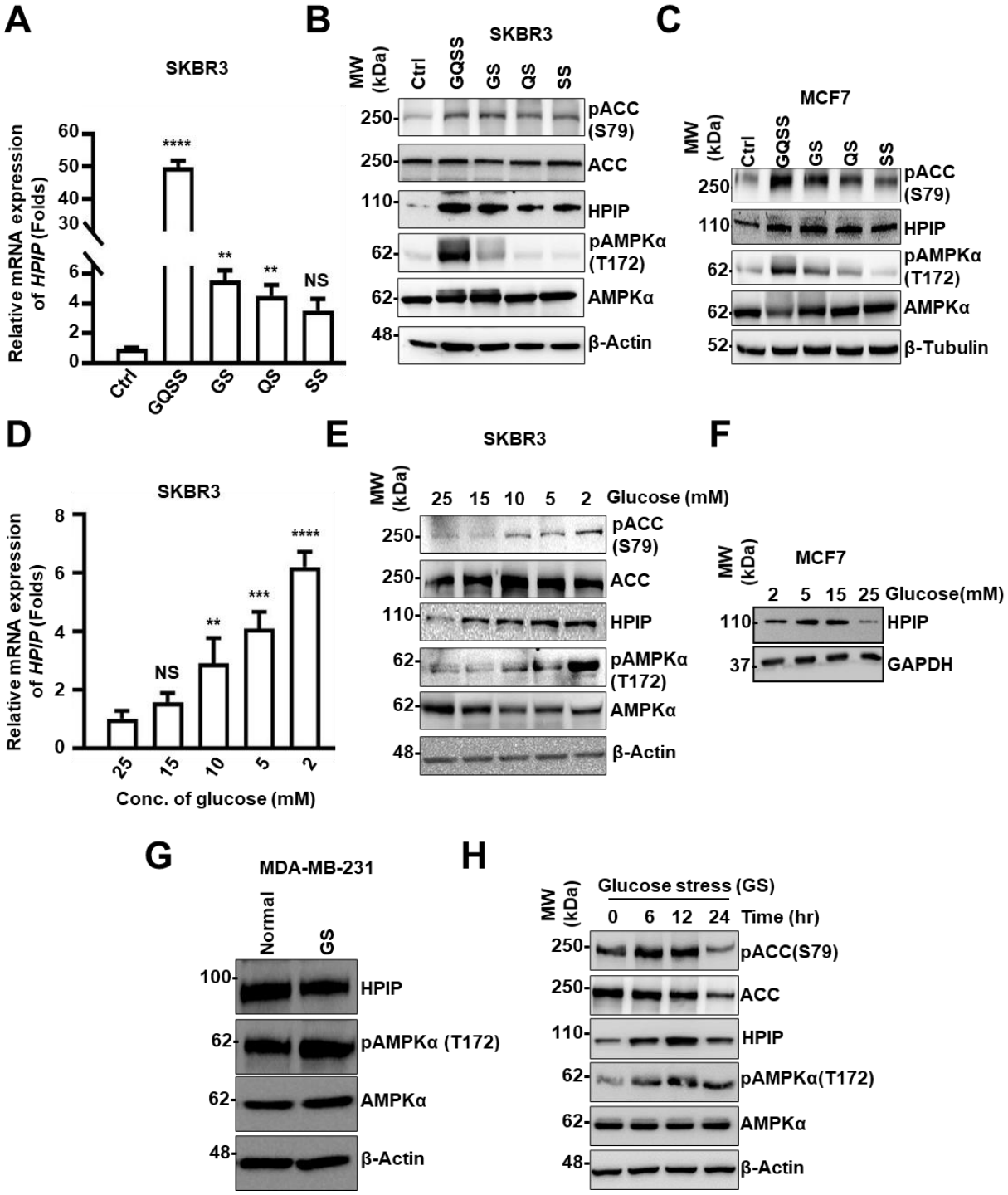

Figure 10: HPIP is a metabolic stress response gene

Quantitative real-time PCR analysis (qRT-PCR) for *HPIP* in SKBR3 cells **(A)**, Immunoblotting analysis for phospho-ACC (S79), ACC, phospho-AMPK (T172), AMPK, and HPIP in SKBR3 cells **(B)** cultured under glucose stress (GS), glutamine stress (QS), pyruvate stress (SS) or combined stress (GQSS) for 12 hr. β-Actin served as a loading control. **C)** MCF7 cells cultured under similar conditions as in B and immunoblotted as indicated. **D)** qRT-PCR analysis for *HPIP* in SKBR3 cells treated with varying concentrations of glucose (25 mM to 2 mM) for 12 hr. Immunoblotting analysis for the indicated proteins in SKBR3 cells (**E**) or MCF7 cells (**F**) treated with different concentrations of glucose (25 mM to 2 mM) for 12 hr. **G)** MDA-

MB-231 cells were cultured in normal, and glucose stress medium for 12 hr and then immunoblotting was done as indicated. **H**) Immunoblotting analysis for the indicated proteins in SKBR3 cells cultured in 2 mM glucose at various time points. Statistical significance denoted as *p<0.05; **p<0.01; ***p<0.001; ****p<0.0001; NS-not significant.

7.2. HPIP expression is induced in response to glucose stress depends on the AMPK/FOXO3a axis

Next, whether the AMPK pathway directly regulated HPIP expression in BC cells was investigated. SKBR3 cells treated with AICAR, an AMPK activator, enhanced HPIP expression in a dose-dependent manner (Fig. 11A). Conversely, compound C (CC), an AMPK inhibitor, suppressed HPIP expression in SKBR3 cells, which was accompanied by decreased AMPK activation (Fig. 11B). Consistent with these results, glucose stress (2 mM) induced HPIP expression, whereas CC restrained it (Fig. 11C). A careful perusal of the HPIP promoter, which is located on chromosome 1q21.3, revealed that it harbored three putative FOXO3a response elements (FRE): FRE1: -440 5′-**TTGTTTCC**-3′-433, FRE2: -1058 5′-**CTGTTTTA**-3′ -1051, and FRE3: -1726 5′-**TTGTTTTG**-3′ -1719 (Fig. 11D), in addition to the previously described binding sites for GATA1 (158). Since FOXO3a is the downstream target of AMPK (219), we hypothesized that FOXO3a regulates *HPIP* transcription under glucose stress. Indeed, silencing of *FOXO3a* expression resulted in a marked decrease in *HPIP* expression in SKBR3 cells cultured in low glucose (Fig. 11E). Conversely, overexpression of *FLAG-FOXO3a* increased HPIP expression at the transcript and protein levels in SKBR3 cells under similar conditions (Fig. 11F and G). In support of this, a chromatin immunoprecipitation (ChIP) assay revealed that FOXO3a readily recruited to all three FREs on the *HPIP* promoter, while glucose deprivation further enhanced its enrichment by 3–6 fold (Fig 11H). These results concluded that the AMPK/FOXO3a axis regulated HPIP expression under glucose stress.

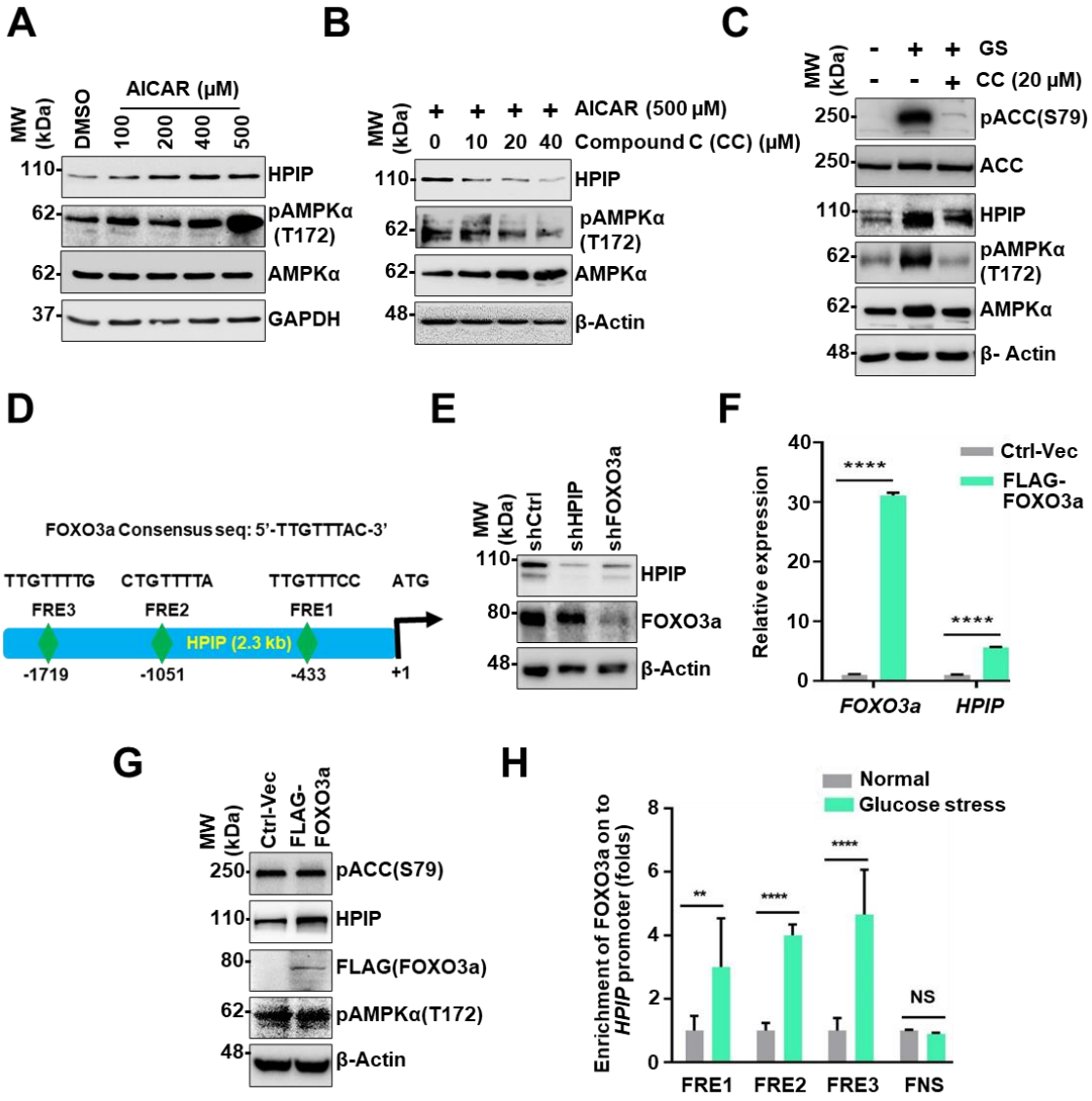

Figure 11: HPIP expression is induced in response to glucose stress depends on the AMPK/FOXO3a axis

A) SKBR3 cells were treated with AICAR (AMPK activator) at various concentrations for 12 hr, and protein lysates were analyzed using immunoblotting. **B)** Compound-C (CC) (AMPK inhibitor) was treated in a dose-dependent fashion for 1 hr before treating with AICAR for the AMPK activation (12 hr) in SKBR3 cells, and cell lysates were analyzed by immunoblotting as indicated. **C)** Immunoblotting analysis for indicated proteins in SKBR3 to show the inhibitory effect of compound C under glucose stress. **D)** Putative FOXO3a response elements (FREs) on HPIP promoter (2.3 kb length), FRE1: -440 5'TTGTTTCC3'-433; FRE2: -1058 5'CTGTTTTA3' -1051; FRE3: -1726 5'TTGTTTTG3' -1719. **E)** Stably knockdown SKBR3 cells (shCtrl, shHPIP, or shFOXO3a) were cultured in 2 mM glucose for 12 hr and analyzed by immunoblotting. qRT-PCR analysis for *HPIP* and *FOXO3a* **(F)**, and immunoblotting analysis for the indicated proteins **(G)** in SKBR3 cells transfected either with empty vector or FOXO3a encoding vector, 48 hr post-transfection cells were incubated in 2 mM glucose for 12 hr. **H)** Chromatin immunoprecipitation (ChIP) assay to show the effect of low glucose (2 mM) on FOXO3a binding to *HPIP* promoter in SKBR3 cells. Statistical significance denoted as *p<0.05; **p<0.01; ***p<0.001; ****p<0.0001; NS-not significant.

7.3. HPIP supports cell survival in response to acute glucose stress in BC cells

After establishing that *HPIP* was a glucose stress response gene, the role of HPIP signaling in cancer cell survival was evaluated. To address this, clones with stable knockdown of *HPIP* or *FOXO3a* in SKBR3 cells were generated. After confirming the efficient knockdown and overexpression of *HPIP* in SKBR3-shFOXO3a cells (Fig. 12A), cell viability under glucose stress was measured using MTT assay. As shown in Fig. 12B, knockdown of *HPIP* or *FOXO3a* results in a significant decrease in cell viability compared to that of the control, while ectopic expression of *FLAG-HPIP* in *FOXO3a* knockdown cells restores cell viability, which is comparable to *FOXO3a* knockdown cells. In support of this, under glucose stress, knockdown of *HPIP* or *FOXO3a* led to a significant decrease in intracellular ATP levels compared to that of the control, while ectopic expression of *FLAG-HPIP* in SKBR3-shFOXO3a cells restored ATP levels (Fig. 12C). Next, the clonogenic capacity and anchorage-independent growth of SKBR3 cells under glucose stress were assessed upon *HPIP* and *FOXO3a* depletion. Both clonogenic and anchorage-independent growth abilities of SKBR3 cells were significantly decreased upon either *HPIP* or *FOXO3a* knockdown compared to those of control cells under glucose stress. However, HPIP ectopic expression partially restored the colony-forming capacity and anchorage-independent growth ability of SKBR3-shFOXO3a cells (Fig. 12D-G). Based on these results, we concluded that HPIP is required for breast cancer cell proliferation and anchorage-independent growth during acute glucose stress.

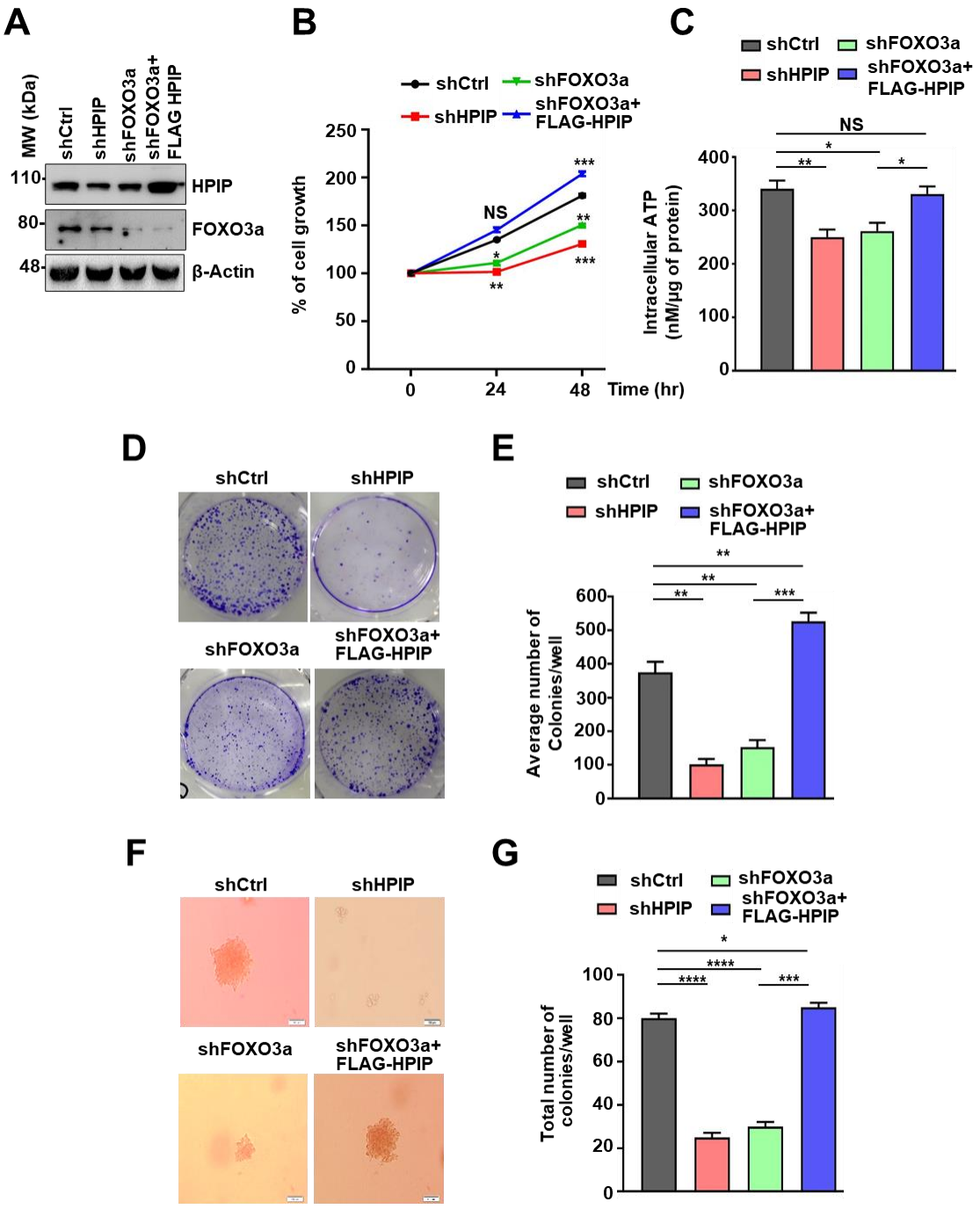

Figure 12: HPIP supports cell survival in response to acute glucose stress in BC cells. A) Immunoblotting analysis for indicated proteins in SKBR3 cells stably knockdown with shCtrl, shHPIP, shFOXO3a, and shFOXO3a cells were ectopically transfected with FLAG-HPIP. **B)** Stably knockdown SKBR3 cells were incubated with 2 mM glucose medium, and then cell growth was monitored up to 48 hr using MTT assay. **C)** Stably knockdown SKBR3 cells were incubated with 2 mM glucose medium for 12 hr, and then intracellular ATP levels were measured using ATP measurement assay. **D)** Representative images of clonogenic assay, stable cells were initially incubated with 2 mM glucose medium for 12 hr, and 0.5×10^3 cells were incubated in complete medium for 14-21 days in 6 well plates. **E)** Quantification from figure D. **F)** Representative images of soft agar assay (*scale=100 µm*), stably knockdown cells were initially incubated with 2 mM glucose medium for 12 hr and 1.0×10^4 cells were seeded in two-

layered agarose plates, grown in complete medium for 14-21 days. **G)** Quantification from figure F. Statistical significance denoted as *p<0.05; **p<0.01; ***p<0.001; ****p<0.0001; NS-not significant.

7.4. HPIP promotes tumor formation in mouse xenografts in response to acute glucose stress

To further assess the tumorigenic capacity of SKBR3 cells upon *HPIP* depletion, nude mice models were utilized. After culturing cells in 2 mM glucose medium for 12 hr, 1×10^6 cells were injected into nude mice, and tumor growth was monitored for 4–5 weeks. HPIP depleted cells showed reduced tumor formation and tumor size compared to control cells (Fig. 13A-E). Furthermore, the mouse tissue samples were examined for HPIP to validate the levels of HPIP using qRT PCR and immunohistochemistry. The results revealed that HPIP expression is absent or very low in shHPIP tumor samples compared to shCtrl tumor samples. These findings show that HPIP plays an essential role in tumor development in mouse xenografts in response to acute glucose stress.

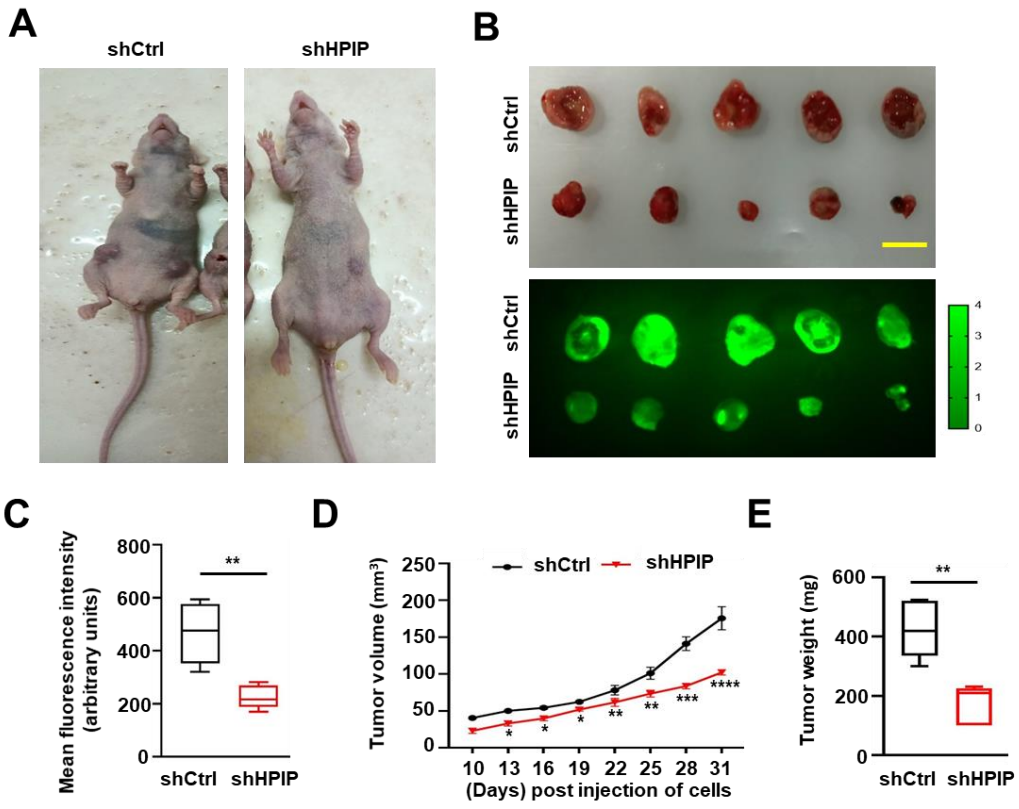

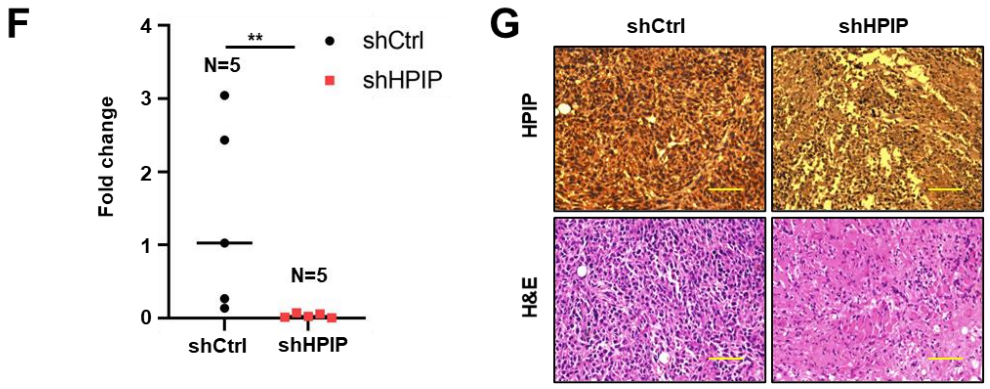

Figure 13: HPIP promotes tumor formation in mouse xenografts in response to acute glucose stress. A) SKBR3 (shCtrl and shHPIP) cells were injected into nude mice, images were taken before sacrificing animals. **B)** Images of excised tumors from the shCtrl and shHPIP stable cells injected into nude mice groups (upper panel) (*scale=1 cm*), Fluorescence (GFP) images of excised tumors (lower panel). **C**) Quantification of mean fluorescence intensity of shCtrl and shHPIP tumor tissues. **D)** Tumor volume at various time intervals shows mean ± S.D (n=5). **E)** Excised tumors were weighed, and the total weight was represented as box plots. **F)** Total RNA was isolated, and HPIP mRNA levels were measured using qRT PCR analysis. **G)** Representative images (scale bar 100 µm) of HPIP expression in shCtrl and shHPIP mice tissue samples were evaluated by immunohistochemistry. Statistical significance denoted as *p<0.05; **p<0.01; ***p<0.001; ****p<0.0001; NS-not significant.

7.5. HPIP increases glutamine import and glutaminolysis under glucose stress

Under glucose stress, cancer cells trigger the AMPK pathway to utilize non-glucose sources to establish energy homeostasis and, thus, cell survival (58, 59). Because AMPK stimulated HPIP expression under glucose stress, we hypothesized that HPIP promoted glutamine metabolism to establish energy homeostasis under these conditions. Therefore, genes involved in glutamine import and metabolism were examined, such as solute carrier family 1 member 5 (*SLC1A5)*, glutaminase (*GLS)*, glutamate dehydrogenase (*GDH)*, and glutamic-oxaloacetic transaminase (*GOT1)* in SKBR3 cells cultured in low glucose upon HPIP depletion. qRT-PCR analysis showed a significant loss of expression of *SLC1A5*, *GLS*, *GDH*, and *GOT1* in HPIP-depleted cells compared to control cells (Fig. 14A). Next, metabolic labeling studies were performed in SKBR3 cells upon *HPIP* depletion, which was confirmed by immunoblotting (Fig. 14B). The typical ^{13}C glutamine metabolism is shown in Fig. 14C. Using ^{13}C glutamine as the tracer with metabolic flux analysis, the fate of glutamine as a function of HPIP loss under glucose stress

was determined. Cells were cultured in 2 mM glucose medium for 12 hr before being transferred to ^{13}C glutamine-supplemented culture medium for 6 hours. As shown in Fig. 14D-F, the conversion of $^{13}C_5$-glutamine (M+5) into $^{13}C_5$-glutamate (M+5) and further conversion of $^{13}C_5$-glutamate (M+5) into $^{13}C_5$-α keto-glutarate (M+5) is significantly decreased.

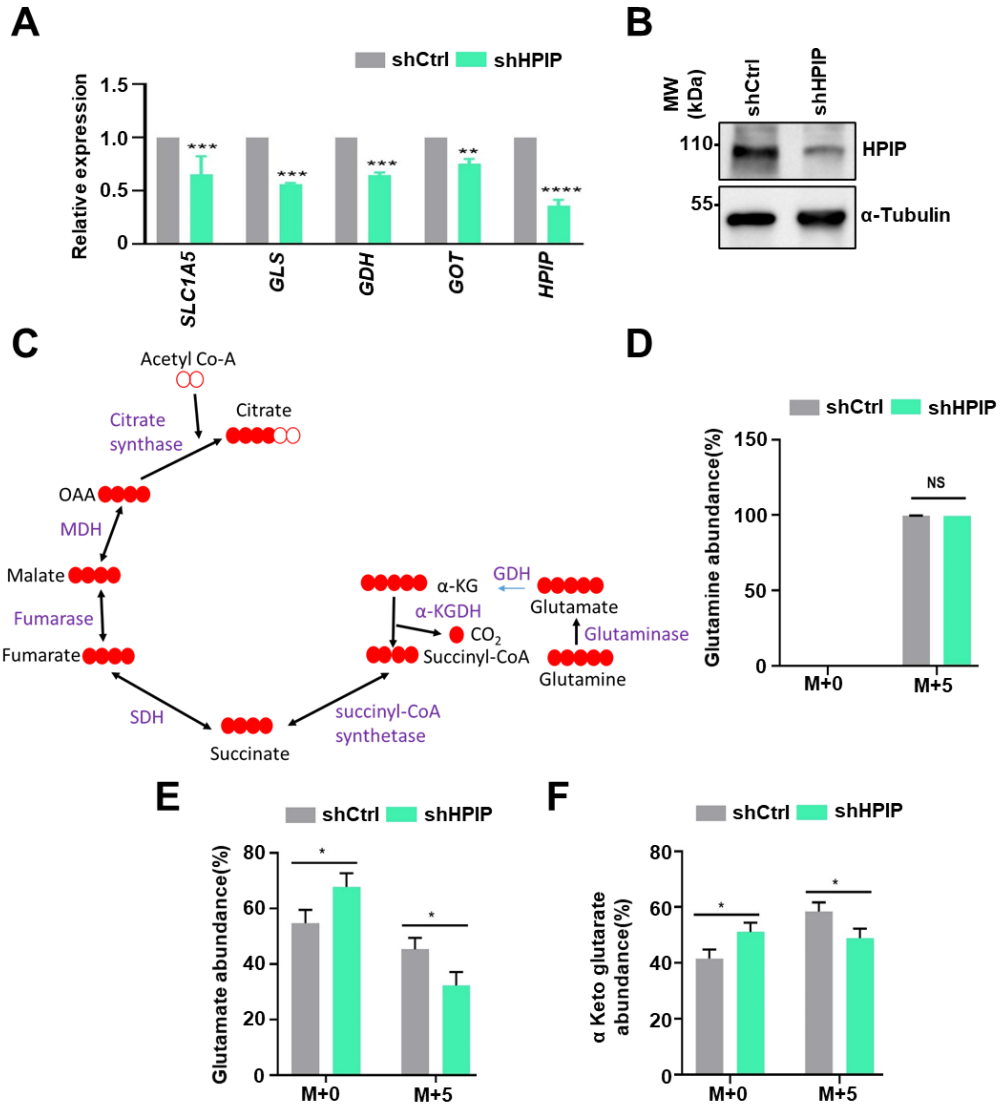

Figure 14: HPIP increases glutamine import and glutaminolysis under glucose stress. A) Stable clones of SKBR3 (shCtrl or shHPIP) cells were cultured in low glucose (2 mM) for 12 hr and were subjected to qRT-PCR analysis for glutamine importer and glutaminolysis genes. **B)** Immunoblotting demonstrating HPIP knockdown in SKBR3 cells. **C)** Schematic model for glutamine-dependent anaplerosis in the TCA cycle, radiolabeled carbons are shown in red circles. ^{13}C labeled glutamine fuels TCA cycle anaplerosis via glutamate to α-ketoglutarate (α-KG) route. Relative abundance of ^{13}C-glutamine incorporation into glutamine (**D**), glutamate (**E**), α-KG (**F**) in SKBR3 cells stably knockdown with shCtrl or shHPIP. Statistical significance denoted as *p<0.05; **p<0.01; ***p<0.001; ****p<0.0001; NS-not significant.

7.6. HPIP increases glutamine import and glutaminolysis under acute glucose stress via AKT/MYC pathway

Based on earlier reports that HPIP activates AKT in cancer cells (160) and AKT is an upstream regulator of the MYC transcription factor that controls the transcription of genes involved in glutamine metabolism (220), we hypothesized that HPIP modulates the expression of glutamine transporters and enzymes involved in glutamine metabolism, possibly via the AKT/MYC pathway. First, we analyzed AKT activation and MYC expression upon glucose stress in SKBR3 cells to test this hypothesis. While glucose stress (2 mM, 12 hr) or treatment with AICAR markedly increased AKT activation and MYC expression, treatment with Compound C restrained it (Fig. 15A). Since FOXO3a mediates AMPK action, we next analyzed AKT activation and MYC expression by altering FOXO3a expression in SKBR3 cells. While FOXO3a knockdown decreased AKT activation and MYC expression, its ectopic expression (Flag-FOXO3a) increased AKT activation and MYC expression (Fig. 15B and C). To further check the involvement of HPIP in AKT activation and MYC expression, *shHPIP*-SKBR3 stable clones were grown under glucose stress, and cell lysates were analyzed by immunoblotting. Indeed, HPIP depletion downregulated MYC expression and AKT activation, measured by AKT phosphorylation at S473 (Fig. 15D). Taken together, these data suggested that under glucose stress, HPIP triggered cancer cells to utilize glutamine as an anaplerotic substrate via the AKT/MYC pathway.

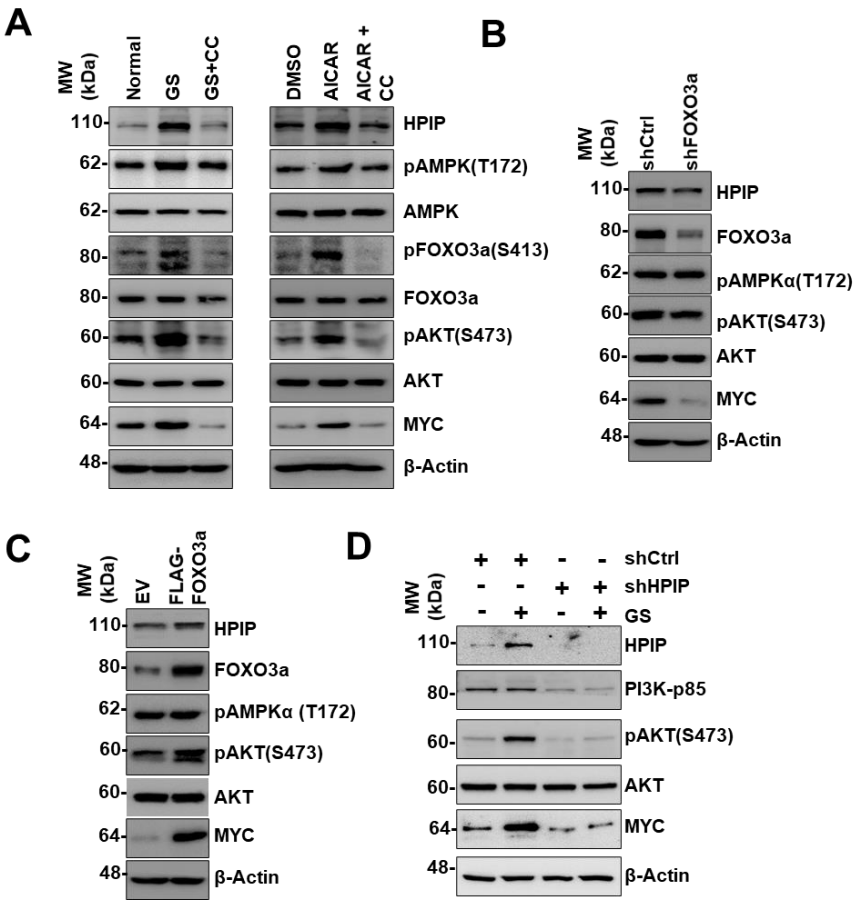

Figure 15: HPIP increases glutamine import and glutaminolysis under acute glucose stress via AKT/MYC pathway. A) Immunoblotting analysis for the indicated proteins in SKBR3 cells cultured in 2 mM glucose and compound c treatment in glucose stress (left panel) or treated with Compound C, 1 hr prior treating with AICAR (12 hr) (right panel). SKBR3 cells were transfected with either control shRNA or FOXO3a shRNA (**B**), an empty vector, or a FLAG-FOXO3a encoding vector (C), 48 hours post-transfection, cells were cultured in glucose stress medium for another 12 hr, and lysates were analyzed by immunoblotting as indicated. **D)** Immunoblotting analysis for indicated proteins in stable clones of SKBR3 (shCtrl or shHPIP) cultured in either 25 mM or 2 mM glucose for 12 hr.

7.7. HPIP acts as a co-activator of MYC in BC cells (SKBR3) under glucose stress

How HPIP enhanced AKT/MYC activation and glutamine import and its metabolic enzymes was further investigated. MYC is a transcription factor that controls the expression of SLC1A5 and GLS in cancer cells (221, 222). HPIP is a protein that shuttles between the cytoplasm and the nucleus (157). Under glucose stress, a considerable fraction of HPIP protein was found in the nucleus under glucose stress (Fig. 16A). It was then determined whether HPIP interacted with MYC to regulate the expression of glutamine metabolic enzymes by MYC activation

during glucose stress. Co-immunoprecipitation (Co-IP) analysis revealed that HPIP could interact with MYC in SKBR3 cells under glucose stress. Although we did not find a marked difference in the interaction between HPIP (increased HPIP at 12 hr is due to its induced expression during acute glucose stress) and MYC during the early phase of glucose stress (0 to 12 hr), complete loss of interaction was observed during chronic glucose stress (48 hr) (Fig. 16B). Next, a ChIP assay was performed on the MYC target genes *SLC1A5* and *GLS* using an HPIP antibody. HPIP readily recruited onto the MYC response elements of the *SLC1A5* and *GLS* promoters and was further enhanced under glucose-limiting conditions (Fig. 16C and D). Furthermore, double ChIP analysis using MYC followed by HPIP antibodies showed a significant increase in the recruitment of the MYC-HPIP transcription complex onto *SLC1A5* and *GLS* promoters under glucose stress (Fig. 16E).

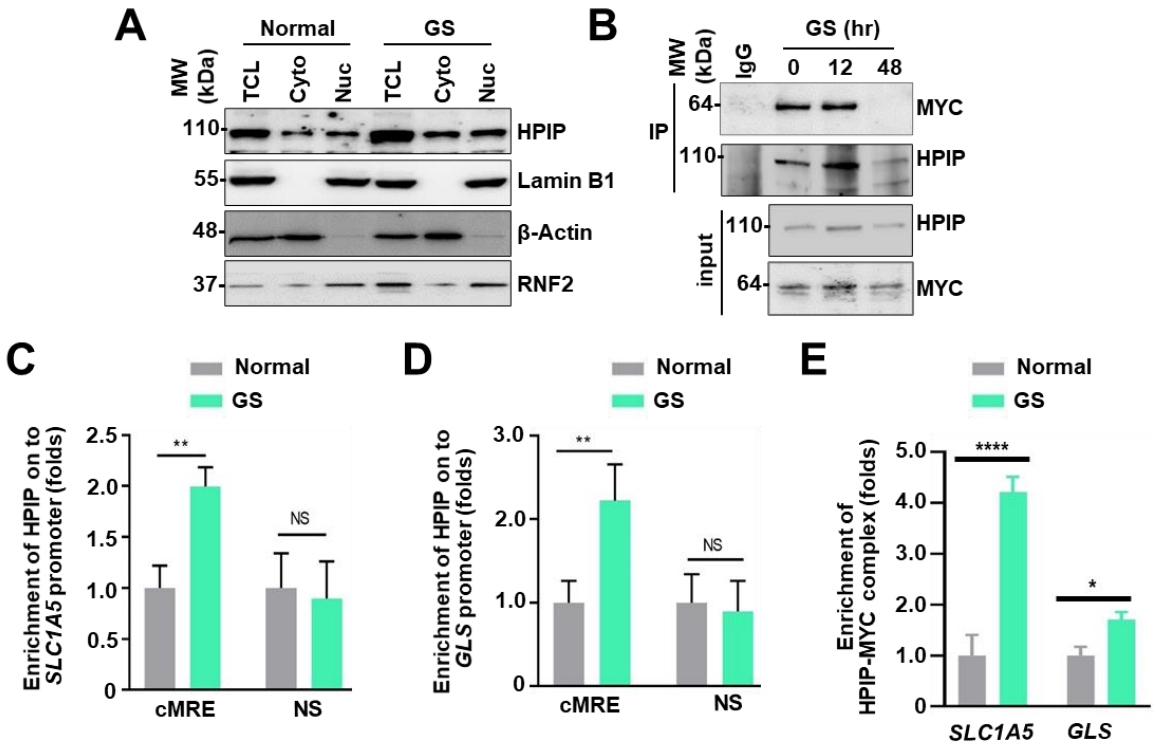

Figure 16: HPIP acts as co-activator of MYC in BC cells (SKBR3) under glucose stress. A) Immunoblotting analysis for the indicated proteins of SKBR3 cells separated into total cell lysates (TCL), cytoplasmic (Cyto), and nuclear fractions (Nuc). **B)** SKBR3 cells were cultured in 2 mM glucose medium for various time points (0, 12, and 48 hr) and co-immunoprecipitated with HPIP antibody, and then immunoblotted as indicated. ChIP analysis determines the effect of low glucose (2 mM) on HPIP binding to MYC response elements (cMRE) on the *SLC1A5* promoter (**C**) or *GLS* promoter (**D**) in SKBR3 cells. **E**) Double ChIP assay shows the glucose

stress on MYC-HPIP transcription complex binding to cMRE of the SLC1A5 and GLS promoters in SKBR3 cells. Statistical significance denoted as *p<0.05; **p<0.01; ***p<0.001; ****p<0.0001; NS-not significant.

To further demonstrate MYC dependence on HPIP, shRNAs were employed to deplete HPIP, and ChIP assays were carried out using an anti-MYC antibody. MYC recruitment onto *SLC1A5* and *GLS* promoters were substantially reduced after HPIP knockdown under glucose stress compared to control cells (Fig. 17A and B). Furthermore, qRT-PCR results revealed that MYC knockdown decreased the expression of SLC1A5 and GLS, while ectopic expression of T7-HPIP increased the expression of these gene transcripts but did not compensate for MYC depletion in the cells (Fig. 17C and D). During these investigations, an exciting discovery was uncovered. When MYC was knocked down using shRNAs, HPIP protein and transcript levels in SKBR3 cells increased (Fig. 17E and F). These results revealed that the HPIP-MYC transcription complex controls the expression of SLC1A5 and GLS, two enzymes involved in glutaminolysis in BC cells.

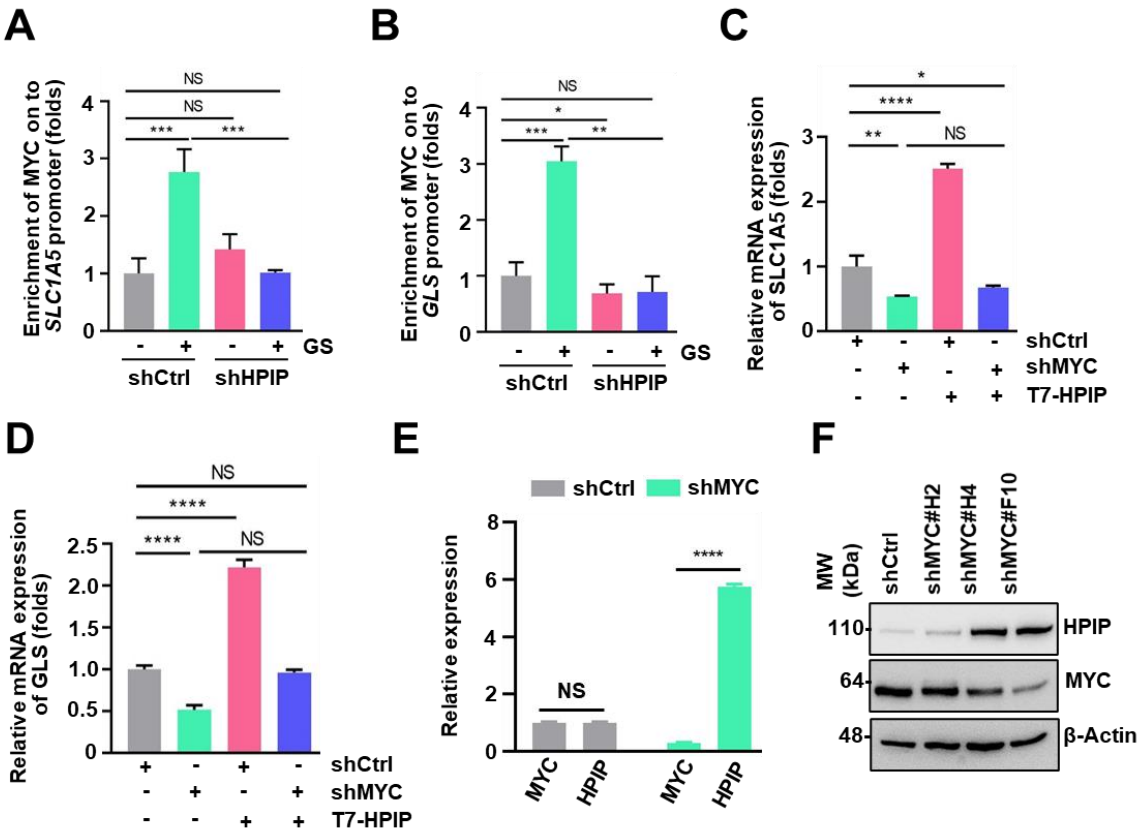

Figure 17: HPIP is required for MYC activity to regulate glutaminolysis in BC cells under glucose stress. ChIP assay demonstrates the effect of HPIP depletion on MYC binding to cMRE of the SLC1A5 (**A**) or GLS (**B**) in SKBR3 cells cultured in 2 mM glucose medium. SLC1A5 (**C**), GLS **(D**) mRNA levels were analyzed by qRT-PCR in SKBR3 cells depleted with MYC and over expressed with HPIP in SKBR3 cells cultured in 2 mM glucose medium. qRT-PCR analysis (**E**) and immunoblotting of indicated proteins (**F**) after SKBR3 cells were depleted with MYC shRNAs grown under 2 mM glucose. Statistical significance denoted as *p<0.05; **p<0.01; ***p<0.001; ****p<0.0001; NS-not significant.

Abbreviations: RNF2-ring finger protein 2; MYC-bHLH transcription factor; cMRE-C-Myc response elements; SLC1A5-Solute Carrier Family 1 Member 5; GLS-Glutaminase; GS-glucose stress; NS- non-specific.

7.8. Breast cancer cells undergo apoptosis as a result of chronic glucose stress

Generally, mammalian cells undergo apoptosis upon prolonged (chronic) glucose stress (223-227). Based on these earlier reports, SKBR3 cell growth was measured under prolonged glucose stress (up to 72 hr). Cells grown under normal conditions (25 mM) showed a continuous proliferation up to 72 hr of incubation with minimal apoptosis, which could be due to the over-confluency of the cells in the culture dish. Conversely, cells cultured under low glucose (2 mM) showed limited cell growth, which was accompanied by increased apoptosis and a declining growth curve, along with excessive apoptosis by 72 hr, as demonstrated by MTT, acridine orange-propidium iodide (AO-PI), acridine orange-ethidium bromide (AO-EtBr), and annexin V-APC assays (Fig. 18A-E). Despite the fact that HPIP inhibits apoptosis in a variety of cancer cells, its functions under metabolic stress remain unknown (169, 170, 180). As a proto-oncogene, HPIP might impede apoptosis induced by metabolic stress. Therefore, the expression of the critical executioner of apoptosis, caspase 3, and poly (ADP-ribose) polymerase (PARP) was investigated in SKBR3 cells upon HPIP depletion under prolonged glucose stress (48 hr). Elevated levels of cleaved caspase 3 and cleaved PARP were observed in HPIP depleted cells cultured under glucose stress, and FOXO3a depleted cells showed increased PARP cleavage, while ectopic expression of FLAG-HPIP restrained PARP cleavage in FOXO3a-depleted cells (Fig. 18F and G). Subsequently, HPIP levels during

prolonged glucose stress were examined. Despite increased HPIP expression during the early phases of glucose stress, its levels decreased under chronic glucose stress (48-72 hr), but AMPK activation was maintained until 72 hr (Fig. 18H). Under these conditions, pFOXO3a (S413) was also elevated during the early phase of glucose stress and then declined later.

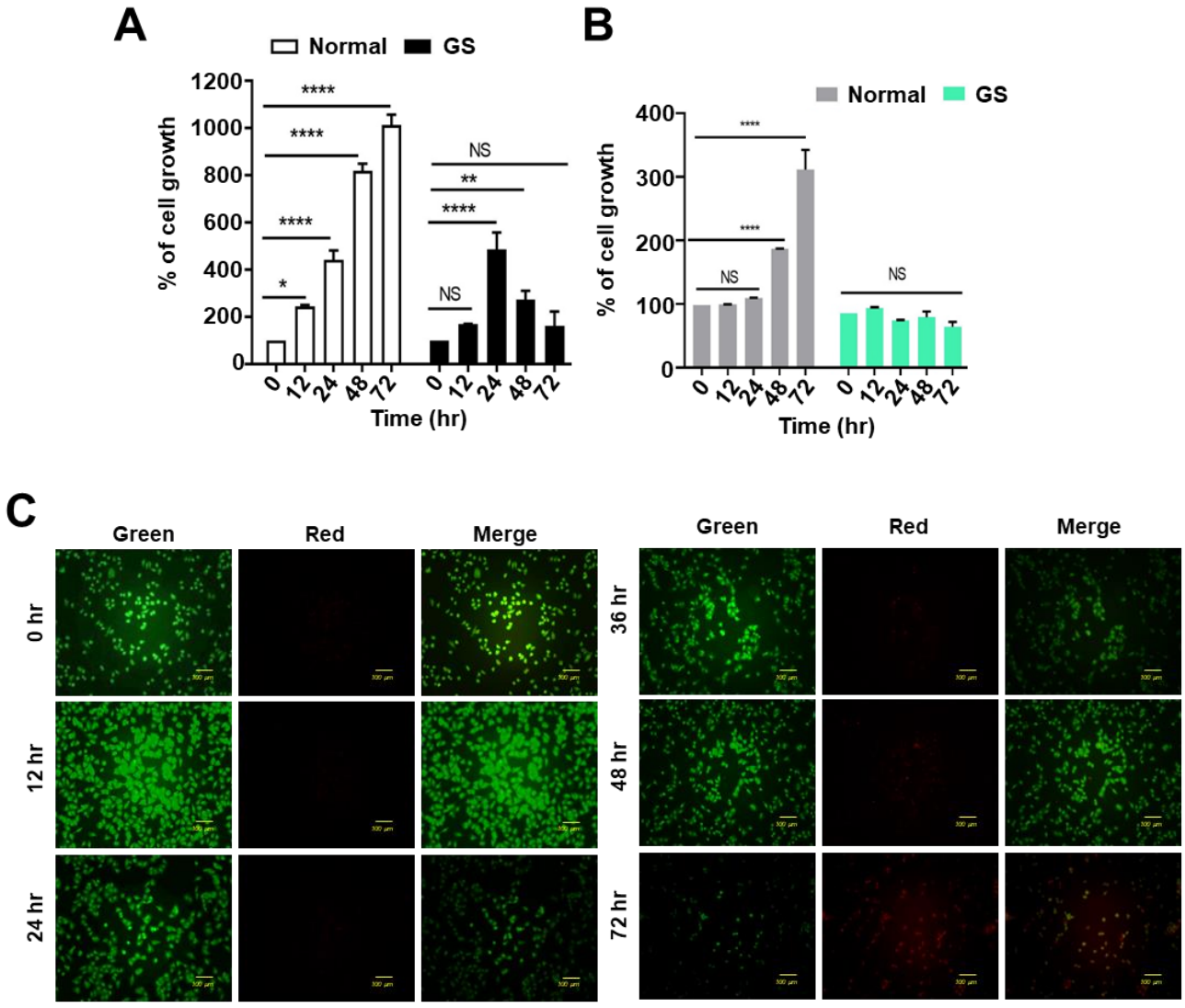

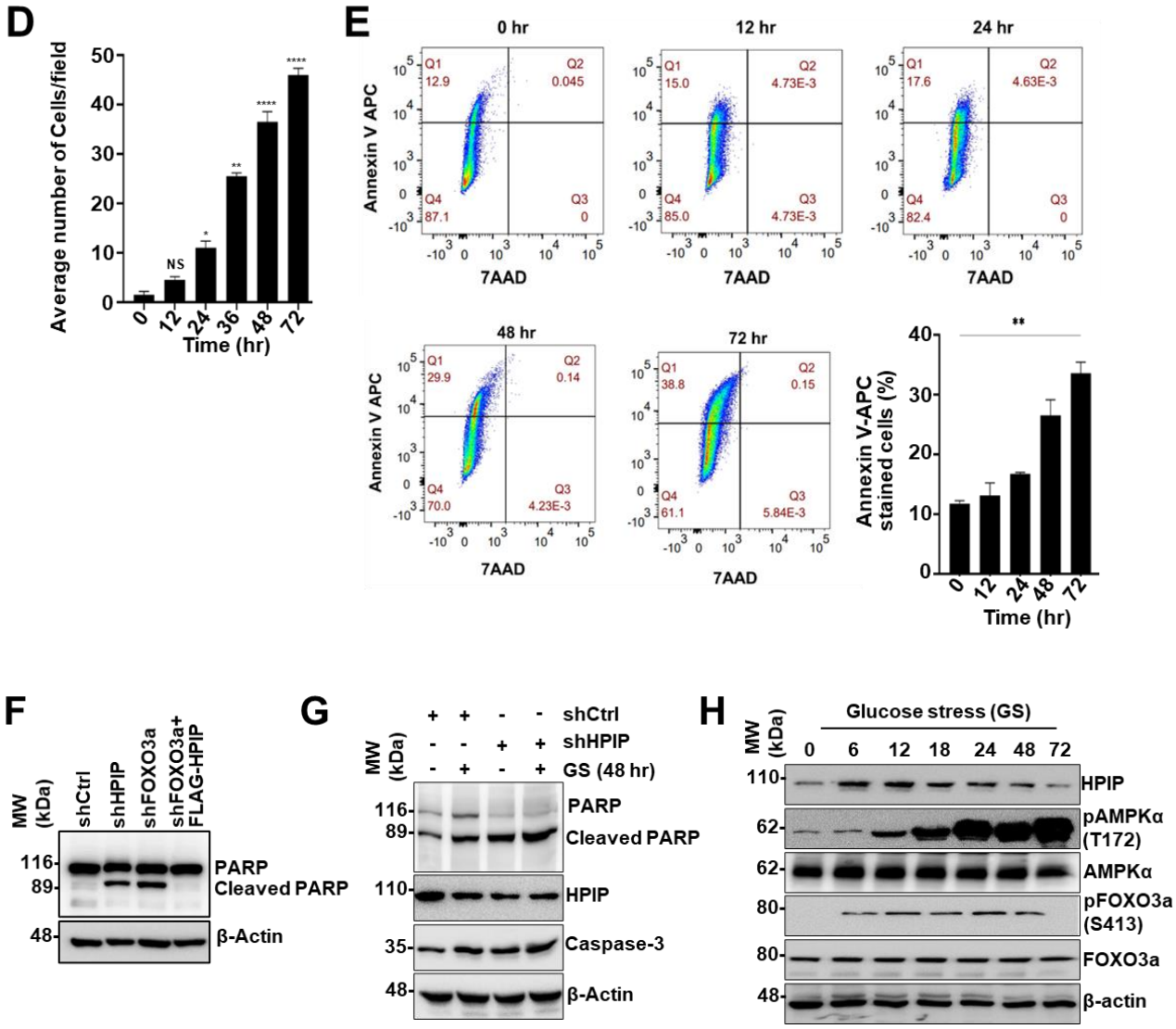

Figure 18: BC cells undergo apoptosis under chronic glucose stress. MTT assay **(A),** AO-PI assay **(B),** AO-EtBr assay **(C-D)** to show the cell growth under normal (25 mM) or glucose stress (2 mM) conditions. **E)** Annexin V-APC-stained cells were analyzed by FACS and then quantified, represented in bar graphs to show the effect of low glucose on cell growth. **F)** SKBR3 cells were transfected with shCtrl, shHPIP, shFOXO3a, or shFOXO3a plus FLAG-HPIP were grown in 2 mM glucose for 48 hr and immunoblotted as indicated. **G)** Stable clones of SKBR3 (shCtrl or shHPIP) cells were cultured either in normal or low glucose (2 mM) medium for 48 hr and immunoblotted as indicated. **H)** SKBR3 cells were grown at various time intervals under glucose stress (2 mM) and immunoblotted as indicated. Statistical significance denoted as *p<0.05; **p<0.01; ***p<0.001; ****p<0.0001; NS-not significant.

7.9. RNF2 degrades HPIP during prolonged glucose stress, and loss of HPIP triggers apoptosis.

Generally, mammalian cells undergo ubiquitination-dependent degradation of specific cellular

proteins as part of adaptation to chronic energy stress (228). Using the Mentha protein-protein interactome browser, RNF2 (an E3 ubiquitin [Ub] ligase) was identified as a potential HPIP interacting partner (Table 5).

Source ID	Source Name	Source Category	Target ID	Target Name	Target Category	Effect
Q96AQ6	PBXIP1	protein	P54646	PRKAA2	protein	ppi
Q96AQ6	PBXIP1	protein	P55201	BRPF1	protein	ppi
Q96AQ6	PBXIP1	protein	P55854	SUMO3	protein	ppi
Q96AQ6	PBXIP1	protein	P43115	PTGER3	protein	ppi
Q96AQ6	PBXIP1	protein	P60371	P60371	protein	ppi
Q96IK5	GMCL1	protein	Q96AQ6	PBXIP1	protein	ppi
Q9ULU4	ZMYND8	protein	Q96AQ6	PBXIP1	protein	ppi
Q9UMX0	UBQLN1	protein	Q96AQ6	PBXIP1	protein	ppi
Q9Y3C0	CCDC53	protein	Q96AQ6	PBXIP1	protein	ppi
Q96AQ6	PBXIP1	protein	P13747	HLA-E	protein	ppi
Q96AQ6	PBXIP1	protein	P49069	CAMLG	protein	ppi
Q96AQ6	PBXIP1	protein	Q8NI37	PPTC7	protein	ppi
Q96AQ6	PBXIP1	protein	Q8N490	PNKD	protein	ppi
Q96AQ6	PBXIP1	protein	O94766	B3GAT3	protein	ppi
Q96AQ6	PBXIP1	protein	O95447	LCA5L	protein	ppi
Q96AQ6	PBXIP1	protein	Q86VU5	COMTD1	protein	ppi
Q9UGM1	CHRNA9	protein	Q96AQ6	PBXIP1	protein	ppi
Q96AQ6	PBXIP1	protein	Q5QGZ9	Q5QGZ9	protein	ppi
Q9H0R8	GABARAPL1	protein	Q96AQ6	PBXIP1	protein	ppi
Q96AQ6	PBXIP1	protein	Q6AZY7	SCARA3	protein	ppi
Q99750	MDFI	protein	Q96AQ6	PBXIP1	protein	ppi
Q9UER7	DAXX	protein	Q96AQ6	PBXIP1	protein	ppi
Q96AQ6	PBXIP1	protein	P24863	CCNC	protein	ppi
Q9UBM8	Q9UBM8	protein	Q96AQ6	PBXIP1	protein	ppi
Q9H813	TMEM206	protein	Q96AQ6	PBXIP1	protein	ppi
Q9NRR5	UBQLN4	protein	Q96AQ6	PBXIP1	protein	ppi
Q9Y6K9	IKBKG	protein	Q96AQ6	PBXIP1	protein	ppi
Q96AQ6	PBXIP1	protein	O43765	SGTA	protein	ppi
Q96AQ6	PBXIP1	protein	Q6IQ23	PLEKHA7	protein	ppi
Q96AQ6	PBXIP1	protein	P06460	P06460	nonhuman	ppi
Q96AQ6	PBXIP1	protein	P06461	P06461	nonhuman	ppi
Q96AQ6	PBXIP1	protein	P06792	P06792	nonhuman	ppi
Q96AQ6	PBXIP1	protein	P21709	EPHA1	protein	ppi
Q96AQ6	PBXIP1	protein	O60477	BRINP1	protein	ppi
Q96AQ6	PBXIP1	protein	Q7Z7J5	DPPA2	protein	ppi
Q96AQ6	PBXIP1	protein	Q81XX8	Q81XX8	nonhuman	ppi
Q96AQ6	PBXIP1	protein	P04629	NTRK1	protein	ppi
Q96AQ6	PBXIP1	protein	Q8AZJ3	Q8AZJ3	nonhuman	ppi
Q96AQ6	PBXIP1	protein	Q8IWL3	HSCB	protein	ppi

Q96AQ6	PBXIP1	protein	Q8IYH5	ZZZ3	protein	ppi
Q96AQ6	PBXIP1	protein	Q00987	MDM2	protein	ppi
Q96AQ6	PBXIP1	protein	P62993	GRB2	protein	ppi
Q99598	TSNAX	protein	Q96AQ6	PBXIP1	protein	ppi
Q96AQ6	PBXIP1	protein	Q15834	CCDC85B	protein	ppi
Q9H0N5	PCBD2	protein	Q96AQ6	PBXIP1	protein	ppi
Q9H4E7	DEF6	protein	Q96AQ6	PBXIP1	protein	ppi
Q9UHD2	TBK1	protein	Q96AQ6	PBXIP1	protein	ppi
Q9RMZ3	CAPR	protein	Q96AQ6	PBXIP1	protein	ppi
Q9UBU8	MORF4L1	protein	Q96AQ6	PBXIP1	protein	ppi
Q96AQ6	PBXIP1	protein	P0CK58	P0CK58	nonhuman	ppi
Q99496	**RNF2**	**protein**	**Q96AQ6**	**PBXIP1**	**protein**	**ppi**
Q96AQ6	PBXIP1	protein	Q8N5C8	TAB3	protein	ppi
Q96AQ6	PBXIP1	protein	P0C739	P0C739	nonhuman	ppi
Q96AQ6	PBXIP1	protein	P03182	P03182	nonhuman	ppi
Q96AQ6	PBXIP1	protein	P03246	P03246	nonhuman	ppi
Q96AQ6	PBXIP1	protein	Q92844	TANK	protein	ppi
Q96AQ6	PBXIP1	protein	Q93086	P2RX5	protein	ppi
Q96AQ6	PBXIP1	protein	P69901	P69901	nonhuman	ppi
Q96AQ6	PBXIP1	protein	Q53SE7	FLJ13057	protein	ppi
Q96AQ6	PBXIP1	protein	Q53F39	MPPE1	protein	ppi

Table 5: Mentha protein-protein interactome data for PBXIP1 interacting partners (ppi means protein-protein interactions)

First, we analyzed whether RNF2 degrades HPIP in SKBR3 cells by altering RNF2 levels. Indeed, ectopic expression of green fluorescent protein (GFP)-RNF2 decreased HPIP expression, while RNF2 knockdown resulted in elevated HPIP expression in SKBR3 and MCF7 cells (Fig. 19A-C). In support of this data, wild-type GFP-RNF2 decreased HPIP levels, but treatment with MG132 (a proteasomal inhibitor) restored HPIP levels, while mutant RNF2, i.e., GFP-RNF2 (H69Y), an inactive mutant of RNF2, failed to do so (Fig. 19D). Next, we examined whether glucose stress modulates the interaction between HPIP and RNF2 and HPIP ubiquitination by RNF2 in SKBR3 cells cultured under glucose stress (2 mM) for various time points (0, 12, and 48 hr). Co-IP analysis revealed a weak interaction of HPIP during the early phase of glucose stress, however moderately increased binding of HPIP with RNF2 was observed during the late phase of glucose stress (Fig. 19E). This is further accompanied by a

gradual increase in the ubiquitination of HPIP during the early to late phase of glucose stress (Fig. 19E). Next, the half-life ($t_{1/2}$) of HPIP expression upon RNF2 knockdown was measured in SKBR3 cells. As compared to control cells ($t_{1/2}$ = 6.057 ± 0.2 h), HPIP was expressed longer ($t_{1/2}$ = 13.092 ± 0.3 h) in RNF2 knockdown cells (Fig. 19F and G). Together, this compelling evidence suggested that RNF2 degrades HPIP during prolonged glucose stress in BC cells.

Since it was demonstrated that RNF2 degrades HPIP during prolonged glucose stress, we hypothesized that HPIP degradation by RNF2 might affect cell growth and trigger apoptosis in cancer cells. Cell growth was examined for 72 hr under glucose stress upon RNF2 knockdown in SKBR3 cells. RNF2 depletion, which elevated HPIP levels, yielded increased cell growth, as anticipated (Fig. 19H), while HPIP knockdown resulted in decreased cell growth. Taken together, these data suggested that RNF2 was a bonafide E3 Ub ligase of HPIP during glucose stress.

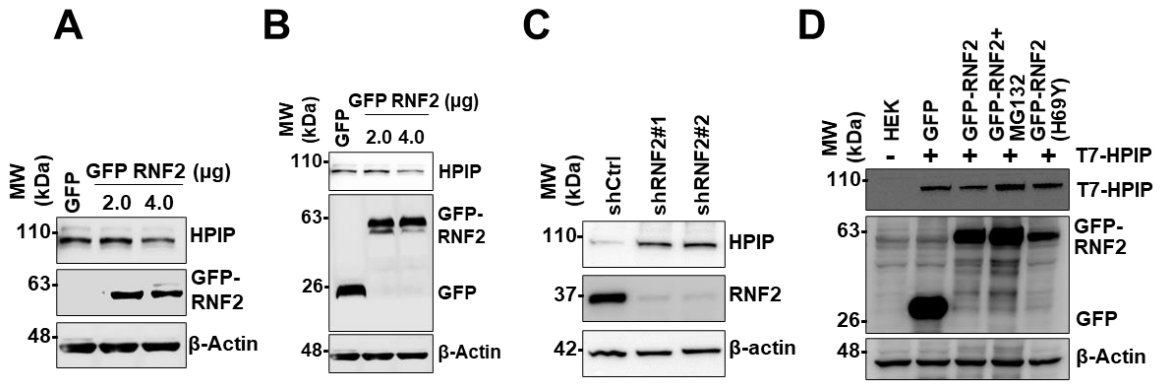

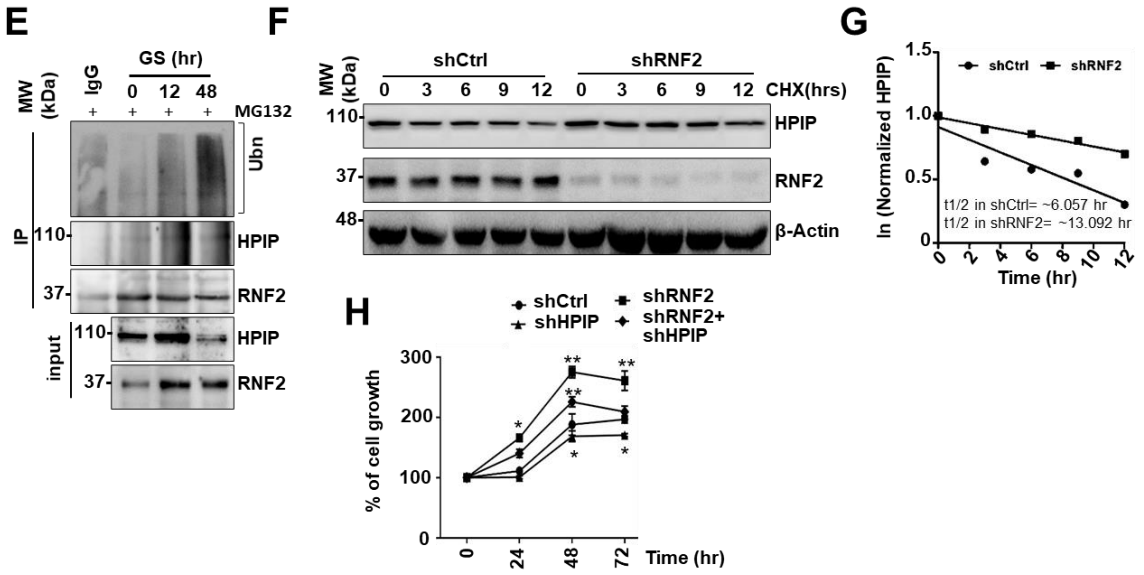

Figure 19: RNF2 degrades HPIP during prolonged glucose stress, and loss of HPIP triggers apoptosis. SKBR3 **(A)** or MCF7 **(B)** cells were transfected either with GFP vector or increasing concentration of GFP-RNF2 construct and then immunoblotted as indicated. **C)** SKBR3 cells were stably transfected with shRNF2 (1 and 2) and then cultured under 2 mM glucose for 48 hr followed by immunoblotting for the indicated proteins. **D)** HEK293T cells were co-transfected either with GFP or GFP-RNF2 or GFP-RNF2 (H69Y) constructs along with T7-HPIP construct, 48 hr post-transfection cells were incubated with 2 mM glucose medium for 48 hr and then treated with MG132 (4 hr), cell lysates were subjected to immunoblotting as indicated. **E)** SKBR3 cells were cultured in 2 mM glucose medium for various time points (0, 12, and 48 hr) and co-immunoprecipitated with HPIP antibody, and then immunoblotted as indicated. **F)** Stable clones of SKBR3 (shCtrl or shRNF2) were cultured in 2 mM glucose medium and treated with cycloheximide (30 µg/ml) for the indicated time points and cell lysates were then analyzed by immunoblotting. **G)** The line graph represents the quantification of HPIP signal intensities from **F**. **H)** Stable clones of SKBR3 cells with indicated shRNAs were cultured in 2 mM glucose medium for indicated time points, and cell growth was monitored using MTT assay. Statistical significance denoted as *p<0.05; **p<0.01; ***p<0.001; ****p<0.0001; NS-not significant.

7.10. HPIP expression positively correlates with AMPK activation in a subset of breast cancers

AMPK overexpression is reported in several cancers, including prostate, pancreatic, and glioblastoma (229-231). Similarly, HPIP overexpression is also documented in various cancers, including breast (160), hepatocellular carcinoma (174), ovarian carcinoma (169, 171), gastric cancer (164, 177), colorectal cancer (170), and renal carcinoma (166, 202). However, the clinical correlation between AMPK and HPIP in BC remains largely unknown. Therefore,

the potential clinical significance of AMPK and HPIP correlative expression in BC development was explored. First, levels of phospho-AMPKα (T172) were determined, which indicates the activation of AMPK, total AMPK, and HPIP in a panel of BC cell lines. These results indicated that although HPIP expression was low to high across the cell lines tested, phospho-AMPK was very low/absent in triple-negative breast cancer cells (TNBC), but its expression in other cell lines correlated with HPIP expression (Fig. 20A and B). Next, *HPIP* transcript levels were determined using qRT-PCR, whereas HPIP protein, pAMPKα (T172), and RNF2 levels were determined in BC and adjacent tissue samples by immunoblotting. These results revealed that patients with BC (C) had significantly higher levels of HPIP, pAMPKα (T172), and relatively low levels of RNF2 compared to those of normal subjects (N) (Fig. 20C-E). Moreover, immunohistochemistry (IHC) was employed to analyze the expression of HPIP, pACC (known substrate of AMPK), and RNF2 in a cohort of 65 clinicopathologically characterized BC tissues and 20 adjacent tissues. IHC analysis revealed that HPIP and pACC (S79) had low expression in adjacent tissue samples, while their expression ranged from medium (signal intensity-1) to very high (signal intensity-3) in BC samples; there was no change in RNF2 expression (Fig. 20F-G). The Pearson correlation between HPIP and pACC (S79) (R = 0.4425) further indicated a slight correlation in their expression with disease (Fig. 20H).

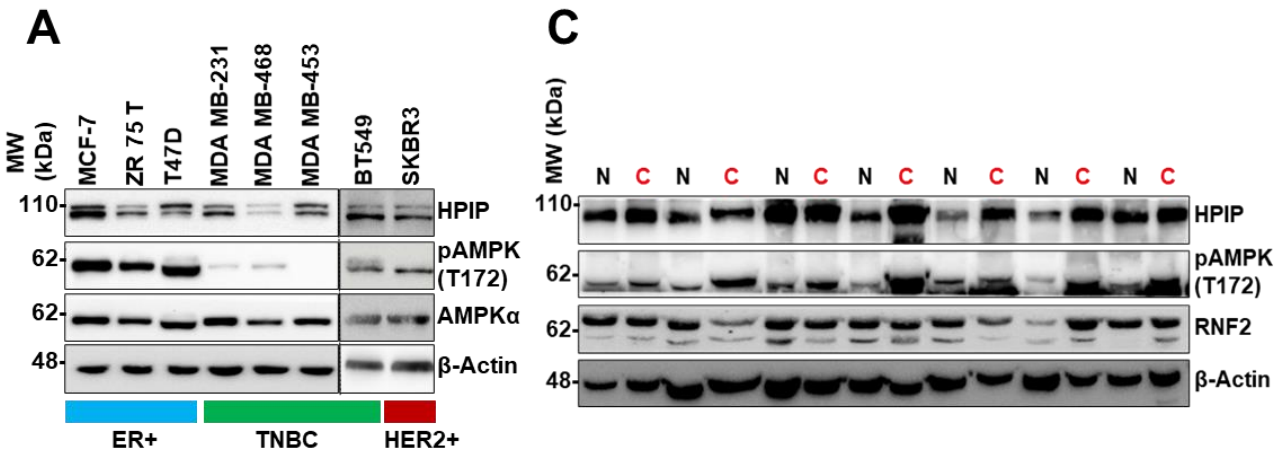

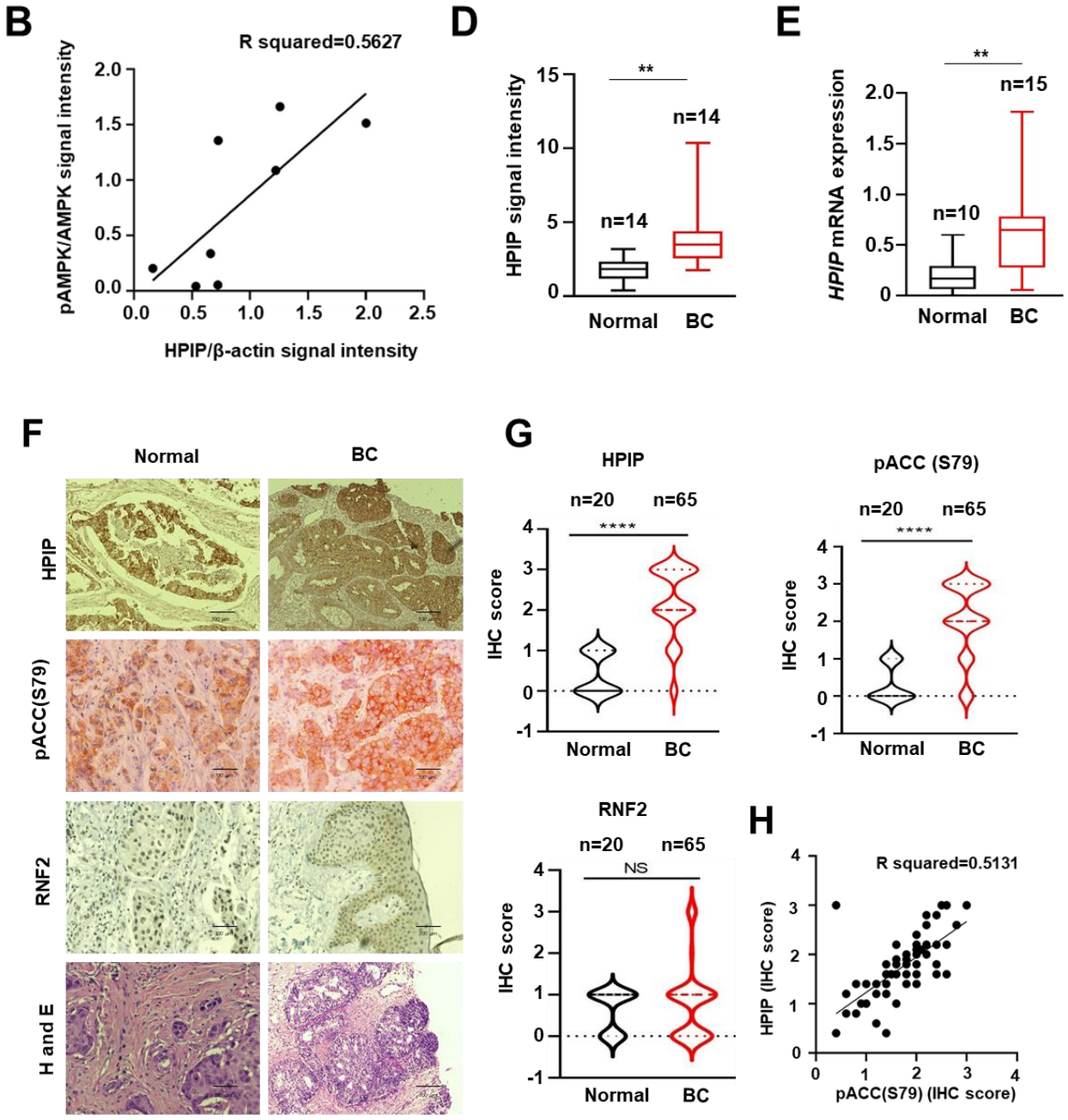

Figure 20: HPIP expression positively correlates with AMPK activation in a subset of BC cells and tissue samples. A) Immunoblotting analysis for the indicated proteins from a panel of BC cell lines. β-Actin is used as a loading control. **B)** Correlative expression plot of pAMPK and HPIP protein expression in BC cell lines. **C)** Expression level of HPIP, pAMPKα (T172), and RNF2 in breast cancer tissue (7 sets) samples were analyzed by immunoblotting; (N= Normal tissue, C=Breast cancer tissue). **D)** Signal intensities were quantified for HPIP protein and represented as box plots (n=14). **E)** qRT-PCR analysis for *HPIP* in normal (n=10) vs. breast cancer tissue samples (n=15). **F)** Representative images of H&E and immunohistochemistry (IHC) for HPIP, pACC (S79) and RNF2 in adjacent vs. breast cancer tissue samples (Scale bar =100 µm). **G)** IHC staining was scored using the IHC profiler plugin in ImageJ software and represented violin plots for HPIP, pACC (S79), and RNF2. Staining intensities were given as negative (0), low positive (1), positive (2), and high positive (3). **H)** Correlative analysis of HPIP and pACC (S79) from the IHC data**.** Statistical significance

denoted as *p<0.05; **p<0.01; ***p<0.001; ****p<0.0001.

Furthermore, we validated our results from cell lines and tissue samples using Gene expression profiling interactive analysis (GEPIA) and Oncomine datasets. The results demonstrated that the expression of HPIP and AMPK in BC samples is significantly higher than the normal tissue samples or corresponding blood samples (Fig. 21A-D). Following that, we utilized Kaplan-Meier plots to see whether HPIP, AMPK, and RNF2 had a role in patient survival. The KM plotter findings indicated that, unlike RNF2, HPIP or AMPK expression in patients with BC was significantly associated with survival time. Furthermore, the survival plots demonstrated that patients with low HPIP or AMPK expression had a longer overall survival time than those with high HPIP or AMPK expression (Fig. 21E). Similarly, RNF2 survival plots revealed that patients with low expression had a shorter overall survival time than those with high expression (Fig. 21E). When we evaluated both proteins combined based on the expression parameters, such as low HPIP and low AMPK (HPIP, EXP<0.5; AMPK, EXP<0.5) or high HPIP and high AMPK (HPIP, EXP>0.5; AMPK, EXP>0.5). Patients with low HPIP and low AMPK survived longer than patients with high HPIP and high AMPK (Fig. 21F). Following that, we examined the correlation between HPIP and AMPK expression levels using GEPIA datasets. The studies revealed that the expression of HPIP and AMPK in breast cancer samples was positively correlated (Fig. 21G). These findings suggested that AMPK and HPIP expression levels are significantly elevated in breast cancer samples and that their levels are positively correlated with each other. While RNF2 levels were low or absent in HER2+ breast cancer tissue samples, this suggests that low levels contribute to HPIP stability in HER2+ breast cancers. In conclusion, the AMPK-HPIP pathway or activating RNF2 in HER2+ breast cancer represents a promising target for breast cancer therapy.

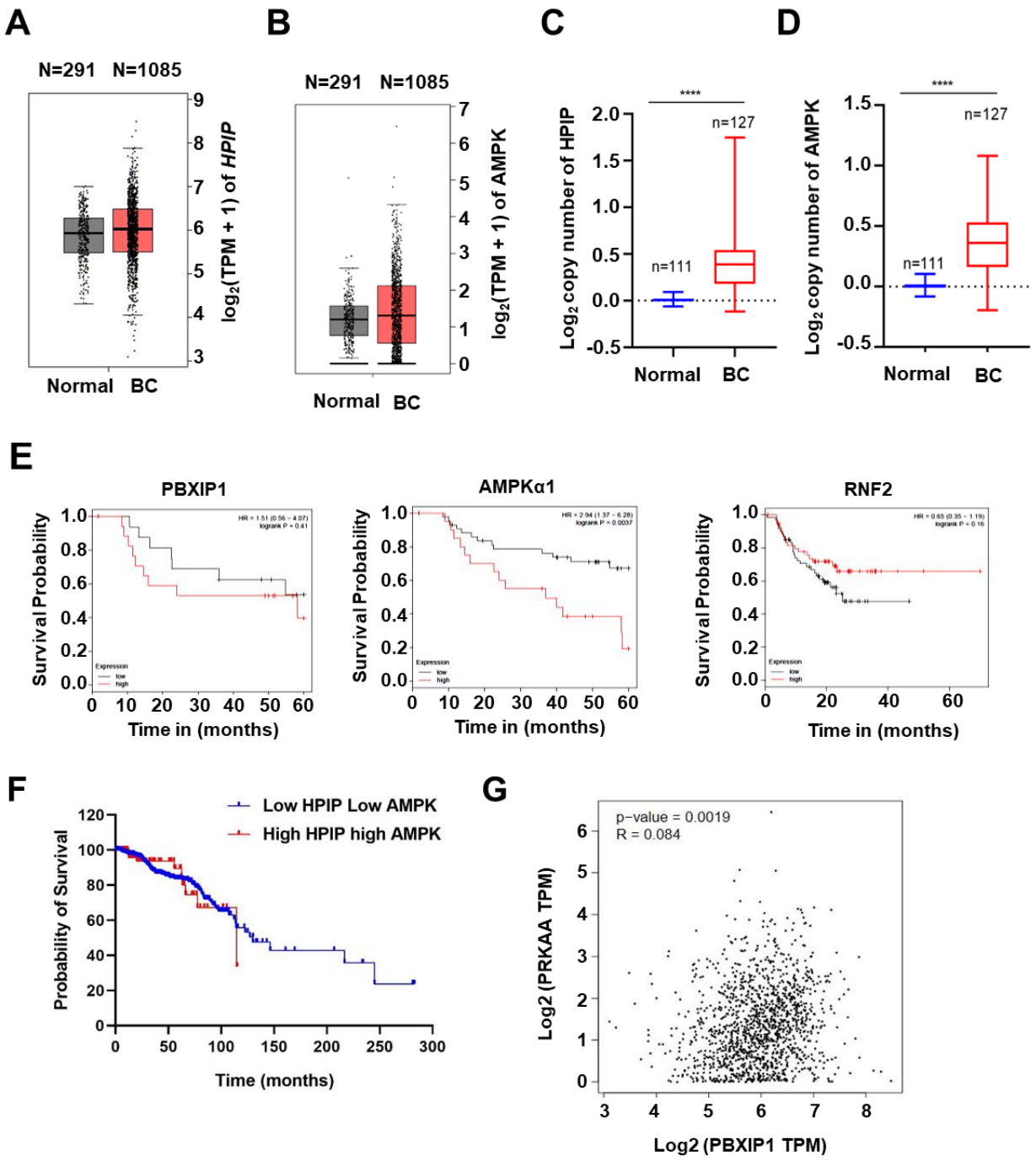

Figure 21: HPIP expression positively correlates with AMPK activation in a subset of breast cancers. HPIP **(A)** or AMPK **(B)** expression analysis from the Gene expression profiling interactive analysis (GEPIA) datasets. HPIP **(C)** or AMPK **(D)** expression analysis from the oncomine datasets. **E)** Kaplan-Meier plots showing survival probability of breast invasive cancer patients (TCGA) with high or low expression of HPIP, AMPK, and RNF2. **F)** cBioPortal database was used to plot the survival probability of breast cancer patients with low HPIP/low AMPK or high HPIP/high AMPK. **G)** The correlation plot depicts the expression of AMPK and HPIP in breast cancer samples obtained from the GEPIA data sets. Statistical significance denoted as *p<0.05; **p<0.01; ***p<0.001; ****p<0.0001.

8. Discussion

Solid tumors, such as BC, are characterized by the presence of a heterogeneous population of cells with a high demand for metabolic energy due to continuous cell proliferation and aberrant vascularization. It remains unclear as to how cancer cells survive and simultaneously maintain cell growth during metabolic stress. Herein, a new molecular mechanism of cancer cell adaptation was identified during metabolic stress. Cancer cells switch from survival to death during early to late (acute to chronic) phases of metabolic stress by employing a team of signaling molecules, including AMPK, HPIP, and RNF2. During the early phase of metabolic stress, AMPK upregulates HPIP expression, which ensures cancer cell survival under glucose stress by rewiring glutamine metabolism. In chronic glucose stress, cancer cells succumbed to apoptosis-mediated cell death because of HPIP loss due to RNF2-mediated degradation. This study highlighted the important role of HPIP as a downstream regulator of AMPK in energy homeostasis and in promoting cell survival under glucose-limiting conditions.

AMPK is a stress response kinase that is activated when cellular ATP levels are below the threshold (232). AMPK activation occurs when it is phosphorylated at T172 by liver kinase B1 (LKB1) during energy stress (233). LKB1 or AMPK inactivation renders cells resistant to oncogenic transformation and tumorigenesis (117). AMPK activation prolongs cell survival during metabolic stress by regulating diverse metabolic pathways, including glycolysis, the pentose phosphate pathway, the TCA cycle, and fatty acid oxidation (234). This study demonstrated that AMPK was active in a subset of BC, $ER^{+,}$ or $Her2^{+}$ but not in TNBC. Furthermore, AMPK activation was correlated with HPIP expression in these cell lines, suggesting that HPIP expression was AMPK-dependent. HPIP expression is also induced in endometrial cancer cells in response to glucose stress in an AMPK dependent manner, suggesting that this pathway is not restricted to breast cancer but also active in other solid tumors such as endometrial cancer (Fig. 22A-F).

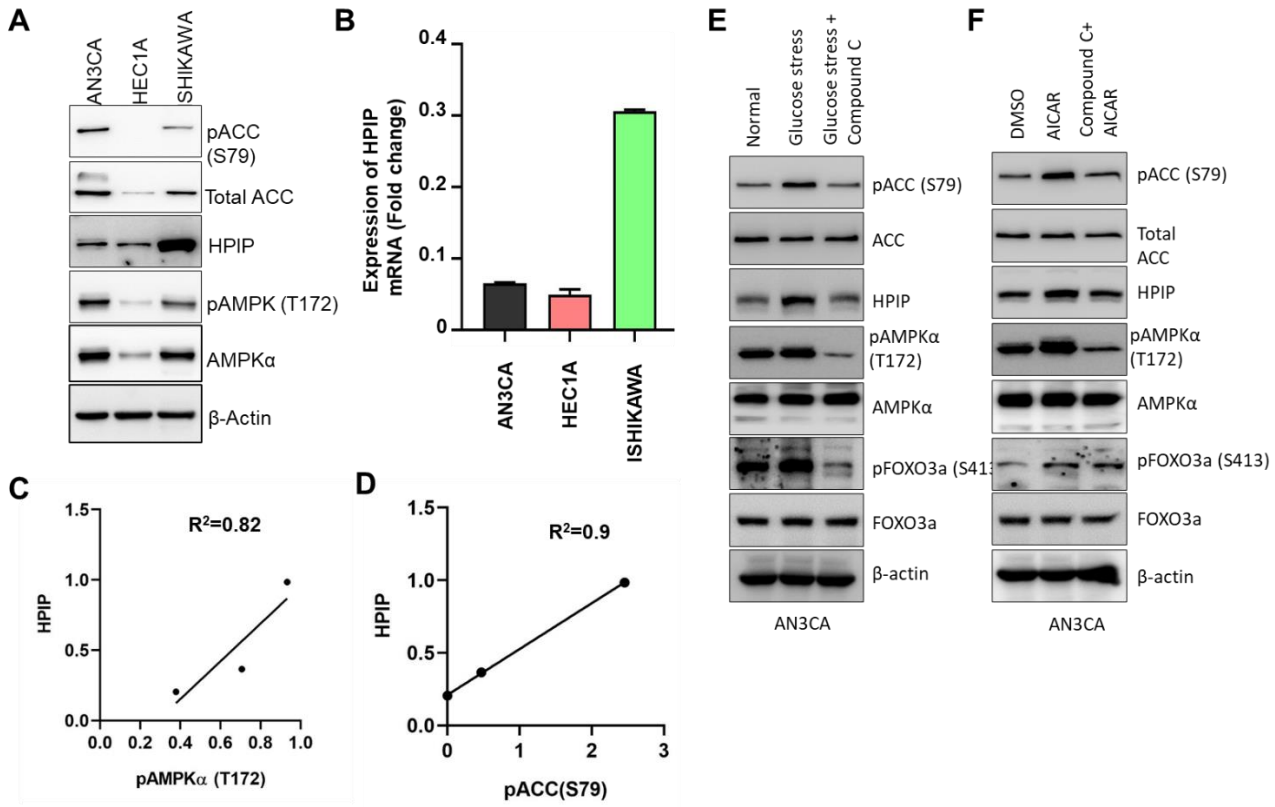

Figure 22: HPIP expression positively correlates with AMPK activation in endometrial cancer cells. A) Immunoblotting analysis for the indicated proteins from a panel of endometrial cancer cell lines, AN3CA, HEC-1-A, and Ishikawa; β-Actin used as a loading control. **B)** Real-time PCR analysis for HPIP in endometrial cancer cell lines. **C-D)** Correlative expression of HPIP with pAMPK or pACC in these cancer cell lines. **E)** Immunoblotting analysis for the indicated proteins in AN3CA cells cultured in 2 mM glucose followed by Compound C for 12 hr. **F)** AN3CA cells were treated with AICAR (AMPK activator) for 12 hr followed by Compound C, and protein lysates were analyzed by immunoblotting. Cells were treated with Compound-C (CC) (AMPK inhibitor) 1 hr prior to the AICAR treatment for the AMPK activation (12 hr).

Indeed, AMPK activation induced *HPIP* expression via *FOXO3a*-mediated transcription in Her2^{+} BC cells and also in EC cell lines (Fig. 22A-F). Loss of function in tumor suppressors or activation of oncogenes is often associated with altered metabolism in cancer cells (235). As a proto-oncogene, *HPIP* supported breast and endometrial cancer cell survival and during the early phase of glucose stress, as loss of *HPIP* expression dampened cell viability and colony-forming ability of SKBR3 and AN3CA cells (Fig. 23A-D), which is accompanied by diminished levels of cellular ATP.

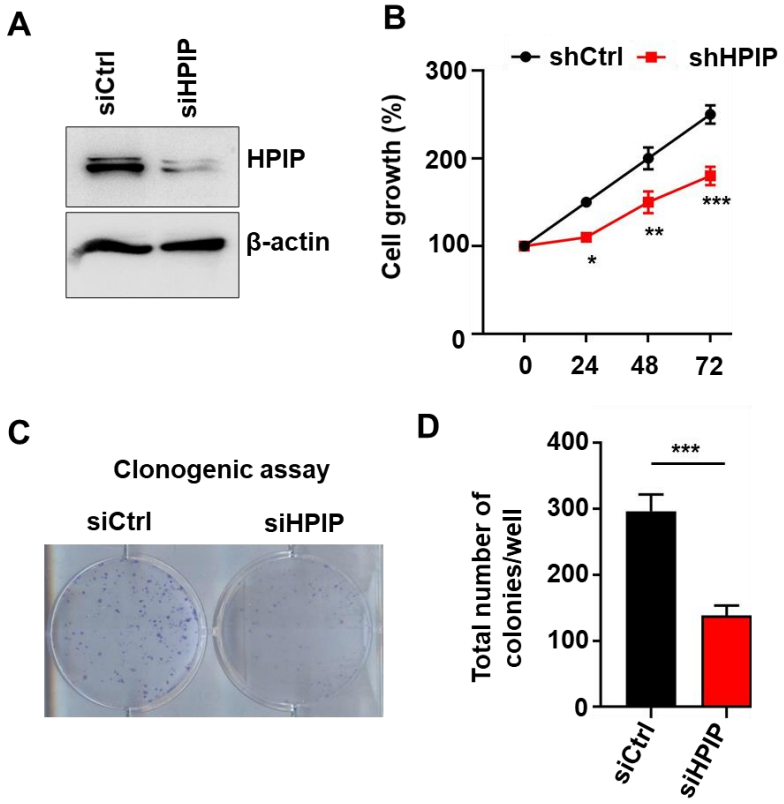

Figure 23: HPIP is required for endometrial cancer growth under acute glucose stress. A) Immunoblotting analysis demonstrates HPIP knockdown by HPIP-siRNA in AN3CA cells. **B)** Control siRNA or HPIP siRNA transfected AN3CA cells were incubated with 2 mM glucose medium, and then cell growth was monitored up to 72 hr using MTT assay. **C)** Representative images of the clonogenic assay. Control siRNA or HPIP siRNA transfected AN3CA cells were initially incubated with 2 mM glucose medium for 12 hr, and 0.5×10^3 cells were incubated in complete medium for 14-21 days in 6 well plates. **D)** Quantification of the data from C.

AMPK depletion in lung cancer cells results in lack of growth under glucose-deprived conditions despite supplementation with glutamine, lactate, and palmitate (58). This implies that under glucose-limiting conditions, AMPK instigates cancer cells to utilize non-glucose carbon sources, such as fatty acids, lactate, and glutamine, to promote oxidative phosphorylation via mitochondrial metabolism (58). The loss of HPIP expression affected the expression of SLC1A5 and glutaminolysis enzymes. Corroborating these findings, metabolic labeling studies further provided evidence that HPIP was essential for glutamine entry into the TCA cycle, perhaps to support anaplerosis. Together, these data imply that HPIP expression

via AMPK during metabolic stress serves as a molecular switch that helps in rewiring glutamine metabolism to ensure breast and endometrial cancer cell survival.

Activation of AKT signaling is associated with cancer cell survival during glucose stress (220). Moreover, via the MYC transcription factor, the AKT pathway regulates glutamine metabolism by controlling *SLC1A5* and *GLS* expression (221, 222), and HPIP activates AKT and MYC expression in cancer cells (158). We hypothesized that HPIP mediated glutamine transport and metabolism, possibly via the AKT/MYC pathway. Under glucose stress, a loss of AKT activation upon HPIP depletion and concomitant loss of expression of MYC and enzymes involved in glutamine metabolism was observed. In support of these findings, we further report that HPIP acts as a coactivator of MYC to regulate *SLC1A5* and *GLS* gene expression. During glucose stress, HPIP recruits MYC onto these promoters as depletion of HPIP abrogates it. Moreover, recent findings established that HPIP is a phosphoprotein (161). Indeed, our findings revealed that AMPK phosphorylates HPIP (Penugurti et al., unpublished), however, further characterization is required to establish this observation fully. Therefore, we cannot rule out the possible post-translational modifications such as phosphorylation on HPIP and its interaction with chromatin-modifying enzymes, which influence gene expression during glucose stress. Together, it implied that HPIP mediated cell survival under glucose stress via activation of signaling pathways involving AKT and MYC. During glucose deprivation, various glucose transporters (GLUTs) are upregulated to support the cancer cell survival to avoid cell death (236). For instance, GLUT1 prevents cell death in prostate cancer cells caused by glucose deprivation (135). During oxidative stress, GLUT4 translocation is induced by the activation of PI3K/AKT pathway and AMPK kinase in cardiac myocytes (237). It will be interesting to see if HPIP induces GLUT's expression via PI3K/AKT and AMPK pathways under glucose stress in breast cancer cells and warrants further investigation.

The role of AMPK and FOXOs in autophagy and cancer is well documented (41, 238). AMPK activation triggers autophagy by inhibiting mTOR pathway while activating ULK1 complex (239). HPIP is also known to activate mTOR signaling in renal cell carcinoma (202). However, whether HPIP activates mTOR signaling to inhibit autophagy is yet to be known. Hence, it will be interesting to study HPIP's role in autophagy in the context of metabolic stress in breast cancer cells and warrants further investigation.

Intriguingly, AMPK acts as an oncogene or tumor suppressor in a context-dependent manner (117). In cancer cells during metabolic stress, AMPK acts as an oncogene as cancer cells fail to survive in the absence of AMPK (240). This study demonstrated that AMPK could activate HPIP to promote cancer cell survival. Overexpression of both HPIP and AMPK in various tumors, including breast tumors, is well documented (169, 182, 241). This study further provided evidence that both HPIP and AMPK were both overexpressed and positively correlated with poor prognosis in BC. Since the AMPK/HPIP pathway is functional in the oncogenic context and both proteins are overexpressed in a subset of BC, this pathway may be considered as a potential therapeutic target.

Physiological stress disrupts homeostasis, which determines whether the cell survives or undergoes apoptosis (242). Extended periods of glucose starvation trigger apoptosis-mediated cell death in cancer cells (223, 224). Ubiquitination-mediated degradation of critical regulators of cell survival is an important mechanism implicated in the cellular stress response; for example, PGC-1α (a mitochondrial regulator) undergoes RNF2-mediated proteasomal degradation upon prolonged glucose stress, which results in p53-dependent apoptosis in HepG2 cells (223). In addition to PGC-1α, RNF2 is an E3 Ub ligase for H2A and Geminin1, but in various cellular contexts (223, 243). In BRCA1-associated protein 1 mutated cells, RNF2 induces apoptosis by silencing the prosurvival genes *Bcl2* and *Mcl1* (244). Under prolonged glucose stress, HPIP was ubiquitinated by RNF2 and subsequently degraded by the

proteasome-mediated pathway. Based on these data, we propose a model wherein cancer cells switch from survival to death during the early to late phase of metabolic stress by employing a novel signaling switch from the AMPK-FOXO3a-HPIP pathway to the RNF2-HPIP-Ub pathway (Fig. 24).

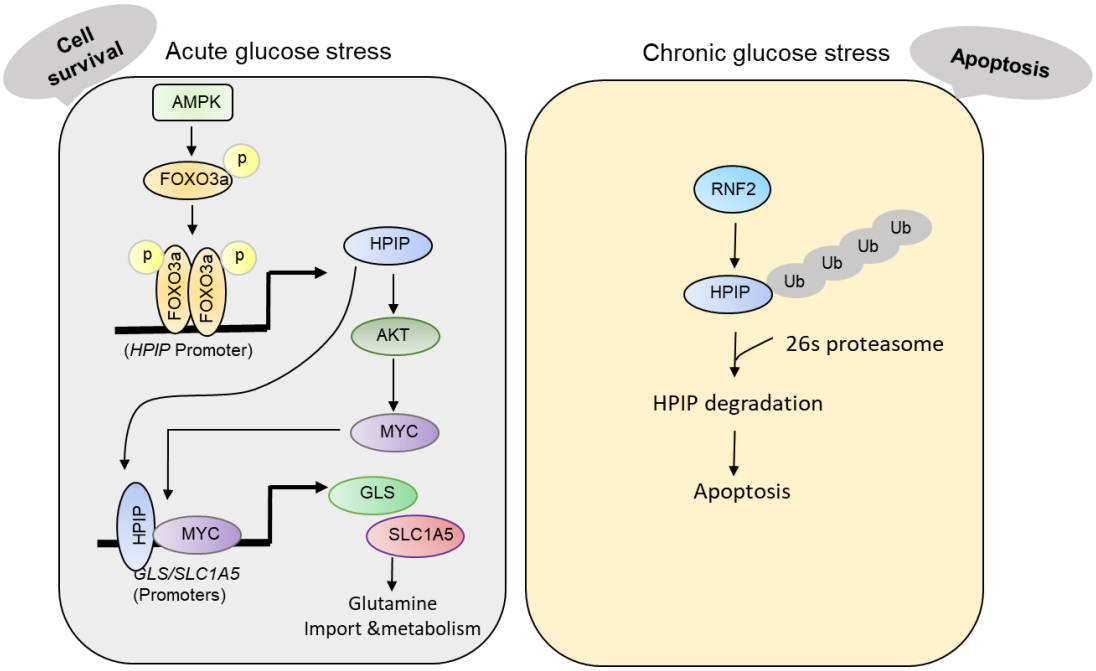

Figure 24: AMPK-FOXO3a-HPIP oncogenic axis promotes cell survival in response to acute glucose stress by rewiring glutamine metabolism. HPIP-MYC transcription complex regulates *GLS/SLC1A5* gene transcription to support glutamine metabolism. Whereas in response to chronic glucose stress, HPIP is ubiquitinated by RNF2 and subsequently degraded by the 26s proteasome pathway resulting in cell death.

9. Conclusions

According to the findings of this research, breast cancer cells increase the expression of HPIP as a part of an adaptive process under metabolic stress. Cancer cells activate AMPK in response to metabolic stress, and AMPK phosphorylates FOXO3a. This phosphorylated FOXO3a enters into the nucleus and subsequently upregulates the expression of HPIP through transcription. In the absence of glucose, HPIP triggers glutaminolysis, which is necessary for anaplerosis. Mechanistically HPIP promotes glutaminolysis by activating AKT and MYC pathways. This study further demonstrates that HPIP forms a transcription complex with MYC, and it is subsequently recruited to SLC1A5 and GLS promoters, resulting in the induction of SLC1A5 and GLS under glucose stress conditions.

Further, we found that HPIP and AMPK expression/activation is significantly higher in HER2+ breast cancer samples when compared to normal tissue samples. We observed that HPIP and AMPK have a positive correlation in HER2+ breast cancers. Hence targeting this pathway might have potential benefits for patients with HER2+ breast cancer.

Under prolonged glucose stress, mammalian cells generally undergo apoptosis. We found a new mechanism that controls cell growth under chronic glucose stress. RNF2 is a new interaction partner with HPIP; we identified RNF2-mediated ubiquitination of HPIP during prolonged glucose stress, which leads to apoptotic initiation.

Bibliography

1. Hanahan D, Weinberg RA. Hallmarks of cancer: the next generation. Cell. 2011;144(5):646-74.

2. Malhotra GK, Zhao X, Band H, Band V. Histological, molecular and functional subtypes of breast cancers. Cancer Biol Ther. 2010;10(10):955-60.

3. Fragomeni SM, Sciallis A, Jeruss JS. Molecular Subtypes and Local-Regional Control of Breast Cancer. Surg Oncol Clin N Am. 2018;27(1):95-120.

4. Gajulapalli VNR, Malisetty VL, Chitta SK, Manavathi B. Oestrogen receptor negativity in breast cancer: a cause or consequence? Biosci Rep. 2016;36(6).

5. Mahdavi M, Nassiri M, Kooshyar MM, Vakili-Azghandi M, Avan A, Sandry R, et al. Hereditary breast cancer; Genetic penetrance and current status with BRCA. J Cell Physiol. 2019;234(5):5741-50.

6. Andreopoulou E, Sparano JA. Chemotherapy in Patients with Anthracycline- and Taxane-Pretreated Metastatic Breast Cancer: An Overview. Curr Breast Cancer Rep. 2013;5(1):42-50.

7. Abotaleb M, Kubatka P, Caprnda M, Varghese E, Zolakova B, Zubor P, et al. Chemotherapeutic agents for the treatment of metastatic breast cancer: An update. Biomedicine & pharmacotherapy = Biomedecine & pharmacotherapie. 2018;101:458-77.

8. Chumsri S, Howes T, Bao T, Sabnis G, Brodie A. Aromatase, aromatase inhibitors, and breast cancer. J Steroid Biochem Mol Biol. 2011;125(1-2):13-22.

9. Peng J, Sengupta S, Jordan VC. Potential of selective estrogen receptor modulators as treatments and preventives of breast cancer. Anticancer Agents Med Chem. 2009;9(5):481-99.

10. Sung H, Ferlay J, Siegel RL, Laversanne M, Soerjomataram I, Jemal A, et al. Global Cancer Statistics 2020: GLOBOCAN Estimates of Incidence and Mortality Worldwide for 36 Cancers in 185 Countries. CA Cancer J Clin. 2021;71(3):209-49.

11. Akhtar M, Akulwar V, Gandhi D, Chandak K. Is locally advanced breast cancer a neglected disease? Indian J Cancer. 2011;48(4):403-5.

12. Rivera-Franco MM, Leon-Rodriguez E. Delays in Breast Cancer Detection and Treatment in Developing Countries. Breast Cancer (Auckl). 2018;12:1178223417752677.

13. Pavlova NN, Thompson CB. The Emerging Hallmarks of Cancer Metabolism. Cell Metab. 2016;23(1):27-47.

14. Quail DF, Joyce JA. Microenvironmental regulation of tumor progression and metastasis. Nat Med. 2013;19(11):1423-37.

15. Condeelis J, Pollard JW. Macrophages: obligate partners for tumor cell migration, invasion, and metastasis. Cell. 2006;124(2):263-6.

16. Musolino C, Allegra A, Pioggia G, Gangemi S. Immature myeloid-derived suppressor cells: A bridge between inflammation and cancer (Review). Oncol Rep. 2017;37(2):671-83.

17. Sahai E, Astsaturov I, Cukierman E, DeNardo DG, Egeblad M, Evans RM, et al. A framework for advancing our understanding of cancer-associated fibroblasts. Nat Rev Cancer. 2020;20(3):174-86.

18. Pickup MW, Mouw JK, Weaver VM. The extracellular matrix modulates the hallmarks of cancer. EMBO Rep. 2014;15(12):1243-53.

19. Walker C, Mojares E, Del Rio Hernandez A. Role of Extracellular Matrix in Development and Cancer Progression. Int J Mol Sci. 2018;19(10).

20. Petrova V, Annicchiarico-Petruzzelli M, Melino G, Amelio I. The hypoxic tumour microenvironment. Oncogenesis. 2018;7(1):10.

21. Krock BL, Skuli N, Simon MC. Hypoxia-induced angiogenesis: good and evil. Genes Cancer. 2011;2(12):1117-33.

22. Dupuy F, Tabaries S, Andrzejewski S, Dong Z, Blagih J, Annis MG, et al. PDK1-Dependent Metabolic Reprogramming Dictates Metastatic Potential in Breast Cancer. Cell metabolism. 2015;22(4):577-89.

23. Guo C, Huang T, Wang QH, Li H, Khanal A, Kang EH, et al. Monocarboxylate transporter 1 and monocarboxylate transporter 4 in cancer-endothelial co-culturing microenvironments promote proliferation, migration, and invasion of renal cancer cells. Cancer cell international. 2019;19:170.

24. Zheng J. Energy metabolism of cancer: Glycolysis versus oxidative phosphorylation (Review). Oncol Lett. 2012;4(6):1151-7.

25. Marijt KA, Sluijter M, Blijleven L, Tolmeijer SH, Scheeren FA, van der Burg SH, et al. Metabolic stress in cancer cells induces immune escape through a PI3K-dependent blockade of IFNgamma receptor signaling. Journal for immunotherapy of cancer. 2019;7(1):152.

26. Al Tameemi W, Dale TP, Al-Jumaily RMK, Forsyth NR. Hypoxia-Modified Cancer Cell Metabolism. Front Cell Dev Biol. 2019;7:4.

27. Schiliro C, Firestein BL. Mechanisms of Metabolic Reprogramming in Cancer Cells Supporting Enhanced Growth and Proliferation. Cells. 2021;10(5).

28. Warburg O. On the origin of cancer cells. Science. 1956;123(3191):309-14.

29. DeBerardinis RJ, Chandel NS. Fundamentals of cancer metabolism. Sci Adv. 2016;2(5):e1600200.

30. Yang C, Ko B, Hensley CT, Jiang L, Wasti AT, Kim J, et al. Glutamine oxidation maintains the TCA cycle and cell survival during impaired mitochondrial pyruvate transport. Molecular cell. 2014;56(3):414-24.

31. Huang F, Zhao Y, Zhao J, Wu S, Jiang Y, Ma H, et al. Upregulated SLC1A5 promotes cell growth and survival in colorectal cancer. Int J Clin Exp Pathol. 2014;7(9):6006-14.

32. Jiang S, Wang Y, Luo L, Shi F, Zou J, Lin H, et al. AMP-activated protein kinase regulates cancer cell growth and metabolism via nuclear and mitochondria events. J Cell Mol Med. 2019;23(6):3951-61.

33. Pascual G, Dominguez D, Benitah SA. The contributions of cancer cell metabolism to metastasis. Disease models & mechanisms. 2018;11(8).

34. Gonzalez H, Hagerling C, Werb Z. Roles of the immune system in cancer: from tumor initiation to metastatic progression. Genes Dev. 2018;32(19-20):1267-84.

35. Steinert G, Scholch S, Niemietz T, Iwata N, Garcia SA, Behrens B, et al. Immune escape and survival mechanisms in circulating tumor cells of colorectal cancer. Cancer Res. 2014;74(6):1694-704.

36. Wang WC, Zhang XF, Peng J, Li XF, Wang AL, Bie YQ, et al. Survival Mechanisms and Influence Factors of Circulating Tumor Cells. Biomed Res Int. 2018;2018:6304701.

37. Han Y, Liu D, Li L. PD-1/PD-L1 pathway: current researches in cancer. Am J Cancer Res. 2020;10(3):727-42.

38. Nunes-Xavier CE, Angulo JC, Pulido R, Lopez JI. A Critical Insight into the Clinical Translation of PD-1/PD-L1 Blockade Therapy in Clear Cell Renal Cell Carcinoma. Curr Urol Rep. 2019;20(1):1.

39. Lin A, Yan WH. Heterogeneity of HLA-G Expression in Cancers: Facing the Challenges. Front Immunol. 2018;9:2164.

40. Klionsky DJ, Baehrecke EH, Brumell JH, Chu CT, Codogno P, Cuervo AM, et al. A comprehensive glossary of autophagy-related molecules and processes (2nd edition). Autophagy. 2011;7(11):1273-94.

41. Mizushima N, Komatsu M. Autophagy: renovation of cells and tissues. Cell. 2011;147(4):728-41.

42. Tan Q, Wang M, Yu M, Zhang J, Bristow RG, Hill RP, et al. Role of Autophagy as a Survival Mechanism for Hypoxic Cells in Tumors. Neoplasia. 2016;18(6):347-55.

43. Degenhardt K, Mathew R, Beaudoin B, Bray K, Anderson D, Chen G, et al. Autophagy promotes tumor cell survival and restricts necrosis, inflammation, and tumorigenesis. Cancer Cell. 2006;10(1):51-64.

44. Qiang L, Wu C, Ming M, Viollet B, He YY. Autophagy controls p38 activation to promote cell survival under genotoxic stress. J Biol Chem. 2013;288(3):1603-11.

45. Santanam U, Banach-Petrosky W, Abate-Shen C, Shen MM, White E, DiPaola RS. Atg7 cooperates with Pten loss to drive prostate cancer tumor growth. Genes Dev. 2016;30(4):399-407.

46. Karsli-Uzunbas G, Guo JY, Price S, Teng X, Laddha SV, Khor S, et al. Autophagy is required for glucose homeostasis and lung tumor maintenance. Cancer Discov. 2014;4(8):914-27.

47. Lock R, Kenific CM, Leidal AM, Salas E, Debnath J. Autophagy-dependent production of secreted factors facilitates oncogenic RAS-driven invasion. Cancer Discov. 2014;4(4):466-79.

48. Lock R, Debnath J. Ras, autophagy and glycolysis. Cell Cycle. 2011;10(10):1516-7.

49. Yang S, Kimmelman AC. A critical role for autophagy in pancreatic cancer. Autophagy. 2011;7(8):912-3.

50. Guo JY, Chen HY, Mathew R, Fan J, Strohecker AM, Karsli-Uzunbas G, et al. Activated Ras requires autophagy to maintain oxidative metabolism and tumorigenesis. Genes Dev. 2011;25(5):460-70.

51. Guo JY, Karsli-Uzunbas G, Mathew R, Aisner SC, Kamphorst JJ, Strohecker AM, et al. Autophagy suppresses progression of K-ras-induced lung tumors to oncocytomas and maintains lipid homeostasis. Genes Dev. 2013;27(13):1447-61.

52. Han Y, Fan S, Qin T, Yang J, Sun Y, Lu Y, et al. Role of autophagy in breast cancer and breast cancer stem cells (Review). Int J Oncol. 2018;52(4):1057-70.

53. Wei H, Wei S, Gan B, Peng X, Zou W, Guan JL. Suppression of autophagy by FIP200 deletion inhibits mammary tumorigenesis. Genes Dev. 2011;25(14):1510-27.

54. Jornayvaz FR, Shulman GI. Regulation of mitochondrial biogenesis. Essays Biochem. 2010;47:69-84.

55. Boushel R, Lundby C, Qvortrup K, Sahlin K. Mitochondrial plasticity with exercise training and extreme environments. Exerc Sport Sci Rev. 2014;42(4):169-74.

56. Porporato PE, Filigheddu N, Pedro JMB, Kroemer G, Galluzzi L. Mitochondrial metabolism and cancer. Cell Res. 2018;28(3):265-80.

57. Vyas S, Zaganjor E, Haigis MC. Mitochondria and Cancer. Cell. 2016;166(3):555-66.

58. Chaube B, Malvi P, Singh SV, Mohammad N, Viollet B, Bhat MK. AMPK maintains energy homeostasis and survival in cancer cells via regulating p38/PGC-1alpha-mediated mitochondrial biogenesis. Cell Death Discov. 2015;1:15063.

59. Chaube B, Bhat MK. AMPK, a key regulator of metabolic/energy homeostasis and mitochondrial biogenesis in cancer cells. Cell death & disease. 2016;7:e2044.

60. Bergeron R, Ren JM, Cadman KS, Moore IK, Perret P, Pypaert M, et al. Chronic activation of AMP kinase results in NRF-1 activation and mitochondrial biogenesis. Am J Physiol Endocrinol Metab. 2001;281(6):E1340-6.

61. Warburg O. The Metabolism of Carcinoma Cells. 1925;9(1):148-63.

62. Ward PS, Thompson CB. Metabolic reprogramming: a cancer hallmark even warburg did not anticipate. Cancer Cell. 2012;21(3):297-308.

63. Phan LM, Yeung SC, Lee MH. Cancer metabolic reprogramming: importance, main features, and potentials for precise targeted anti-cancer therapies. Cancer Biol Med. 2014;11(1):1-19.

64. Jang M, Kim SS, Lee J. Cancer cell metabolism: implications for therapeutic targets. Exp Mol Med. 2013;45:e45.

65. Lum JJ, Bui T, Gruber M, Gordan JD, DeBerardinis RJ, Covello KL, et al. The transcription factor HIF-1alpha plays a critical role in the growth factor-dependent regulation of both aerobic and anaerobic glycolysis. Genes Dev. 2007;21(9):1037-49.

66. He G, Jiang Y, Zhang B, Wu G. The effect of HIF-1alpha on glucose metabolism, growth and apoptosis of pancreatic cancerous cells. Asia Pac J Clin Nutr. 2014;23(1):174-80.

67. Yu L, Chen X, Wang L, Chen S. The sweet trap in tumors: aerobic glycolysis and potential targets for therapy. Oncotarget. 2016;7(25):38908-26.

68. Dang CV, Le A, Gao P. MYC-induced cancer cell energy metabolism and therapeutic opportunities. Clin Cancer Res. 2009;15(21):6479-83.

69. Elstrom RL, Bauer DE, Buzzai M, Karnauskas R, Harris MH, Plas DR, et al. Akt stimulates aerobic glycolysis in cancer cells. Cancer Res. 2004;64(11):3892-9.

70. Coloff JL, Mason EF, Altman BJ, Gerriets VA, Liu T, Nichols AN, et al. Akt requires glucose metabolism to suppress puma expression and prevent apoptosis of leukemic T cells. J Biol Chem. 2011;286(7):5921-33.

71. Nogueira V, Park Y, Chen CC, Xu PZ, Chen ML, Tonic I, et al. Akt determines replicative senescence and oxidative or oncogenic premature senescence and sensitizes cells to oxidative apoptosis. Cancer Cell. 2008;14(6):458-70.

72. Makinoshima H, Takita M, Saruwatari K, Umemura S, Obata Y, Ishii G, et al. Signaling through the Phosphatidylinositol 3-Kinase (PI3K)/Mammalian Target of Rapamycin (mTOR) Axis Is Responsible for Aerobic Glycolysis mediated by Glucose Transporter in Epidermal Growth Factor Receptor (EGFR)-mutated Lung Adenocarcinoma. J Biol Chem. 2015;290(28):17495-504.

73. Puzio-Kuter AM. The Role of p53 in Metabolic Regulation. Genes Cancer. 2011;2(4):385-91.

74. Zhang C, Liu J, Wu R, Liang Y, Lin M, Liu J, et al. Tumor suppressor p53 negatively regulates glycolysis stimulated by hypoxia through its target RRAD. Oncotarget. 2014;5(14):5535-46.

75. Kawauchi K, Araki K, Tobiume K, Tanaka N. p53 regulates glucose metabolism through an IKK-NF-kappaB pathway and inhibits cell transformation. Nat Cell Biol. 2008;10(5):611-8.

76. Yoo HC, Yu YC, Sung Y, Han JM. Glutamine reliance in cell metabolism. Exp Mol Med. 2020;52(9):1496-516.

77. Wei Z, Liu X, Cheng C, Yu W, Yi P. Metabolism of Amino Acids in Cancer. Front Cell Dev Biol. 2020;8:603837.

78. Scalise M, Pochini L, Console L, Losso MA, Indiveri C. The Human SLC1A5 (ASCT2) Amino Acid Transporter: From Function to Structure and Role in Cell Biology. Front Cell Dev Biol. 2018;6:96.

79. Gao P, Tchernyshyov I, Chang TC, Lee YS, Kita K, Ochi T, et al. c-Myc suppression of miR-23a/b enhances mitochondrial glutaminase expression and glutamine metabolism. Nature. 2009;458(7239):762-5.

80. Xiang Y, Stine ZE, Xia J, Lu Y, O'Connor RS, Altman BJ, et al. Targeted inhibition of tumor-specific glutaminase diminishes cell-autonomous tumorigenesis. J Clin Invest. 2015;125(6):2293-306.

81. Dang CV. MYC, metabolism, cell growth, and tumorigenesis. Cold Spring Harb Perspect Med. 2013;3(8).

82. Herzig S, Shaw RJ. AMPK: guardian of metabolism and mitochondrial homeostasis. Nat Rev Mol Cell Biol. 2018;19(2):121-35.

83. Ghislat G, Patron M, Rizzuto R, Knecht E. Withdrawal of essential amino acids increases autophagy by a pathway involving Ca2+/calmodulin-dependent kinase kinase-beta (CaMKK-beta). J Biol Chem. 2012;287(46):38625-36.

84. Mungai PT, Waypa GB, Jairaman A, Prakriya M, Dokic D, Ball MK, et al. Hypoxia triggers AMPK activation through reactive oxygen species-mediated activation of calcium release-activated calcium channels. Molecular and cellular biology. 2011;31(17):3531-45.

85. Salle-Lefort S, Miard S, Nolin MA, Boivin L, Pare ME, Debigare R, et al. Hypoxia upregulates Malat1 expression through a CaMKK/AMPK/HIF-1alpha axis. Int J Oncol. 2016;49(4):1731-6.

86. Sundararaman A, Amirtham U, Rangarajan A. Calcium-Oxidant Signaling Network Regulates AMP-activated Protein Kinase (AMPK) Activation upon Matrix Deprivation. J Biol Chem. 2016;291(28):14410-29.

87. Willows R, Sanders MJ, Xiao B, Patel BR, Martin SR, Read J, et al. Phosphorylation of AMPK by upstream kinases is required for activity in mammalian cells. Biochem J. 2017;474(17):3059-73.

88. Lan F, Cacicedo JM, Ruderman N, Ido Y. SIRT1 modulation of the acetylation status, cytosolic localization, and activity of LKB1. Possible role in AMP-activated protein kinase activation. J Biol Chem. 2008;283(41):27628-35.

89. Jeon SM. Regulation and function of AMPK in physiology and diseases. Exp Mol Med. 2016;48(7):e245.

90. Oakhill JS, Chen ZP, Scott JW, Steel R, Castelli LA, Ling N, et al. beta-Subunit myristoylation is the gatekeeper for initiating metabolic stress sensing by AMP-activated protein kinase (AMPK). Proc Natl Acad Sci U S A. 2010;107(45):19237-41.

91. Zong Y, Zhang CS, Li M, Wang W, Wang Z, Hawley SA, et al. Hierarchical activation of compartmentalized pools of AMPK depends on severity of nutrient or energy stress. Cell Res. 2019;29(6):460-73.

92. Lyons CL, Roche HM. Nutritional Modulation of AMPK-Impact upon Metabolic-Inflammation. Int J Mol Sci. 2018;19(10).

93. Kim J, Yang G, Kim Y, Kim J, Ha J. AMPK activators: mechanisms of action and physiological activities. Exp Mol Med. 2016;48:e224.

94. Steneberg P, Lindahl E, Dahl U, Lidh E, Straseviciene J, Backlund F, et al. PAN-AMPK activator O304 improves glucose homeostasis and microvascular perfusion in mice and type 2 diabetes patients. JCI Insight. 2018;3(12).

95. Kanazawa I. Interaction between bone and glucose metabolism [Review]. Endocr J. 2017;64(11):1043-53.

96. Lee NK, Sowa H, Hinoi E, Ferron M, Ahn JD, Confavreux C, et al. Endocrine regulation of energy metabolism by the skeleton. Cell. 2007;130(3):456-69.

97. Packer M. Autophagy-dependent and -independent modulation of oxidative and organellar stress in the diabetic heart by glucose-lowering drugs. Cardiovasc Diabetol. 2020;19(1):62.

98. Visnjic D, Lalic H, Dembitz V, Tomic B, Smoljo T. AICAr, a Widely Used AMPK Activator with Important AMPK-Independent Effects: A Systematic Review. Cells. 2021;10(5).

99. Xiao B, Sanders MJ, Carmena D, Bright NJ, Haire LF, Underwood E, et al. Structural basis of AMPK regulation by small molecule activators. Nat Commun. 2013;4:3017.

100. Xu Y, Yu T, Ma G, Zheng L, Jiang X, Yang F, et al. Berberine modulates deacetylation of PPARgamma to promote adipose tissue remodeling and thermogenesis via AMPK/SIRT1 pathway. Int J Biol Sci. 2021;17(12):3173-87.

101. Mo Y, Zhu JL, Jiang A, Zhao J, Ye L, Han B. Compound 13 activates AMPK-Nrf2 signaling to protect neuronal cells from oxygen glucose deprivation-reoxygenation. Aging (Albany NY). 2019;11(24):12032-42.

102. Park JB, Lee MS, Cha EY, Lee JS, Sul JY, Song IS, et al. Magnolol-induced apoptosis in HCT-116 colon cancer cells is associated with the AMP-activated protein kinase signaling pathway. Biol Pharm Bull. 2012;35(9):1614-20.

103. Kaur H, Moreau R. Curcumin represses mTORC1 signaling in Caco-2 cells by a two-sided mechanism involving the loss of IRS-1 and activation of AMPK. Cell Signal. 2021;78:109842.

104. Pournourmohammadi S, Grimaldi M, Stridh MH, Lavallard V, Waagepetersen HS, Wollheim CB, et al. Epigallocatechin-3-gallate (EGCG) activates AMPK through the inhibition of glutamate dehydrogenase in muscle and pancreatic ss-cells: A potential beneficial effect in the pre-diabetic state? Int J Biochem Cell Biol. 2017;88:220-5.

105. Zhang H, Yang X, Pang X, Zhao Z, Yu H, Zhou H. Genistein protects against ox-LDL-induced senescence through enhancing SIRT1/LKB1/AMPK-mediated autophagy flux in HUVECs. Mol Cell Biochem. 2019;455(1-2):127-34.

106. Zheng Z, Wang M, Cheng C, Liu D, Wu L, Zhu J, et al. Ginsenoside Rb1 reduces H2O2induced HUVEC dysfunction by stimulating the sirtuin1/AMPactivated protein kinase pathway. Molecular medicine reports. 2020;22(1):247-56.

107. Zadra G, Photopoulos C, Tyekucheva S, Heidari P, Weng QP, Fedele G, et al. A novel direct activator of AMPK inhibits prostate cancer growth by blocking lipogenesis. EMBO Mol Med. 2014;6(4):519-38.

108. Coletta DK, Sriwijitkamol A, Wajcberg E, Tantiwong P, Li M, Prentki M, et al. Pioglitazone stimulates AMP-activated protein kinase signalling and increases the expression of genes involved in adiponectin signalling, mitochondrial function and fat oxidation in human skeletal muscle in vivo: a randomised trial. Diabetologia. 2009;52(4):723-32.

109. Jensen TE, Ross FA, Kleinert M, Sylow L, Knudsen JR, Gowans GJ, et al. PT-1 selectively activates AMPK-gamma1 complexes in mouse skeletal muscle, but activates all three gamma subunit complexes in cultured human cells by inhibiting the respiratory chain. Biochem J. 2015;467(3):461-72.

110. Kim SG, Kim JR, Choi HC. Quercetin-Induced AMP-Activated Protein Kinase Activation Attenuates Vasoconstriction Through LKB1-AMPK Signaling Pathway. J Med Food. 2018;21(2):146-53.

111. Lan F, Weikel KA, Cacicedo JM, Ido Y. Resveratrol-Induced AMP-Activated Protein Kinase Activation Is Cell-Type Dependent: Lessons from Basic Research for Clinical Application. Nutrients. 2017;9(7).

112. Liu Y, Hu X, Shan X, Chen K, Tang H. Rosiglitazone metformin adduct inhibits hepatocellular carcinoma proliferation via activation of AMPK/p21 pathway. Cancer Cell Int. 2019;19:13.

113. O'Brien AJ, Villani LA, Broadfield LA, Houde VP, Galic S, Blandino G, et al. Salicylate activates AMPK and synergizes with metformin to reduce the survival of prostate and lung cancer cells ex vivo through inhibition of de novo lipogenesis. Biochem J. 2015;469(2):177-87.

114. Ren Y, Chen J, Chen P, Hao Q, Cheong LK, Tang M, et al. Oxidative stress-mediated AMPK inactivation determines the high susceptibility of LKB1-mutant NSCLC cells to glucose starvation. Free Radic Biol Med. 2021;166:128-39.

115. Tsai JS, Chuang LM, Chen CS, Liang CJ, Chen YL, Chen CY. Troglitazone and Delta2Troglitazone enhance adiponectin expression in monocytes/macrophages through the AMP-activated protein kinase pathway. Mediators Inflamm. 2014;2014:726068.

116. Lee WJ, Song KH, Koh EH, Won JC, Kim HS, Park HS, et al. Alpha-lipoic acid increases insulin sensitivity by activating AMPK in skeletal muscle. Biochem Biophys Res Commun. 2005;332(3):885-91.

117. Liang J, Mills GB. AMPK: a contextual oncogene or tumor suppressor? Cancer Res. 2013;73(10):2929-35.

118. Endo H, Owada S, Inagaki Y, Shida Y, Tatemichi M. Glucose starvation induces LKB1-AMPK-mediated MMP-9 expression in cancer cells. Sci Rep. 2018;8(1):10122.

119. Qian X, Li X, Tan L, Lee JH, Xia Y, Cai Q, et al. Conversion of PRPS Hexamer to Monomer by AMPK-Mediated Phosphorylation Inhibits Nucleotide Synthesis in Response to Energy Stress. Cancer Discov. 2018;8(1):94-107.

120. Chan LN, Chen Z, Braas D, Lee JW, Xiao G, Geng H, et al. Metabolic gatekeeper function of B-lymphoid transcription factors. Nature. 2017;542(7642):479-83.

121. Chhipa RR, Fan Q, Anderson J, Muraleedharan R, Huang Y, Ciraolo G, et al. AMP kinase promotes glioblastoma bioenergetics and tumour growth. Nat Cell Biol. 2018;20(7):823-35.

122. Li X, Yu W, Qian X, Xia Y, Zheng Y, Lee JH, et al. Nucleus-Translocated ACSS2 Promotes Gene Transcription for Lysosomal Biogenesis and Autophagy. Mol Cell. 2017;66(5):684-97 e9.

123. Qiu S, Liu T, Piao C, Wang Y, Wang K, Zhou Y, et al. AMPKalpha2 knockout enhances tumour inflammation through exacerbated liver injury and energy deprivation-associated AMPKalpha1 activation. J Cell Mol Med. 2019;23(3):1687-97.

124. Prakasam G, Singh RK, Iqbal MA, Saini SK, Tiku AB, Bamezai RNK. Pyruvate kinase M knockdown-induced signaling via AMP-activated protein kinase promotes mitochondrial biogenesis, autophagy, and cancer cell survival. J Biol Chem. 2017;292(37):15561-76.

125. Jeon SM, Chandel NS, Hay N. AMPK regulates NADPH homeostasis to promote tumour cell survival during energy stress. Nature. 2012;485(7400):661-5.

126. Li Y, Liang R, Sun M, Li Z, Sheng H, Wang J, et al. AMPK-dependent phosphorylation of HDAC8 triggers PGM1 expression to promote lung cancer cell survival under glucose starvation. Cancer Lett. 2020;478:82-92.

127. Wu Y, Sarkissyan M, McGhee E, Lee S, Vadgama JV. Combined inhibition of glycolysis and AMPK induces synergistic breast cancer cell killing. Breast Cancer Res Treat. 2015;151(3):529-39.

128. Barbosa AM, Martel F. Targeting Glucose Transporters for Breast Cancer Therapy: The Effect of Natural and Synthetic Compounds. Cancers (Basel). 2020;12(1).

129. Zaugg K, Yao Y, Reilly PT, Kannan K, Kiarash R, Mason J, et al. Carnitine palmitoyltransferase 1C promotes cell survival and tumor growth under conditions of metabolic stress. Genes Dev. 2011;25(10):1041-51.

130. Ma Y, Cui D, Xiong X, Inuzuka H, Wei W, Sun Y, et al. SCFbeta-TrCP ubiquitinates CHK1 in an AMPK-dependent manner in response to glucose deprivation. Mol Oncol. 2019;13(2):307-21.

131. Han F, Li CF, Cai Z, Zhang X, Jin G, Zhang WN, et al. The critical role of AMPK in driving Akt activation under stress, tumorigenesis and drug resistance. Nat Commun. 2018;9(1):4728.

132. Hindupur SK, Balaji SA, Saxena M, Pandey S, Sravan GS, Heda N, et al. Identification of a novel AMPK-PEA15 axis in the anoikis-resistant growth of mammary cells. Breast Cancer Res. 2014;16(4):420.

133. Saxena M, Balaji SA, Deshpande N, Ranganathan S, Pillai DM, Hindupur SK, et al. AMP-activated protein kinase promotes epithelial-mesenchymal transition in cancer cells through Twist1 upregulation. J Cell Sci. 2018;131(14).

134. Park HU, Suy S, Danner M, Dailey V, Zhang Y, Li H, et al. AMP-activated protein kinase promotes human prostate cancer cell growth and survival. Molecular cancer therapeutics. 2009;8(4):733-41.

135. Gonzalez-Menendez P, Hevia D, Alonso-Arias R, Alvarez-Artime A, Rodriguez-Garcia A, Kinet S, et al. GLUT1 protects prostate cancer cells from glucose deprivation-induced oxidative stress. Redox Biol. 2018;17:112-27.

136. Kim SM, Nguyen TT, Ravi A, Kubiniok P, Finicle BT, Jayashankar V, et al. PTEN Deficiency and AMPK Activation Promote Nutrient Scavenging and Anabolism in Prostate Cancer Cells. Cancer Discov. 2018;8(7):866-83.

137. Wang MD, Wu H, Huang S, Zhang HL, Qin CJ, Zhao LH, et al. HBx regulates fatty acid oxidation to promote hepatocellular carcinoma survival during metabolic stress. Oncotarget. 2016;7(6):6711-26.

138. Kazyken D, Magnuson B, Bodur C, Acosta-Jaquez HA, Zhang D, Tong X, et al. AMPK directly activates mTORC2 to promote cell survival during acute energetic stress. Sci Signal. 2019;12(585).

139. Ferretti AC, Tonucci FM, Hidalgo F, Almada E, Larocca MC, Favre C. AMPK and PKA interaction in the regulation of survival of liver cancer cells subjected to glucose starvation. Oncotarget. 2016;7(14):17815-28.

140. Liu M, Zhang Z, Wang H, Chen X, Jin C. Activation of AMPK by metformin promotes renal cancer cell proliferation under glucose deprivation through its interaction with PKM2. Int J Biol Sci. 2019;15(3):617-27.

141. Patergnani S, Guzzo S, Mangolini A, dell'Atti L, Pinton P, Aguiari G. The induction of AMPK-dependent autophagy leads to P53 degradation and affects cell growth and migration in kidney cancer cells. Exp Cell Res. 2020;395(1):112190.

142. Tang H, Chen Y, Liu X, Wang S, Lv Y, Wu D, et al. Downregulation of HSP60 disrupts mitochondrial proteostasis to promote tumorigenesis and progression in clear cell renal cell carcinoma. Oncotarget. 2016;7(25):38822-34.

143. Wang YN, Lu YX, Liu J, Jin Y, Bi HC, Zhao Q, et al. AMPKalpha1 confers survival advantage of colorectal cancer cells under metabolic stress by promoting redox balance through the regulation of glutathione reductase phosphorylation. Oncogene. 2020;39(3):637-50.

144. Wang Z, Zhu Z, Li C, Zhang Y, Li Z, Sun S. NMIIA promotes tumorigenesis and prevents chemosensitivity in colorectal cancer by activating AMPK/mTOR pathway. Exp Cell Res. 2021;398(1):112387.

145. Zhan P, Zhao S, Yan H, Yin C, Xiao Y, Wang Y, et al. alpha-enolase promotes tumorigenesis and metastasis via regulating AMPK/mTOR pathway in colorectal cancer. Mol Carcinog. 2017;56(5):1427-37.

146. Zhao Y, Liu Y, Lin L, Huang Q, He W, Zhang S, et al. The lncRNA MACC1-AS1 promotes gastric cancer cell metabolic plasticity via AMPK/Lin28 mediated mRNA stability of MACC1. Mol Cancer. 2018;17(1):69.

147. Cheng G, Li B, Sun X, Cao Z, Zhang G, Zhao Z, et al. LncRNA LOC730101 promotes osteosarcoma cell survival under energy stress. Biochem Biophys Res Commun. 2018;496(1):1-6.

148. Leprivier G, Remke M, Rotblat B, Dubuc A, Mateo AR, Kool M, et al. The eEF2 kinase confers resistance to nutrient deprivation by blocking translation elongation. Cell. 2013;153(5):1064-79.

149. Takahashi Y, Serada S, Ohkawara T, Fujimoto M, Hiramatsu K, Ueda Y, et al. LSR promotes epithelial ovarian cancer cell survival under energy stress through the LKB1-AMPK pathway. Biochem Biophys Res Commun. 2021;537:93-9.

150. Rauner M, Baschant U, Roetto A, Pellegrino RM, Rother S, Salbach-Hirsch J, et al. Transferrin receptor 2 controls bone mass and pathological bone formation via BMP and Wnt signaling. Nat Metab. 2019;1(1):111-24.

151. Saito S, Furuno A, Sakurai J, Park HR, Shin-ya K, Tomida A. Compound C prevents the unfolded protein response during glucose deprivation through a mechanism independent of AMPK and BMP signaling. PloS one. 2012;7(9):e45845.

152. Saito Y, Chapple RH, Lin A, Kitano A, Nakada D. AMPK Protects Leukemia-Initiating Cells in Myeloid Leukemias from Metabolic Stress in the Bone Marrow. Cell Stem Cell. 2015;17(5):585-96.

153. Jin P, Jiang J, Xie N, Zhou L, Huang Z, Zhang L, et al. MCT1 relieves osimertinib-induced CRC suppression by promoting autophagy through the LKB1/AMPK signaling. Cell death & disease. 2019;10(8):615.

154. Li FL, Liu JP, Bao RX, Yan G, Feng X, Xu YP, et al. Acetylation accumulates PFKFB3 in cytoplasm to promote glycolysis and protects cells from cisplatin-induced apoptosis. Nat Commun. 2018;9(1):508.

155. Rasheduzzaman M, Moon JH, Lee JH, Nazim UM, Park SY. Telmisartan generates ROS-dependent upregulation of death receptor 5 to sensitize TRAIL in lung cancer via inhibition of autophagy flux. Int J Biochem Cell Biol. 2018;102:20-30.

156. Abramovich C, Shen WF, Pineault N, Imren S, Montpetit B, Largman C, et al. Functional cloning and characterization of a novel nonhomeodomain protein that inhibits the binding of PBX1-HOX complexes to DNA. J Biol Chem. 2000;275(34):26172-7.

157. Abramovich C, Chavez EA, Lansdorp PM, Humphries RK. Functional characterization of multiple domains involved in the subcellular localization of the hematopoietic Pbx interacting protein (HPIP). Oncogene. 2002;21(44):6766-71.

158. Manavathi B, Lo D, Bugide S, Dey O, Imren S, Weiss MJ, et al. Functional regulation of pre-B-cell leukemia homeobox interacting protein 1 (PBXIP1/HPIP) in erythroid differentiation. J Biol Chem. 2012;287(8):5600-14.

159. Yu YH, Siao FP, Hsu LC, Yen PH. TEX11 modulates germ cell proliferation by competing with estrogen receptor beta for the binding to HPIP. Molecular endocrinology. 2012;26(4):630-42.

160. Manavathi B, Acconcia F, Rayala SK, Kumar R. An inherent role of microtubule network in the action of nuclear receptor. Proc Natl Acad Sci U S A. 2006;103(43):15981-6.

161. Shostak K, Patrascu F, Goktuna SI, Close P, Borgs L, Nguyen L, et al. MDM2 restrains estrogen-mediated AKT activation by promoting TBK1-dependent HPIP degradation. Cell death and differentiation. 2014;21(5):811-24.

162. Wang X, Yang Z, Zhang H, Ding L, Li X, Zhu C, et al. The estrogen receptor-interacting protein HPIP increases estrogen-responsive gene expression through activation of MAPK and AKT. Biochim Biophys Acta. 2008;1783(6):1220-8.

163. Xu X, Fan Z, Kang L, Han J, Jiang C, Zheng X, et al. Hepatitis B virus X protein represses miRNA-148a to enhance tumorigenesis. The Journal of clinical investigation. 2013;123(2):630-45.

164. Feng Y, Li L, Zhang X, Zhang Y, Liang Y, Lv J, et al. Hematopoietic pre-B cell leukemia transcription factor interacting protein is overexpressed in gastric cancer and promotes gastric cancer cell proliferation, migration, and invasion. Cancer Sci. 2015;106(10):1313-22.

165. Li P, Cao S, Huang Y, Zhang Y, Liu J, Cai X, et al. A novel chemical inhibitor suppresses breast cancer cell growth and metastasis through inhibiting HPIP oncoprotein. Cell Death Discov. 2021;7(1):198.

166. Khumukcham SS, Manavathi B. Two decades of a protooncogene HPIP/PBXIP1: Uncovering the tale from germ cell to cancer. Biochim Biophys Acta Rev Cancer. 2021;1876(1):188576.

167. Wang D, Wang L, Zhou Y, Zhao X, Xiong H. The involvement of hematopoietic pre-B cell leukemia transcription factor-interacting protein in regulating epithelial-mesenchymal transition of human spinal glioblastoma. Tumour biology : the journal of the International Society for Oncodevelopmental Biology and Medicine. 2016;37(5):5897-903.

168. Ning YX, Wang XY, Wang JQ, Zeng R, Wang GQ. miR152 regulates TGFbeta1induced epithelialmesenchymal transition by targeting HPIP in tubular epithelial cells. Molecular medicine reports. 2018;17(6):7973-9.

169. Bugide S, Gonugunta VK, Penugurti V, Malisetty VL, Vadlamudi RK, Manavathi B. HPIP promotes epithelial-mesenchymal transition and cisplatin resistance in ovarian cancer cells through PI3K/AKT pathway activation. Cellular oncology. 2017;40(2):133-44.

170. Feng Y, Xu X, Zhang Y, Ding J, Wang Y, Zhang X, et al. HPIP is upregulated in colorectal cancer and regulates colorectal cancer cell proliferation, apoptosis and invasion. Sci Rep. 2015;5:9429.

171. Zhang GY, Liu AH, Li GM, Wang JR. HPIP Silencing Prevents Epithelial-Mesenchymal Transition Induced by TGF-beta1 in Human Ovarian Cancer Cells. Oncology research. 2016;24(1):33-9.

172. Wang SC, Chai DS, Chen CB, Wang ZY, Wang L. HPIP promotes thyroid cancer cell growth, migration and EMT through activating PI3K/AKT signaling pathway. Biomedicine & pharmacotherapy = Biomedecine & pharmacotherapie. 2015;75:33-9.

173. Shi S, Zhao J, Wang J, Mi D, Ma Z. HPIP silencing inhibits TGF-beta1-induced EMT in lung cancer cells. International journal of molecular medicine. 2017;39(2):479-83.

174. Xu X, Jiang C, Wang S, Tai Y, Wang T, Kang L, et al. HPIP is upregulated in liver cancer and promotes hepatoma cell proliferation via activation of G2/M transition. IUBMB life. 2013;65(10):873-82.

175. van Vuurden DG, Aronica E, Hulleman E, Wedekind LE, Biesmans D, Malekzadeh A, et al. Pre-B-cell leukemia homeobox interacting protein 1 is overexpressed in astrocytoma and promotes tumor cell growth and migration. Neuro-oncology. 2014;16(7):946-59.

176. Okada S, Irie T, Tanaka J, Yasuhara R, Yamamoto G, Isobe T, et al. Potential role of hematopoietic pre-B-cell leukemia transcription factor-interacting protein in oral carcinogenesis. Journal of oral pathology & medicine : official publication of the International Association of Oral Pathologists and the American Academy of Oral Pathology. 2015;44(2):115-25.

177. Chen Y, Zhao R, Zhao Q, Shao Y, Zhang S. Knockdown of HPIP Inhibits the Proliferation and Invasion of Head-and-Neck Squamous Cell Carcinoma Cells by Regulating PI3K/Akt Signaling Pathway. Oncology research. 2016;24(3):153-60.

178. Cheng L, Zhao T, Li S, Wang Y, Fei H, Meng F. Overexpression of HPIP as a biomarker for metastasis and prognosis prediction in endometrial cancer patients. Journal of clinical laboratory analysis. 2019;33(8):e22959.

179. Meng F, Liu H, Liu S, Ma R. The clinical significance of HPIP and the associated prognosis in cervical cancer. Oncotarget. 2017;8(41):70262-70.

180. Zhao YM, Yang G, You L, Hu Y, Zhao YP. [Effect of Hematopoietic Pre-B-cell Leukemia Transcription Factor Interacting Protein Knockdown on Proliferation,Cell Cycle and Apoptosis in Pancreatic Cancer Cells]. Zhongguo Yi Xue Ke Xue Yuan Xue Bao. 2020;42(1):7-15.

181. Jiang L, Hu G, Chen FF, Du XY, Liu B, Liu C. CSR1 suppresses tumor growth and metastasis of human hepatocellular carcinoma via inhibition of HPIP. Eur Rev Med Pharmacol Sci. 2017;21(17):3813-20.

182. Bugide S, David D, Nair A, Kannan N, Samanthapudi VS, Prabhakar J, et al. Hematopoietic PBX-interacting protein (HPIP) is over expressed in breast infiltrative ductal carcinoma and regulates cell adhesion and migration through modulation of focal adhesion dynamics. Oncogene. 2015;34(35):4601-12.

183. Ji Q, Xu X, Kang L, Xu Y, Xiao J, Goodman SB, et al. Hematopoietic PBX-interacting protein mediates cartilage degeneration during the pathogenesis of osteoarthritis. Nat Commun. 2019;10(1):313.

184. Khumukcham SS, Samanthapudi VSK, Penugurti V, Kumari A, Kesavan PS, Velatooru LR, et al. Hematopoietic PBX-interacting protein is a substrate and an inhibitor of the APC/C-Cdc20 complex and regulates mitosis by stabilizing cyclin B1. J Biol Chem. 2019;294(26):10236-52.

185. Dongre A, Weinberg RA. New insights into the mechanisms of epithelial-mesenchymal transition and implications for cancer. Nat Rev Mol Cell Biol. 2019;20(2):69-84.

186. Mittal V. Epithelial Mesenchymal Transition in Tumor Metastasis. Annu Rev Pathol. 2018;13:395-412.

187. Choi D, Lee SJ, Hong S, Kim IH, Kang S. Prohibitin interacts with RNF2 and regulates E2F1 function via dual pathways. Oncogene. 2008;27(12):1716-25.

188. Di Croce L, Helin K. Transcriptional regulation by Polycomb group proteins. Nat Struct Mol Biol. 2013;20(10):1147-55.

189. Lee SJ, Choi D, Rhim H, Choo HJ, Ko YG, Kim CG, et al. PHB2 interacts with RNF2 and represses CP2c-stimulated transcription. Mol Cell Biochem. 2008;319(1-2):69-77.

190. Bosch A, Panoutsopoulou K, Corominas JM, Gimeno R, Moreno-Bueno G, Martin-Caballero J, et al. The Polycomb group protein RING1B is overexpressed in ductal breast carcinoma and is required to sustain FAK steady state levels in breast cancer epithelial cells. Oncotarget. 2014;5(8):2065-76.

191. Su WJ, Fang JS, Cheng F, Liu C, Zhou F, Zhang J. RNF2/Ring1b negatively regulates p53 expression in selective cancer cell types to promote tumor development. Proc Natl Acad Sci U S A. 2013;110(5):1720-5.

192. Qu C, Qu Y. Down-regulation of salt-inducible kinase 1 (SIK1) is mediated by RNF2 in hepatocarcinogenesis. Oncotarget. 2017;8(2):3144-55.

193. Rai K, Akdemir KC, Kwong LN, Fiziev P, Wu CJ, Keung EZ, et al. Dual Roles of RNF2 in Melanoma Progression. Cancer Discov. 2015;5(12):1314-27.

194. Zhang J, Sun Z, Han Y, Yao R, Yue L, Xu Y, et al. Rnf2 knockdown reduces cell viability and promotes cell cycle arrest in gastric cancer cells. Oncol Lett. 2017;13(5):3817-22.

195. Wei M, Jiao D, Han D, Wu J, Wei F, Zheng G, et al. Knockdown of RNF2 induces cell cycle arrest and apoptosis in prostate cancer cells through the upregulation of TXNIP. Oncotarget. 2017;8(3):5323-38.

196. Scharping NE, Delgoffe GM. Tumor Microenvironment Metabolism: A New Checkpoint for Anti-Tumor Immunity. Vaccines. 2016;4(4).

197. Kumar A, Giri S, Shaha C. Sestrin2 facilitates glutamine-dependent transcription of PGC-1alpha and survival of liver cancer cells under glucose limitation. FEBS J. 2018;285(7):1326-45.

198. Jones RG, Thompson CB. Tumor suppressors and cell metabolism: a recipe for cancer growth. Genes Dev. 2009;23(5):537-48.

199. Shortt J, Johnstone RW. Oncogenes in cell survival and cell death. Cold Spring Harb Perspect Biol. 2012;4(12).

200. Choo AY, Kim SG, Vander Heiden MG, Mahoney SJ, Vu H, Yoon SO, et al. Glucose addiction of TSC null cells is caused by failed mTORC1-dependent balancing of metabolic demand with supply. Mol Cell. 2010;38(4):487-99.

201. Marin-Aguilar F, Pavillard LE, Giampieri F, Bullon P, Cordero MD. Adenosine Monophosphate (AMP)-Activated Protein Kinase: A New Target for Nutraceutical Compounds. Int J Mol Sci. 2017;18(2).

202. Mai H, Xu X, Mei G, Hong T, Huang J, Wang T, et al. The interplay between HPIP and casein kinase 1alpha promotes renal cell carcinoma growth and metastasis via activation of mTOR pathway. Oncogenesis. 2016;5(10):e260.

203. Dwivedi A, Padala C, Kumari A, Khumukcham SS, Penugurti V, Ghosh S, et al. Hematopoietic PBX-interacting protein is a novel regulator of mammary epithelial cell differentiation. FEBS J. 2021.

204. Brunet A, Sweeney LB, Sturgill JF, Chua KF, Greer PL, Lin Y, et al. Stress-dependent regulation of FOXO transcription factors by the SIRT1 deacetylase. Science. 2004;303(5666):2011-5.

205. T.Tsunoda TT. Estimating Transcription Factor Bindability on DNA. BIOINFORMATICS. 1999;Vol.15, No.7/8:pp.622-30.

206. Messeguer X, Escudero R, Farre D, Nunez O, Martinez J, Alba MM. PROMO: detection of known transcription regulatory elements using species-tailored searches. Bioinformatics. 2002;18(2):333-4.

207. Farre D, Roset R, Huerta M, Adsuara JE, Rosello L, Alba MM, et al. Identification of patterns in biological sequences at the ALGGEN server: PROMO and MALGEN. Nucleic Acids Res. 2003;31(13):3651-3.

208. Webb AE, Kundaje A, Brunet A. Characterization of the direct targets of FOXO transcription factors throughout evolution. Aging Cell. 2016;15(4):673-85.

209. Peng GH. CS. Double Chromatin Immunoprecipitation: Analysis of Target Co-occupancy of Retinal Transcription Factors.: Humana Press, Totowa, NJ; 2012 22 September 2012.

210. Rueden CT, Schindelin J, Hiner MC, DeZonia BE, Walter AE, Arena ET, et al. ImageJ2: ImageJ for the next generation of scientific image data. BMC bioinformatics. 2017;18(1):529.

211. Gilkerson J, Kelley DR, Tam R, Estelle M, Callis J. Lysine Residues Are Not Required for Proteasome-Mediated Proteolysis of the Auxin/Indole Acidic Acid Protein IAA1. Plant Physiol. 2015;168(2):708-20.

212. J. Gilkerson RT, A. Zhang, K. Dreher, J. Callis. Cycloheximide assays to measure protein degradation in vivo in plants. BioProtocol. 2016;6.

213. Have KHSt. Cellular Fractionation Protocol. 2012.

214. Liu K, Liu PC, Liu R, Wu X. Dual AO/EB staining to detect apoptosis in osteosarcoma cells compared with flow cytometry. Med Sci Monit Basic Res. 2015;21:15-20.

215. Cerami E, Gao J, Dogrusoz U, Gross BE, Sumer SO, Aksoy BA, et al. The cBio cancer genomics portal: an open platform for exploring multidimensional cancer genomics data. Cancer Discov. 2012;2(5):401-4.

216. Gao J, Aksoy BA, Dogrusoz U, Dresdner G, Gross B, Sumer SO, et al. Integrative analysis of complex cancer genomics and clinical profiles using the cBioPortal. Sci Signal. 2013;6(269):pl1.

217. Rhodes DR, Yu J, Shanker K, Deshpande N, Varambally R, Ghosh D, et al. ONCOMINE: a cancer microarray database and integrated data-mining platform. Neoplasia. 2004;6(1):1-6.

218. Tang Z, Li C, Kang B, Gao G, Li C, Zhang Z. GEPIA: a web server for cancer and normal gene expression profiling and interactive analyses. Nucleic Acids Res. 2017;45(W1):W98-W102.

219. Greer EL, Oskoui PR, Banko MR, Maniar JM, Gygi MP, Gygi SP, et al. The energy sensor AMP-activated protein kinase directly regulates the mammalian FOXO3 transcription factor. The Journal of biological chemistry. 2007;282(41):30107-19.

220. Lee JV, Carrer A, Shah S, Snyder NW, Wei S, Venneti S, et al. Akt-dependent metabolic reprogramming regulates tumor cell histone acetylation. Cell metabolism. 2014;20(2):306-19.

221. Zhao X, Petrashen AP, Sanders JA, Peterson AL, Sedivy JM. SLC1A5 glutamine transporter is a target of MYC and mediates reduced mTORC1 signaling and increased fatty acid oxidation in long-lived Myc hypomorphic mice. Aging Cell. 2019;18(3):e12947.

222. Li J, Li X, Wu L, Pei M, Li H, Jiang Y. miR-145 inhibits glutamine metabolism through c-myc/GLS1 pathways in ovarian cancer cells. Cell Biol Int. 2019;43(8):921-30.

223. Sen N, Satija YK, Das S. PGC-1alpha, a key modulator of p53, promotes cell survival upon metabolic stress. Mol Cell. 2011;44(4):621-34.

224. Shin S, Buel GR, Wolgamott L, Plas DR, Asara JM, Blenis J, et al. ERK2 Mediates Metabolic Stress Response to Regulate Cell Fate. Molecular cell. 2015;59(3):382-98.

225. Isono T, Chano T, Kitamura A, Yuasa T. Glucose deprivation induces G2/M transition-arrest and cell death in N-GlcNAc2-modified protein-producing renal carcinoma cells. PloS one. 2014;9(5):e96168.

226. Ding B, Parmigiani A, Divakaruni AS, Archer K, Murphy AN, Budanov AV. Sestrin2 is induced by glucose starvation via the unfolded protein response and protects cells from non-canonical necroptotic cell death. Scientific reports. 2016;6:22538.

227. Redza-Dutordoir M, Averill-Bates DA. Activation of apoptosis signalling pathways by reactive oxygen species. Biochimica et biophysica acta. 2016;1863(12):2977-92.

228. Lilienbaum A. Relationship between the proteasomal system and autophagy. Int J Biochem Mol Biol. 2013;4(1):1-26.

229. Kato K, Ogura T, Kishimoto A, Minegishi Y, Nakajima N, Miyazaki M, et al. Critical roles of AMP-activated protein kinase in constitutive tolerance of cancer cells to nutrient deprivation and tumor formation. Oncogene. 2002;21(39):6082-90.

230. Chhipa RR, Wu Y, Mohler JL, Ip C. Survival advantage of AMPK activation to androgen-independent prostate cancer cells during energy stress. Cellular signalling. 2010;22(10):1554-61.

231. Godlewski J, Nowicki MO, Bronisz A, Nuovo G, Palatini J, De Lay M, et al. MicroRNA-451 regulates LKB1/AMPK signaling and allows adaptation to metabolic stress in glioma cells. Molecular cell. 2010;37(5):620-32.

232. Hardie DG. AMP-activated protein kinase: an energy sensor that regulates all aspects of cell function. Genes Dev. 2011;25(18):1895-908.

233. Shaw RJ, Kosmatka M, Bardeesy N, Hurley RL, Witters LA, DePinho RA, et al. The tumor suppressor LKB1 kinase directly activates AMP-activated kinase and regulates apoptosis in response to energy stress. Proceedings of the National Academy of Sciences of the United States of America. 2004;101(10):3329-35.

234. Shackelford DB, Shaw RJ. The LKB1-AMPK pathway: metabolism and growth control in tumour suppression. Nat Rev Cancer. 2009;9(8):563-75.

235. Cantor JR, Sabatini DM. Cancer cell metabolism: one hallmark, many faces. Cancer Discov. 2012;2(10):881-98.

236. Barron CC, Bilan PJ, Tsakiridis T, Tsiani E. Facilitative glucose transporters: Implications for cancer detection, prognosis and treatment. Metabolism. 2016;65(2):124-39.

237. Horie T, Ono K, Nagao K, Nishi H, Kinoshita M, Kawamura T, et al. Oxidative stress induces GLUT4 translocation by activation of PI3-K/Akt and dual AMPK kinase in cardiac myocytes. J Cell Physiol. 2008;215(3):733-42.

238. Farhan M, Silva M, Li S, Yan F, Fang J, Peng T, et al. The role of FOXOs and autophagy in cancer and metastasis-Implications in therapeutic development. Med Res Rev. 2020;40(6):2089-113.

239. Thorburn A, Thamm DH, Gustafson DL. Autophagy and cancer therapy. Mol Pharmacol. 2014;85(6):830-8.

240. Jeon SM, Hay N. The double-edged sword of AMPK signaling in cancer and its therapeutic implications. Arch Pharm Res. 2015;38(3):346-57.

241. Huang X, Li X, Xie X, Ye F, Chen B, Song C, et al. High expressions of LDHA and AMPK as prognostic biomarkers for breast cancer. Breast. 2016;30:39-46.

242. Simone Fulda AMG, Osamu Hori, Afshin Samali. Cellular Stress Responses: Cell Survival and Cell Death. International Journal of Cell Biology. 2010;vol. 2010:23 pages.

243. Ohtsubo M, Yasunaga S, Ohno Y, Tsumura M, Okada S, Ishikawa N, et al. Polycomb-group complex 1 acts as an E3 ubiquitin ligase for Geminin to sustain hematopoietic stem cell activity. Proceedings of the National Academy of Sciences of the United States of America. 2008;105(30):10396-401.

244. He M, Chaurushiya MS, Webster JD, Kummerfeld S, Reja R, Chaudhuri S, et al. Intrinsic apoptosis shapes the tumor spectrum linked to inactivation of the deubiquitinase BAP1. Science. 2019;364(6437):283-5.

Thesis Publications

Cancer Letters 518 (2021) 243–255

Contents lists available at ScienceDirect

Cancer Letters

journal homepage: www.elsevier.com/locate/canlet

HPIP protooncogene differentially regulates metabolic adaptation and cell fate in breast cancer cells under glucose stress via AMPK and RNF2 dependent pathways

Vasudevarao Penugurti [a], Saratchandra Singh Khumukcham [a], Chiranjeevi Padala [a], Anju Dwivedi [a], Karthik Reddy Kamireddy [b,d], Srinivasulu Mukta [c], Triveni Bhopal [c], Bramanandam Manavathi [a,*]

[a] Molecular and Cellular Oncology Laboratory, Department of Biochemistry, School of Life Sciences, University of Hyderabad, Hyderabad, 500046, Telangana, India
[b] Molecular and Cellular Biology Laboratory, Baylor College of Medicine, Houston, TX, United States
[c] MNJ Institute of Oncology and Regional Cancer Center, Hyderabad, 500004, Telangana, India
[d] Indian Institute of Chemical Technology, Hyderabad, Telangana, 500007, India

ARTICLE INFO

Keywords:
HPIP
FOXO3a
AMPK
MYC
Cell survival
Apoptosis
Glutaminolysis

ABSTRACT

While cancer cells rewire metabolic pathways to sustain growth and survival under metabolic stress in solid tumors, the molecular mechanisms underlying these processes remain largely unknown. In this study, cancer cells switched from survival to death during the early to late phases of metabolic stress by employing a novel signaling switch from AMP activated protein kinase (AMPK)-Forkhead box O3 (FOXO3a)-hematopoietic PBX1-interacting protein (HPIP) to the ring finger protein 2 (RNF2)-HPIP-ubiquitin (Ub) pathway. Acute metabolic stress induced proto-oncogene *HPIP* expression in an AMPK-FOXO3a-dependent manner in breast cancer (BC) cells. HPIP depletion reduced cell survival and tumor formation in mouse xenografts, which was accompanied by diminished intracellular ATP levels and increased apoptosis in BC cells in response to metabolic (glucose) stress. Glutamine flux (^{13}C-labeled) analysis further suggested that HPIP rewired glutamine metabolism by controlling the expression of the solute carrier family 1 member 5 (SLC1A5) and glutaminase (GLS) genes by acting as a coactivator of MYC to ensure cell survival upon glucose deprivation. However, in response to chronic glucose stress, HPIP was ubiquitinated by the E3-Ub ligase, RNF2, and was concomitantly degraded by the proteasome-mediated pathway, ensuring apoptosis. In support of these data, clinical analyses further indicated that elevated levels of HPIP correlated with AMPK activation in BC. Taken together, these data suggest that HPIP is a signal coordinator during metabolic stress and thus serves as a potential therapeutic target in BC.

1. Introduction

For rapidly dividing cells, such as cancer cells, there is a huge demand for metabolic energy to synthesize various biomolecules. To accomplish this, cancer cells often rewire metabolic pathways to suit their needs [1–3]. As glucose is the main energy and carbon source for rapidly dividing cells, cancer cells rely on glycolysis to generate energy; however, under glucose stress, glutamine is utilized as an anaplerotic substance for ATP generation and to control redox homeostasis, thus ensuring cell survival [1,4,5]. Typically, reduced expression of tumor suppressor genes and increased oncogenic gene expression is observed in cancer cells during metabolic stress as a part of cellular adaptation [6]. For example, oncogenes, such as protein kinase B (AKT), c-MYC (hereafter referred to as MYC), and Ras are overexpressed under metabolic stress to support cancer cell survival [7].

A balance between energy production and consumption dictates cell survival under metabolic stress [8]. Accordingly, in such situations, tumor cells acquire certain adaptations for their survival by suppressing energy-consuming pathways and promoting energy-producing pathways [9]. One such adaptation is the expression of AMP activated protein kinase (AMPK), a metabolic sensor, which is activated in response to a low ATP:AMP ratio in cells [10,11]. For example, AMPK-mediated pyruvate kinase M1 expression is essential for cell survival under hypoglycemic conditions [12] and modulates the expression of

* Corresponding author.
E-mail address: manavathibsl@uohyd.ac.in (B. Manavathi).

https://doi.org/10.1016/j.canlet.2021.07.027
Received 23 April 2021; Received in revised form 27 June 2021; Accepted 19 July 2021
Available online 22 July 2021

Other Publications

Hematopoietic PBX-interacting protein is a novel regulator of mammary epithelial cell differentiation

Authors and Affiliations

Anju Dwivedi[a], Chiranjeevi Padala[a], Anita Kumari[a], Saratchandra Singh Khumukcham[a], Vasudevarao Penugurti[a], Sinjini Ghosh[b], Aprotim Mazumder[b], Vincent Goffin[c] and Bramanandam Manavathi[a]*

[a]Department of Biochemistry, School of Life Sciences, University of Hyderabad, Hyderabad, 500046, Telangana, India

[b]TIFR Centre for Interdisciplinary Sciences, Tata Institute of Fundamental Research Hyderabad, Hyderabad, 500046, Telangana, India.

[c]Institut Necker Enfants Malades (INEM), Inserm U1151/CNRS 8253, Université de Paris, 75015, Paris, France

***Correspondence:** Dr. Bramanandam Manavathi, Professor, Department of Biochemistry, School of Life Sciences, University of Hyderabad, Hyderabad-500046, India. Email: manavathibsl@uohyd.ac.in; manavathi.hcu@gmail.com

Running Title: PRL-HPIP-miR-148a loop regulates lactogenic differentiation

Abbreviations

HPIP: Hematopoietic PBX-interacting protein

EMT: Epithelial to mesenchyme transition

PTEN: Phosphatase and Tensin Homolog deleted on Chromosome 10

PI3K: Phosphoinositide 3-kinase

AKT: Protein kinase B

STAT5: Signal transducer and activator of transcription 5

JAK2: Janus kinase 2

miR-148a: microRNA-148a

bPRL: bovine prolactin

PRKCA: Protein kinase Cα

PRL: Prolactin

This article has been accepted for publication and undergone full peer review but has not been through the copyediting, typesetting, pagination and proofreading process, which may lead to differences between this version and the Version of Record. Please cite this article as doi: 10.1111/febs.16242

Hematopoietic PBX-interacting protein is a substrate and an inhibitor of the APC/C–Cdc20 complex and regulates mitosis by stabilizing cyclin B1

Received for publication, November 15, 2018, and in revised form, April 27, 2019 Published, Papers in Press, May 17, 2019, DOI 10.1074/jbc.RA118.006733

Saratchandra Singh Khumukcham[‡1], Venkata Subramanyam Kumar Samanthapudi[‡1], Vasudevarao Penugurti[‡1], Anita Kumari[‡], P. S. Kesavan[§], Loka Reddy Velatooru[‡], Siva Reddy Kotla[‡], Aprotim Mazumder[§], and Bramanandam Manavathi[‡2]

From the [‡]Department of Biochemistry, School of Life Sciences, University of Hyderabad, Hyderabad 500046, India and the [§]Centre for Interdisciplinary Sciences, Tata Institute of Fundamental Research Hyderabad, Hyderabad 500107, Telangana, India

Edited by Xiao-Fan Wang

Proper cell division relies on the coordinated regulation between a structural component, the mitotic spindle, and a regulatory component, anaphase-promoting complex/cyclosome (APC/C). Hematopoietic PBX-interacting protein (HPIP) is a microtubule-associated protein that plays a pivotal role in cell proliferation, cell migration, and tumor metastasis. Here, using HEK293T and HeLa cells, along with immunoprecipitation and immunoblotting, live-cell imaging, and protein-stability assays, we report that HPIP expression oscillates throughout the cell cycle and that its depletion delays cell division. We noted that by utilizing its D box and IR domain, HPIP plays a dual role both as a substrate and inhibitor, respectively, of the APC/C complex. We observed that HPIP enhances the G_2/M transition of the cell cycle by transiently stabilizing cyclin B1 by preventing APC/C–Cdc20–mediated degradation, thereby ensuring timely mitotic entry. We also uncovered that HPIP associates with the mitotic spindle and that its depletion leads to the formation of multiple mitotic spindles and chromosomal abnormalities, results in defects in cytokinesis, and delays mitotic exit. Our findings uncover HPIP as both a substrate and an inhibitor of APC/C–Cdc20 that maintains the temporal stability of cyclin B1 during the G_2/M transition and thereby controls mitosis and cell division.

Accurate chromosome segregation is essential for proper cell division in normal cells. Two important post-translational modifications, phosphorylation, and ubiquitin-mediated proteolysis during mitosis, play crucial roles in this process (1). The anaphase promoting complex/cyclosome (APC/C),[3] a ubiquitin ligase, controls the cell division by regulating mitosis through ubiquitin-directed proteolysis of key substrates in an ordered fashion to direct progression through the mitotic exit, chromosome segregation, and cytokinesis (2–4). The activity of APC/C is coordinated by two regulatory proteins, Cdc20 and Cdh1, through phase-specific interactions during the cell cycle and promotes cell division with precision and accuracy (5). For example, APC/C–Cdc20 degrades Securin and cyclin B1 at anaphase onset. This ensures Separase activation and proteolysis of Cohesin, which holds pair of sister chromatids together during early mitosis. The spindle assembly checkpoint, which depends on multiprotein complexes including Mad2, BubR1, and Bub3, delays APC/C–Cdc20 activation until all chromosomes are properly aligned at the metaphase plate (6, 7). Perturbation of this checkpoint results in chromosomal abnormality (8).

Entry into mitosis is coordinated by cyclin B1–dependent activation of cyclin-dependent kinase 1 (CDK1) during G_2 phase and form a Cdk1–cyclin B1 complex also known as maturation-promoting factor, which is crucial for G_2/M transition (9). Cyclin B1 accumulates in the nucleus as the cells progress to mitosis, although the activation of CDK1–cyclin B1 is initiated at the cytoplasm (10). Cyclin B1 binding triggers a conformational change in Wee1 phosphorylated and inactive CDK1, restoring the activity in CDK1 (11). The activated CDK1–cyclin B1 complex triggers initiation of chromosome condensation, nuclear envelope breakdown, and mitotic spindle assembly through phosphorylation of its substrates (10). It also phosphorylates APC/C–Cdc20 for its complete activation, but later during mitosis cyclin B1 is degraded by APC/C–Cdc20 (12, 13). Abolishing the degradation of cyclin B1 leads to arrest of cells in mitosis, suggesting timely degradation of cyclin B1 by APC/C, is important for proper cell cycle progression (14, 15). Although transcriptional up-regulation of cyclin B1 and its increased stability of mRNA during the G_2 phase has been described before (16), the role of proteasomal pathway in increased cyclin B1 levels is largely unknown.

Hematopoietic PBX-interacting protein (HPIP, also known as PBXIP1) is a protooncoprotein that has been shown to be overexpressed in several cancer types including infiltrative ductal carcinoma (17), hepatocellular carcinoma (18), glioma (19), and ovarian cancer (20). Previous reports have shown that HPIP promotes cell proliferation by modulating the expression of cyclins during the

This work was supported by Department of Biotechnology, India Grants BT/PR7672/BRB/10/1173/2013, BT/Med/30/SP11273/2015, and BT/PR8764/MED/97/104/2013 and Department of Science and Technology, India Grant SB/SO/BB/013/2013 (to B. M.). The authors declare that they have no conflicts of interest with the contents of this article.

This article contains supporting "Materials and methods," Tables S1 and S2, Figs. S1 and S2, and Videos S1–S13.

[1] These authors contributed equally to this work.

[2] To whom correspondence should be addressed. E-mail: manavbrahma@gmail.com.

[3] The abbreviations used are: APC/C, anaphase-promoting complex/cyclosome; HPIP, hematopoietic PBX-interacting protein; CDK, cyclin-dependent kinase; DT, double thymidine; DMEM, Dulbecco's modified Eagle's medium; DAPI, 4′,6′-diamino-2-phenylindole; SAC, spindle assembly checkpoint; MCC, mitotic checkpoint complex.

Cell Oncol.
DOI 10.1007/s13402-016-0308-2

ORIGINAL PAPER

HPIP promotes epithelial-mesenchymal transition and cisplatin resistance in ovarian cancer cells through PI3K/AKT pathway activation

Suresh Bugide[1] · Vijay Kumar Gonugunta[2] · Vasudevarao Penugurti[1] · Vijaya Lakshmi Malisetty[3] · Ratna K. Vadlamudi[2] · Bramanandam Manavathi[1]

Accepted: 1 December 2016

Abstract
Purpose Hematopoietic PBX interacting protein (HPIP), a scaffold protein, is known to regulate the proliferation, migration and invasion in different cancer cell types. The aim of this study was to assess the role of HPIP in ovarian cancer cell migration, invasion and epithelial-mesenchymal transition (EMT), and to unravel the mechanism by which it regulates these processes.
Methods HPIP expression was assessed by immunohistochemistry of tissue microarrays containing primary ovarian tumor samples of different grades. OAW42, an ovarian carcinoma-derived cell line exhibiting a high HPIP expression, was used to study the role of HPIP in cell migration, invasion and EMT. HPIP knockdown in these cells was achieved using a small hairpin RNA (shRNA) approach. Cell migration and invasion were assessed using scratch wound and transwell invasion assays, respectively. The extent of EMT was assessed by determining the expression levels of Snail, Vimentin and E-cadherin using Western blotting. The effect of HPIP expression on AKT and MAPK activation was also investigated by Western blotting. Cell viabilities in response to cisplatin treatment were assessed using a MTT assay, whereas apoptosis was assessed by determining caspase-3 and PARP cleavage in ovarian carcinoma-derived SKOV3 cells.
Results We found that HPIP is highly expressed in high-grade primary ovarian tumors. In addition, we found that HPIP promotes the migration, invasion and EMT in OAW42 cells and induces EMT in these cells via activation of the PI3K/AKT pathway. The latter was found to lead to stabilization of the Snail protein and to repression of E-cadherin expression through inactivation of GSK-3β. We also found that HPIP expression confers cisplatin resistance to SKOV3 cells after prolonged exposure and that its subsequent knockdown decreases the viability of these cells and increases caspase-3 activation and PARP proteolysis in these cells following cisplatin treatment.
Conclusions From these results we conclude that HPIP expression is associated with high-grade ovarian tumors and may promote their migration, invasion and EMT, a process that is associated with metastasis. In addition, we conclude that HPIP may serve as a potential therapeutic target for cisplatin resistant ovarian tumors.

Keywords HPIP/PBXIP1 · PI3K/AKT pathway · Ovarian cancer · Epithelial-mesenchymal transition (EMT) · Cell migration

Abbreviations

HPIP/ PBXIP1	Hematopoietic PBX interacting protein/ pre B-cell leukemia homeobox interacting protein
EMT	Epithelial-mesenchymal transition
GSK-3β	Glycogen synthase kinase-3β

Vijay Kumar Gonugunta and Vasudevarao Penugurti contributed equally to this work

Electronic supplementary material The online version of this article (doi:10.1007/s13402-016-0308-2) contains supplementary material, which is available to authorized users.

✉ Bramanandam Manavathi
manavbrahma@gmail.com; manavathilab@gmail.com

[1] Department of Biochemistry, School of Life Sciences, University of Hyderabad, Hyderabad 500046, India

[2] Department of Obstetrics and Gynecology, UT Health Science Center, San Antonio, USA

[3] Department of Biotechnology, Acharya Nagarjuna University, Guntur, AP, India

Published online: 30 December 2016

Biomedicine & Pharmacotherapy 95 (2017) 956–964

Contents lists available at ScienceDirect

Biomedicine & Pharmacotherapy

journal homepage: www.elsevier.com/locate/biopha

Review

MTA1 expression in human cancers – Clinical and pharmacological significance

Vijaya Lakshmi Malisetty[a], Vasudevarao Penugurti[b], Prashanth Panta[c], Suresh Kumar Chitta[d], Bramanandam Manavathi[b,*]

[a] Department of Biotechnology, Acharya Nagarjuna University, Guntur, AP, India
[b] Department of Biochemistry, School of Life Sciences, University of Hyderabad, Hyderabad, 500046, India
[c] Department of Oral Medicine and Radiology, MNR Dental College and Hospital, Sangareddy, Telangana, India
[d] Department of Biochemistry, Sri Krishnadevaraya University, Anantapuramu, AP, India

ARTICLE INFO

Keywords:
MTA1
Tumor metastasis
NuRD
Epigenetic gene regulation
Drug targets

ABSTRACT

Remarkably, majority of the cancer deaths are due to metastasis, not because of primary tumors. Metastasis is one of the important hallmarks of cancer. During metastasis invasion of primary tumor cells from the site of origin to a new organ occurs. Metastasis associated proteins (MTAs) are a small family of transcriptional co-regulators that are closely associated with tumor metastasis. These proteins are integral components of nuclear remodeling and deacetylation complex (NuRD). By virtue of being integral components of NuRD, these proteins regulate the gene expression by altering the epigenetic changes such as acetylation and methylation on the target gene chromatin. Among the MTA proteins, MTA1 expression is very closely correlated with the aggressiveness of several cancers that includes breast, liver, colon, pancreas, prostate, blood, esophageal, gastro-intestinal etc. Considering its close association with aggressiveness in human cancers, MTA1 may be considered as a potential therapeutic target for cancer treatment. The recent developments in its crystal structure further strengthened the idea of developing small molecule inhibitors for MTA1. In this review, we discuss the recent trends on the diverse functions of MTA1 and its role in various cancers, with the focus to consider MTA1 as a 'druggable' target in the control of human cancers.

1. Introduction

Cancer is a disease of a mass of mutated cells which undergo uncontrollable cell divisions. As mentioned in the book 'The Emperor of All Melodies-A Biography of Cancer'-by Siddartha Mukharjee, cancer is an uncommited crime. Every year, millions of people around the world die of various cancers. Approximately, 1,685,210 new cases were diagnosed and 595,690 deaths were registered duing 2016 in USA [1]. Remarkably, large number of cancer deaths are due to metastasis, and not because of the primary tumors. Metastasis is therefore one of the important hallmarks of cancer [2]. During metastasis, invasion of primary tumor cells from the site of origin to a new organ occur establishing the malignant tumor at distant location. Size of the tumor appears to be one of the critical factor for tumor metastasis. As the tumor size exceeds 1 cm, these tumor cells tend to metastasize to the secondary sites. Typically, metastasis involves the detachment of primary epithelial cancer cells by loss of E-cadherin, an epithelial marker, resulting in acquisition of mesenchymal phenotype, a process known as epithelial to mesenchymal transition (EMT) [3]. After detaching from the primary tumor through EMT, the disseminated cells enter the blood circulation through cell migration and invasion followed by intravasation. The circulating tumor cells enter the secondary site through extravasation and acclimatizes with the tissue to establish metastasis (Fig. 1). Establishment of secondary tumor is dependent on multiple factors and each primary tumor exibits tissue trophism. For instance, breast tumors are known to metastasize into specific tissues in the order of priority: bone, liver, lung and brain. Given the importance, identification and charactarization of the regulators of tumor metastasis and more importantly, understanding the molecular mechanisms and pathways involved in this critical process is crucial to consider them as

Abbreviations: MTAs, metastasis associated proteins; EMT, epithelial to mesenchymal transition; NuRD, nuclear remodeling and deacetylation complex; HDAC1 or HDAC2, histone deacetylases; MBD, methylated CpG binding domain proteins; RbAb46/48, retinoblastoma associated protein; DOC1, deleted in oral cancer; SAHA, suberoylanilide hydroxamic acid; TSA, trichostatin A; PTER, pterostilbene; E2, estradiol; ERα, estrogen receptor alpha; Gd@$C_{82}(OH)_{22}$, a gadolinium metallofullerenol nanoparticles; SERM, selective estrogen receptor modulators

* Corresponding author.
E-mail addresses: manavathibsl@uohyd.ernet.in, manavbrahma@gmail.com (B. Manavathi).

http://dx.doi.org/10.1016/j.biopha.2017.09.025
Received 2 August 2017; Received in revised form 1 September 2017; Accepted 6 September 2017

Journal of Non-Crystalline Solids 574 (2021) 121164

Contents lists available at ScienceDirect

Journal of Non-Crystalline Solids

journal homepage: www.elsevier.com/locate/jnoncrysol

In vitro studies of B_2O_3–SiO_2–Na_2O–CaO–ZnO bioactive glass system

Raj Kumar Samudrala [a], Sushil Patel [a], Vasudevarao Penugurthi [b], Bramanandam Manavathi [b], Abdul Azeem P [a,*]

[a] Department of Physics, National Institute of Technology Warangal, Warangal-506004, India
[b] Department of Biochemistry, School of Life Sciences, University of Hyderabad, Hyderabad, India

ARTICLE INFO

Keywords:
Bioactivity
Cytocompatibility
Osteoblast cells
Tissue engineering

ABSTRACT

The main purpose of the present investigation is to examine in detail *in vitro* studies like bioactivity and cytocompatibility of a novel bioactive glass system i.e., B_2O_3–SiO_2–Na_2O–CaO–ZnO glass composition. Glasses are prepared by the traditional melt quenching method. In vitro studies are performed with ISO standards. Bioactivity has been studied using standard Kokubo's method. Highly sophisticated analytical techniques were utilized for the assessment of apatite forming ability. Scanning electron microscopy micrographs have shown visible evidence of apatite forming ability through cauliflower type of precipitation on the surface of the glass. Cytocompatibility was performed using human osteoblast cells (MG-63). Cytocompatibility of zinc-containing soda lime borosilicate glasses has shown significant results for bone tissue engineering applications.

1. Introduction

One of the important innovations for mankind in the last century was the gold standard 45S5 bioglass. It is the first man-made biomaterial so far. One of the first clinical applications of bioactive glass was to restore the hearing disability of patients by middle ear implants. SiO_2 – Na_2O – CaO – P_2O_5 system has been the first bioactive glass developed by Larry Hench et al [1]. After the invention of the 45S5 glass system, many glass and glass-ceramic systems have been developed for orthopedic and dental applications [2–4].

Since the discovery of glass, borate-based glasses have been very useful materials in optical and most engineering applications. From the past two decades, borate-based glasses have also been used in medical applications such as implant materials [5]. Borate-based glasses were found to be significant materials in curing chronic wounds. Even though borate-based glasses are useful biological materials, there are only limited studies [6–9]. Studies by D. E. Day et al [10] have contributed significantly to the scientific fraternity in terms of the development of new borate-based glass materials. As part of the study, glass spheres were prepared using the glass system B_2O_3– Dy_2O_3– Li_2O – MgO – Al_2O_3– SiO_2. Bioactivity was studied in phosphate-buffered saline. The transformation of glass into medical material depends on glass design, ingredients in the body fluid, and temperature. The transformation rate was also affected by the addition of different oxide materials. Some important findings in the transformation process are, borate glass is fully transformed into strange material within a few hours at low temperatures, say, nearly 50°C. The material composition thus obtained can be modified by altering the composition of starting material and associated body fluid. The size of the glass particle does not change during the transformation process, so the size of the final material can be adjusted by using particles of the desired size.

Several authors have reported that borate and borosilicate bioactive glasses show higher dissolution nature [11,12]. To improve the properties of the glass system, some of the transition elements are the best candidates which can be incorporated during the synthesis process. Zinc is one of the important and essential inorganic trace elements in the human body, which is available in 1.5-2.5 g in different parts of the biological tissues [13]. Zinc plays a unique role in bone formation in vitro by the stimulation of protein synthesis in osteoblast cells and to prevent bone resorption by inhibiting the formation of osteoclast cells [14].

Aina et al [15,16], developed zinc-containing 45S5 bioglass by conventional melt quenching method and studied biological properties with human osteoblast cells and endothelial cells. Irrespective of the concentration of zinc content in the bioactive glass system, the bioactive glass showed toxicity to human osteoblast cells. A higher amount of zinc content inhibited bioactivity. Balamurugan et al [17] synthesized zinc-containing silico phosphate bioactive glass using the sol-gel method. The addition of about 5 mol% of zinc did not retard the bioactivity of the glass system. Biological studies like cell proliferation

* Corresponding author.
E-mail addresses: drazeem2002@yahoo.com, drazeem2002@gmail.com (A.A. P).

https://doi.org/10.1016/j.jnoncrysol.2021.121164
Received 13 July 2021; Received in revised form 29 August 2021; Accepted 2 September 2021

Carbohydrate Polymer Technologies and Applications 2 (2021) 100077

Contents lists available at ScienceDirect

Carbohydrate Polymer Technologies and Applications

journal homepage: www.elsevier.com/locate/carpta

Chitooligosaccharides induce apoptosis in human breast cancer cells

Mohan Krishna Mallakuntla [a], Vasudevarao Penugurti [b], Bramanandam Manavathi [b], Appa Rao Podile [a,*]

[a] Department of Plant Sciences, School of Life Sciences, University of Hyderabad, Gachibowli, Hyderabad, Telangana 500046, India
[b] Department of Biochemistry, School of Life Sciences, University of Hyderabad, Gachibowli, Hyderabad, Telangana 500046, India

ARTICLE INFO

Keywords:
Chitooligosaccharides
Breast cancer and Apoptosis

ABSTRACT

In this study, biologically active chitooligosaccharides (COS) D_{3-7} (D-deacetylated unit) and A_5 (A-acetylated unit) were assessed for their suitability to reduce the viability of human breast cancer cell lines, BT-474 and SUM-159. The treatment with COS resulted in a significant decrease in the viability of breast cancer cells, in a dose-dependent manner. The long-term proliferative potential of breast cancer cells decreased upon COS treatment, suggesting that COS significantly inhibited colony formation in breast cancer cells. The COS-treated cell population significantly underwent apoptosis, confirmed by flow cytometry. Further, the increased expression of BAX, cleaved PARP, and cleaved caspase 3, with increased concentration of COS, conformed that COS-D_{3-7} and A_5 induce apoptosis in BT474 cells through apoptotic signaling. We further investigated the mechanism by which COS promotes apoptosis. The marked inhibition of phosphorylation of EGFR and its downstream signaling molecules FAK, AKT, and MAPKpromote apoptosis.

1. Introduction

In women, breast cancer is the most common cancer in the world. The occurrence of this aggressive disease with approximately 17 million new cases is increasing each year (Anastasiadi, Lianos, Ignatiadou, Harissis, & Mitsis, 2017). Breast cancer remains a major health problem and remained biomedical research priority. Research efforts have been made, over the past decade, to reduce breast cancer burden. Breast cancer is a heterogeneous disease with different molecular, cellular, and morphological features (Gajulapalli, Malisetty, Chitta, & Manavathi, 2016). Due to this very nature, there is a continuous raise in the mortality of breast cancer patients. Various combinations of treatments like surgery, chemotherapy, and radiotherapy are available for treatment. However, most of the drugs have displayed resistance, incomplete effectiveness, toxicity, tumor recurrence, aggressiveness, etc., (Kim, Kang, Choi, & Ko, 2015), leaving scope for the development of natural products with anti-tumor effects.

The hydrolytic products of chitin and chitosan are called chitooligosaccharides (COS). COS have wide-ranging biological applications in agriculture, cosmetics, and health care (Das et al., 2015; Dou et al., 2009; Fernandes et al., 2008). The COS consist of either acetylated units (A) of glucosamine (GlcNAc) or deacetylated units (D) of glucosamine (GlcN) or both A and D units linked through β-1,4 glycosidic bonds. Increasing interest in COS is due to unique properties such as water solubility, cell membrane permeability, easy absorption, and different biological activities. Some of the reported biomedical activities of COS include anti-tumor, antimicrobial, antioxidant, immunoregulatory, antihypertensive, and hypo-cholesterolemic effects (Harish Prashanth & Tharanathan, 2007; Kim & Rajapakse, 2005).

The anti-cancer properties of the COS make them potential anti-cancer agents (Liaqat & Eltem, 2018). The molecular weight (MW), the degree of polymerization (DP), degree of acetylation (DA), and the pattern of acetylation play an important role in biological activities of COS, including anti-tumor activity. For example, COS with low MW showed higher anti-tumor activity and decrease in MW resulted an increased tumor suppression ability (Salah et al., 2013). Chitohexaose was essential to manifest anti-cancer activity (Li et al., 2011; Xiong et al., 2009). Further, COS can inhibit the proliferation and also induce apoptosis in cancer cells. The anti-proliferation effects and apoptosis have been observed upon treatment of COS on human lung and gastric cancer cells (Han, Cui, You, Xing, & Sun, 2015; Luo, Deng, Deng, & Wen, 2016). Promoting apoptosis by chemotherapeutic drugs is an important strategy to counteract cancer (Alimbetov, Askarova, Umbayev, Davis, & Kipling, 2018), as one of the hallmarks of the cancer cells is to evade apoptosis.

We have verified, whether the natural compounds like COS with different DP and DA (D_{3-7} and A_5) possess anti-cancer activity on human breast cancer BT-474 cells. We, now, present evidence on the anti-cancer activities of deacetylated COS with DP_{3-7} (D_{3-7}), and, for the first time, for the acetylated COS with DP5 (A_5), and their potential as therapeutic agents against breast cancer.

* Corresponding author.
E-mail address: arpsl@uohyd.ernet.in (A.R. Podile).

https://doi.org/10.1016/j.carpta.2021.100077
Received 3 December 2020; Received in revised form 9 April 2021; Accepted 13 April 2021
Available online 18 April 2021

IOP Publishing Biomed. Mater. 15 (2020) 055025 https://doi.org/10.1088/1748-605X/ab975d

Biomedical Materials

RECEIVED
19 April 2020

REVISED
21 May 2020

ACCEPTED FOR PUBLICATION
28 May 2020

PUBLISHED
31 July 2020

PAPER

Zirconia-containing wollastonite ceramics derived from biowaste resources for bone tissue engineering

Palakurthy Srinath[1], **P Abdul Azeem**[1,3], **K Venugopal Reddy**[1], **Vasudevarao Penugurti**[2] and **Bramanandam Manavathi**[2]

[1] Department of Physics, National Institute of Technology Warangal, Warangal 506004, India
[2] Department of Biochemistry, School of Life Science, University of Hyderabad, Hyderabad, India
[3] Author to whom any correspondence should be addressed.

E-mail: drazeem2002@yahoo.com

Keywords: *in vitro* bioactivity, sol-gel method, wollastonite, mechanical properties

Abstract

Zirconia-containing wollastonite ($CaSiO_3$) ceramics with partial substitution of zirconia (1, 3 and 5 mol%) were prepared using eggshells and rice husk ash as source materials for calcium oxide and silica, respectively, through a sol–gel technique. The effect of incorporation of zirconia on *in vitro* bioactivity, mechanical properties, degradability and cytocompatibility of wollastonite was studied. Bioactivity was evaluated by *in vitro* assay using simulated body fluid while degradability was tested in Tris-HCl buffer solution for different time periods (1, 3, 7, 14 and 21 d) according to the ISO 10 993-14 standard. Human osteosarcoma (MG-63) cells were used to assess cytocompatibility with the MTT assay. X-ray diffractometry, Fourier transform infrared spectroscopy and scanning electron microscopy–energy dispersive spectroscopy were used to characterize the ceramics before and after *in vitro* studies. The results obtained showed that increasing the zirconia content in the wollastonite phase increases microhardness, compressive strength, bending strength and the elasticity modulus, while slightly decreasing the rate of formation of the hydroxyapatite layer. Moreover, the samples doped with zirconia had a lower degradation rate and it was noticed that cell viability is unaffected by the incorporation of zirconia.

1. Introduction

Calcium silicate-based ceramics, including wollastonite, akermanite, diopside, merwinite and bredigite, have been widely studied in recent years because they support the attachment, proliferation and differentiation of osteoblast-like cells such as human mesenchymal stem cells [1–3]. Ca and Si are two ions that dissolve from these ceramics. Ca ions play an important role in cell reactions in bioceramics including cell proliferation and differentiation into osteoblasts [4]. Si is one of the most significant trace elements in the human body, acting as a key controller of bone calcification and helping to improve bone density and prevent osteoporosis, specifically during the early stage of bone formation [5, 6]. It has also been reported that the dissolution products from calcium silicates enhance the effect of insulin-like growth factor on cell proliferation [7]. Moreover, calcium silicate ceramics show better mechanical properties than other calcium phosphate ceramics [8, 9].

Wollastonite ($CaSiO_3$), which has a monoclinic crystal structure, belongs to the group of calcium silicate ceramics. It exists in two forms: a low-temperature form called β-wollastonite (β-$CaSiO_3$) and a high-temperature form called α-wollastonite (α-$CaSiO_3$) [10–12]. It has received attention for its ability to contribute to hard tissue regeneration due to its progressive bio-functionalities [13, 14]. Siriphannon *et al* [15] showed that the apatite growth rate on wollastonite was faster than on A-W glass ceramics and other bioactive glass ceramics. *In vitro* cell culture assessments demonstrated that wollastonite ceramics can support the attachment of osteoblast-like cells and the proliferation and differentiation of bone marrow mesenchymal stem cells [16–18]. However, the degradation rate of wollastonite ceramics is relatively high, leading to abrupt changes in the pH value of the local environment by dissolution ions which may negatively affect surrounding cells [19]. Additionally, the high rate of solubility is a likely reason for failure of scaffold construc-

Received: 29 May 2019 | Revised: 25 July 2019 | Accepted: 8 August 2019

DOI: 10.1111/jace.16745

Journal of the American Ceramic Society

ORIGINAL ARTICLE

A comparative study on in vitro behavior of calcium silicate ceramics synthesized from biowaste resources

Srinath Palakurthy[1] | **P. Abdul Azeem**[1] | **K. Venugopal Reddy**[1] | **Vasudevarao Penugurti**[2] | **Bramanandam Manavathi**[2]

[1]Department of Physics, National Institute of Technology Warangal, Warangal, India

[2]Department of Biochemistry, School of Life Science, University of Hyderabad, Hyderabad, India

Correspondence
P. Abdul Azeem, Department of Physics, National Institute of Technology Warangal, Warangal 506004, India.
Email: drazeem2002@yahoo.com

Funding information
Science and Engineering Research Board; MHRD, Government of India

Abstract

Calcium silicate ceramics have received significant attention for biomedical applications for their excellent bioactivity and osteoconduction properties. Sol-gel process is extensively used for the fabrication of calcium silicates. In sol-gel process, calcium nitrate tetra hydrate ($Ca(NO_3)_2{\cdot}4H_2O$) and tetraethylorthosilicate (TEOS) are used as precursors. However, these precursors are expensive. The objective of this work was to compare in vitro behavior of calcium silicate ($CaSiO_3$) produced using biowaste such as rice husk ash (RHA) and eggshells (coded; NCS) with $CaSiO_3$ prepared using TEOS and $Ca(NO_3)_2{\cdot}4H_2O$ (coded; CCS). Thermal investigation results revealed that the crystallization temperature for NCS is relatively lower (772°C) than for CCS (870°C). Bioactivity was studied in vitro using simulated body fluid (SBF) with respect to mineralization rate of hydroxyapatite. Mineralization of a greater hydroxyapatite was observed on NCS ceramics than CCS ceramics after incubation for 3, 7, 14 days in SBF solution, which was confirmed using X-ray diffractometer, Fourier transform infrared spectroscopy, scanning electron microscopy-energy dispersive spectroscopy. Degradation studies were conducted in Tris-HCl solution and the test results revealed that NCS ceramics has lower dissolution rate than CCS ceramics. The antimicrobial assay has shown that NCS samples exhibit significant zone of inhibition against *Escherichia coli* and *Staphylococcus aureus* which confirmed that the $CaSiO_3$ prepared from RHA and eggshell can prevent bacteria from adhering to the surface. In addition cell culture studies revealed that NCS ceramics possess good cytocompatibility with MG-63 cells and significantly promoted cell proliferation.

KEYWORDS

bioactivity, calcium silicate, hydroxyapatite, sol-gel

1 | INTRODUCTION

Calcium silicate ceramics have been identified as bioactive and prospective candidates for bone tissue engineering applications.[1–3] Researchers have reported that bone tissue can be produced on calcium silicate ceramics with hydroxyl carbonated apatite layer deposition.[4,5] Moreover, these ceramics can support the attachment of human bone-derived cells, their proliferation and differentiation.[6–8] The conventional starting materials used to synthesize calcium silicates are calcium oxide (CaO) and silica (SiO_2). Commercial calcium oxide and calcium nitrate tetra hydrate ($Ca(NO_3)_2{\cdot}4H_2O$) are

Journal of Alloys and Compounds 764 (2018) 1072–1078

Contents lists available at ScienceDirect

Journal of Alloys and Compounds

journal homepage: http://www.elsevier.com/locate/jalcom

In vitro evaluation of niobia added soda lime borosilicate bioactive glasses

Rajkumar Samudrala [a], P. Abdul Azeem [a, *], Vasudevarao Penugurti [b], Bramanandam Manavathi [b]

[a] Department of Physics, National Institute of Technology Warangal, Warangal, 506004, India
[b] Department of Biochemistry, School of Life Sciences, University of Hyderabad, Hyderabad, India

ARTICLE INFO

Article history:
Received 17 February 2018
Received in revised form
5 June 2018
Accepted 6 June 2018
Available online 7 June 2018

Keywords:
Bioactivity
Cell viability
Human osteoblast cells
Cytocompatibility

ABSTRACT

In the present study, systematic and detailed investigations have been reported, in terms of bioactivity, cytocompatibility and mechanical hardness of a synthetic material that is proposed as a bone implant material in *in-vitro* conditions. The objective of the present study is to explore the effect of niobium addition on bioactivity and cytocompatibility of soda lime borosilicate bioglasses. Synthesis of bioglasses is carried out by conventional melt-quenching method. Simulated body fluid is prepared by Tas method. The bioactivity study was done for twenty-one days of immersion in simulated body fluid. XRD, FTIR, and SEM-EDS are showed formation of hydroxyapatite layer on the niobium added soda lime borosilicate glass even at a higher concentration (10 mol %) of niobium content. Degradation test was performed as per ISO 10993. The results obtained from degradation studies have demonstrated that weight loss of niobia mixed soda lime borosilicate glasses decreased with the increase of niobia. Cytocompatibility study has been studied by MTT Assay with osteoblast cells (MG-63). Cell viability is not affected by the addition of niobium content. Niobium added soda lime borosilicate glasses are both bioactive and cytocompatible. Hence it can be concluded that niobia mixed borosilicate glasses may be used as potential material in bone tissue engineering.

1. Introduction

Biomaterials have played very important role in recent times and have been used for different types of medical applications. More significantly, biomaterials have been used for not only bone-related hard tissue problems but also soft tissue regeneration and these materials including a combination of metals, polymers, ceramics, with the combination involving any of them [1,2]. Among different types of biomaterials, bioactive glass has attracted huge attention because of easy processing and controllable properties [3]. Bioglass was discovered by Larry Hench in 1969, which was the first man-made synthetic material that could bond chemically with living bone [4]. Hench formulated a composition of silicate-calcium-sodium-phosphorus in which the ratio of Ca/P matches with the Ca/P of bone. This is an exciting alternative for first-generation inert biomaterials. Silica-based materials have been extensively studied for bone tissue engineering applications due to their characteristic feature of apatite-forming ability, i.e., ability to form carbonated hydroxyapatite layer on the surface of the materials when exposed to physiological fluids [5,6]. Most commercial bioactive glasses contain SiO_2 as a basic constituent. However, the degradation of silica-based glasses is highly time-dependent, which rather restrict their usage as bone implants [7]. As a result, borate glasses were shown to have potential in bone bonding ability as their corrosion mechanism match with Hench's composition [8–12]. Because of low mechanical strength, the application of borate-based glass with different chemical compositions has been continuously investigated.

The primary test for a bioactive material that is going to be used in implants is performed in vitro using a simulated body fluid (SBF). Niobium is a comparatively less investigated transition metal and it exhibits good biocompatibility and osteoconductivity and has excellent corrosion resistance [13–15]. Niobium has been reported that toxicity levels are very less compare to other transition metals like titanium(Ti) [16] and it has the capability of angiogenesis for bone regenerative applications [17]. Niobium oxide has the ability

* Corresponding author.
E-mail addresses: drazeem2002@yahoo.com, drazeem2002@gmail.com, drazeem2002@nitw.ac.in (P. Abdul Azeem).

https://doi.org/10.1016/j.jallcom.2018.06.069
0925-8388/

Biomedical Materials

PAPER

Bio-inspired synthesis of a hierarchical self-assembled zinc phosphate nanostructure in the presence of cowpea mosaic virus: *in vitro* cell cycle, proliferation and prospects for tissue regeneration

Koushi Kumar[1], **Vasudevarao Penugurti**[2], **Gila Levi**[3], **Yitzhak Mastai**[3], **Bramanandam Manavathi**[2] and **Pradip Paik**[1]

[1] School of Engineering Sciences and Technology, University of Hyderabad, Hyderabad, India
[2] Molecular and Cellular Oncology Laboratory, Department of Biochemistry, School of Life Sciences, University of Hyderabad, Hyderabad, India
[3] Department of Chemistry and the Institute of Nanotechnology, Bar-Ilan University, Ramat-Gan, Israel

E-mail: ppse@uohyd.ernet.ac.in, paik@uohyd.ac.in and pradip.paik@gmail.com

Keywords: self-assembly nanoparticles, zinc phosphate, bio-synthesis, cowpea mosaic virus, cell proliferation, tissue engineering

Supplementary material for this article is available online

RECEIVED
27 May 2017

REVISED
25 July 2017

ACCEPTED FOR PUBLICATION
8 August 2017

PUBLISHED
7 December 2017

Abstract

Self-assembly is an important auto-organization process used in designing structural biomaterials which have the potential capability to heal tissues after traumatic injury. Although various materials having the ability to heal after injury are available, there is still a substantial need to develop new improved materials. To address this issue, we have developed hierarchical three-dimensional (3D) self-assembled zinc phosphate ($Zn_3(PO_4)_2$) in the presence of cowpea mosaic virus (CPMV). $Zn_3(PO_4)_2$ nanoparticles are self-assembled into nanosheets with a high degree of isotropy and then self-organized into a 3D structure that can enhance surface interactions with biological entities. The self-assembled structure is formed through the auto-organization of nanoparticles of size ~50 nm under the influence of CPMV. The cellular response of self-assembled $Zn_3(PO_4)_2$ and cell–particle adhesion behavior have been investigated through *in vitro* studies using modeled osteoblast-like MG63 cells. Self-assembled $Zn_3(PO_4)_2$ resulted in proliferation of MG63 cells of up to 310% within 7 days of incubation. A 15% higher proliferation was obtained than with commercially available hydroxyapatite (HAp). Immunofluorescent analysis of MG63 cells after co-culturing with self-assembled $Zn_3(PO_4)_2$ confirmed the healthy cytoskeletal organization and dense proliferation of MG63 cells. Further, $Zn_3(PO_4)_2$ exhibited ~28% cell-cycle progression in S phase, which is higher than obtained with commercially available HAp. Overall, these results demonstrate the multiple functions of hierarchical self-assembled $Zn_3(PO_4)_2$ in the regeneration of bone tissue without defects and increasing the formation of cellular networks, and suggest its use in bone tissue engineering.

1. Introduction

Self-assembled nanostructured materials have recently attracted attention in biotechnology [1] and cell-based therapy for the treatment of damaged tissues [2–4] because the self-assembly approach can generate many complex structures that mimic the chemical and physical properties of the extracellular matrix. The main driving force for the self-assembled organization of biomaterials is the van der Waals force of interaction [5]. Self-assembled ceramic, polymer and hydro-gel biomaterials are used for tissue engineering to enhance biological activities [1, 6, 7], and most of these have been used to enhance cell adhesion and proliferation.

Zinc phosphate ($Zn_3(PO_4)_2$) has recently been recognized as a biomaterial, and due to its biocompatibility is widely used as a nontoxic anticorrosive agent [8], in dental cements [9] and as a drug delivery vehicle [10]. Naturally occurring $Zn_3(PO_4)_2$ is found in orthorhombic hopeite and triclinic parahopeite crystalline forms and is not available in pure form [11]; however, $Zn_3(PO_4)_2$ can be chemically synthesized in the presence of templating agents [12] by varying the reaction conditions [13, 14]. Notably, small

Materials Science and Engineering C 77 (2017) 772–779

Contents lists available at ScienceDirect

Materials Science and Engineering C

journal homepage: www.elsevier.com/locate/msec

Cytocompatibility studies of titania-doped calcium borosilicate bioactive glasses *in-vitro*

Rajkumar Samudrala [a], Abdul Azeem P [a,*], Vasudevarao Penugurti [b], Bramanandam Manavathi [b]

[a] Department of Physics, National Institute of Technology Warangal, Warangal 506004, India
[b] Department of Biochemistry, School of Life Sciences, University of Hyderabad, Hyderabad, India

ARTICLE INFO

Article history:
Received 23 October 2016
Received in revised form 26 January 2017
Accepted 25 March 2017
Available online 27 March 2017

Keywords:
Biocompatible material
Bioactivity
Cell viability
Cytocompatibility
Proliferation
Human osteoblast cells

ABSTRACT

The present study aims to elucidate the applications of Titania (TiO_2) doped calcium borosilicate glass as a biocompatible material in regenerative orthopedic applications. In this context, we have examined the bioactivity of various concentrations of TiO_2 doped glasses with the help of simulated body fluid (SBF). Cytocompatibility, cell proliferation, and protein expression studies revealed the potential candidature of TiO_2 doped glasses on osteoblast cell lines (MG-63). We hypothesized that TiO_2 doped calcium borosilicate glasses are most cytocompatible material for bone implants. Glasses with composition $31B_2O_3$-$20SiO_2$-$24.5Na_2O$-$(24.5 - x)$ CaO- x TiO_2 ($x = 0,0.5,1,2$) have been prepared by the conventional melt-quenching technique. After immersion of glasses in the SBF, formation of hydroxyapatite layer on the surface was confirmed by X-ray Diffractometer (XRD), Fourier Transform Infrared Spectroscopy (FT-IR) and Scanning Electron Microscopy-Energy Dispersive Spectroscopy (SEM-EDS) analysis. Significant change in the pH of the body fluid was observed with the addition of titania. Degradation test was performed as per the ISO 10993. The results showed that partial substitution of TiO_2 with CaO negatively influenced bioactivity; it decreased with increase in concentration of TiO_2. Vickers hardness tester was used to measure the microhardness values of the prepared glasses. With the increasing of TiO_2 content, the microhardness of the glass samples was increased from 545 Hv to 576 Hv. Cytocompatibility has been evaluated with MG-63 cells by using MTT assay. Further, we observed that there was no change in expressions of cyclin levels even after the incorporation of titania. The antibacterial properties were examined against *E. coli* and *S. aureus*. Strong antibacterial efficacy was observed for 2% TiO_2 in the system. Hence it can be concluded that titania-doped borosilicate glasses may be used as potential materials in bone tissue engineering.

1. Introduction

'Bioceramics' are biocompatible materials, which find use in several clinical applications. Bioceramics can be produced in crystalline and amorphous forms and they are generally classified into two groups based on their chemical composition; calcium phosphates and others, including yttria-stabilized tetragonal zirconia, alumina ceramics, silicate and phosphate families of glasses and glass-ceramics [1]. Bioactive glasses are considered as potential materials for bone substitution, as they can form a direct bond with the living bone without formation of bond with surrounding fibrous tissue. One of the essential conditions for the bioactive material is that it should form a biologically active apatite called hydroxylapatite layer (HAp) on its surface through which the material could form a bond with both soft tissues as well as hard tissues [2]. 45S5 is the best implant material, not only for dental and orthopedic applications but also, for ossicular prostheses, endosseous ridge maintenance, and other applications [1,3].

Boron plays a vital role in bone formation and depends on its concentration in the composition. The highest concentrations of boron are found in bone, nails, and hair [4]. Day et al. [5–9] have extensively studied the use of borate glasses in biomedical applications. Recent studies have demonstrated that the potential bioactivity of borate glasses comes from their lower chemical durability, faster degradation rate and almost complete conversion to hydroxyapatite (HAp) than the widely studied 45S5 bioglass when placed in SBF. Studies have shown that some borate glasses have the ability to support the growth and differentiation of human mesenchymal stem cells, and to promote bone formation more rapidly than silicate based 45S5 glass [10,11]. S. M. Wiederhorn et al. [10] reported that higher amount of borate content weakens the glass structure. Glass structure was strengthened by incorporation of silica as former and CaO as modifier respectively [12].

Titanium has gained importance recently for its broad range of applications in the biomedical field [13]; it is one of the earliest transition metals to be investigated for antitumor properties; also it is found to elicit favorable cell response and is concluded to be one of the best materials suited for biological requirements [14]. Hence, titanium is widely used as a biomaterial for several dental and orthopedic clinical

* Corresponding author.
E-mail address: drazeem2002@nitw.ac.in (Abdul Azeem P).

http://dx.doi.org/10.1016/j.msec.2017.03.245
0928-4931/

Conferences participated

Certificate of participation

This is to certify that

Mr./Ms./Dr. **Vasudevarao Penugurti** has participated in the conference

"Phenotypic heterogeneity as a driver of cancer progression"

held from 5-6th January, 2019 at the Indian Institute of Science, Bengaluru

Organizing Committee

Funder: IDRC CRDI Canada

Organizers: SickKids; האוניברסיטה העברית בירושלים THE HEBREW UNIVERSITY OF JERUSALEM; הפקולטה לרפואה FACULTY OF MEDICINE; Indian Institute of Science भारतीय विज्ञान संस्थान

XLII ALL INDIA CELL BIOLOGY CONFERENCE

and 2ND International Conference on

TRENDS IN CELL AND MOLECULAR BIOLOGY

BITS Pilani K K Birla Goa Campus

Indian Society of Cell Biology (Regd.) Estd. 1975

December 21 - 23, 2018

CERTIFICATE

This is to certify that Prof./Dr./Mr./Ms. VASUDEVARAO PENUGURTI of UNIVERSITY OF HYDERABAD has participated in the XLII All India Cell Biology Conference.

He/~~she~~ has presented a paper entitled " HPIP Signalling reprograms breast Cancer cell metabolism for survival under energy stress " in ~~oral~~/poster session of the conference.

Prof. Pradeep K. Burma
Secretary, ISCB

Dr. Angshuman Sarkar
Convener

International Conference on Reproductive Biology and Comparative Endocrinology (ICRBCE)

and

35th Annual Meeting of The Society for Reproductive Biology and Comparative Endocrinology (SRBCE-XXXV)

9-11 February, 2017

University of Hyderabad, Hyderabad, India

Certificate

This is to certify that Prof./Dr./Mr./Ms. Vasudevarao Penugurti *of* University of Hyderabad *made an ~~oral~~/poster presentation at the "International Conference on Reproductive Biology and Comparative Endocrinology and 35th Annual Meeting of The Society for Reproductive Biology and Comparative Endocrinology" held during February 9-11, 2017 organised by the Dept. of Animal Biology, University of Hyderabad, Hyderabad, India.*

Dr. T. Shivanandappa
President, SRBCE

Dr. T. G. Shrivastav
Secretary, SRBCE

Dr. B. Senthilkumaran
Convenor

Dr. Suresh Yenugu
Organising Secretary

XL All India Cell Biology Conference & International Symposium on

Functional Genomics and Epigenomics

Jiwaji University, Gwalior

November 17-19, 2016

Certificate

This is to certify that Dr./Mr./Ms. Penugurti Vasudevarao *of* University of Hyderabad *has participated in the XL All India Cell Biology Conference.*

He/She has presented a paper entitled " _____ *" in the Oral/Poster session of the conference.*

Dr. H.S. Misra
Secretary, ISCB

Prof. I.K. Patro
Convenor

Prof. P.K. Tiwari
Organizing Secretary

Certificate of Training

RADIOACTIVE FACILITY

School of Life Sciences
University of Hyderabad

This is to certify that VASUDEVARAO PENUGURTI has successfully completed the orientation course on radioactivity usage and safety at School of Life Sciences, University of Hyderabad on 09th January 2020.

Faculty, In charge

Radiation Safety Officer

Dean

UKIERI
UK-India Education and Research Initiative

ज्ञान-विज्ञान विमुक्तये

UGC-UKIERI
Thematic Partnership

Workshop on Animal Models in Cancer Research

Organized by

School of Medical Sciences, University of Hyderabad, India

24th - 25th October **2017**

CERTIFICATE

This is to certify that ~~Dr.~~/Mr./~~Ms.~~/~~Shri.~~ P. Vasudeva Rao has participated in the workshop on **Animal Models in Cancer Research** conducted by School of Medical Sciences, University of Hyderabad.

Prof. Geeta Vemuganti,
Dean, School of Medical Science,
University of Hyderabad

Prof. Sarah E Coupland
Department of Molecular & Clinical Cancer Medicine
University of Liverpool

Plagiarism report

Prof. Bramanandam Manavathi Ph.D.,
Department of Biochemistry,
School of Life Sciences,
University of Hyderabad,
Hyderabad - 500046,
Telangana, India

प्रतिष्ठित संस्थान
INSTITUTION OF EMINENCE

CERTIFICATE

This is to certify that the similarity index of this thesis, as evaluated by the Librarian of the University of Hyderabad, is 44%. There is a 40% similarity in Vasudevarao Penugurti's publications.

- 35% from the publication: **Penugurti V**, Khumukcham SS, Padala C, Dwivedi A, Kamireddy KR, Mukta S, Bhopal T, **Manavathi B**. HPIP protooncogene differentially regulates metabolic adaptation and cell fate in breast cancer cells under glucose stress via AMPK and RNF2 dependent pathways. ***Cancer Letters.*** 2021 Oct 10;518:243-255.
- 5% from the publication: Student paper submitted to the University of Hyderabad (The above publication)

In the current thesis, only 4% similarity was found from external sources such as the internet and other publications. Hence, the present thesis is considered free of plagiarism.

Prof. Bramanandam Manavathi Ph.D.,

Supervisor

Prof. Bramanandam Manavathi, PhD
Department of Biochemistry
School of Life Sciences
University of Hyderabad
Hyderabad-500 046. (TS), INDIA

Role of HPIP signaling in cellular adaptation and cell fate regulation in response to metabolic stress: Implications in breast cancer development

by Penugurti Vasudevarao

Submission date: 01-Nov-2021 05:22PM (UTC+0530)
Submission ID: 1689927380
File name: Penugurti_Vasudevarao.docx (10.1M)
Word count: 19682
Character count: 114002

Role of HPIP signaling in cellular adaptation and cell fate regulation in response to metabolic stress: Implications in breast cancer development

ORIGINALITY REPORT

44%	7%	42%	23%
SIMILARITY INDEX	INTERNET SOURCES	PUBLICATIONS	STUDENT PAPERS

PRIMARY SOURCES

1	Vasudevarao Penugurti, Saratchandra Singh Khumukcham, Chiranjeevi Padala, Anju Dwivedi et al. "HPIP protooncogene differentially regulates metabolic adaptation and cell fate in breast cancer cells under glucose stress via AMPK and RNF2 dependent pathways", Cancer Letters, 2021 Publication	35%
2	Submitted to University of Hyderabad, Hyderabad Student Paper	5%
3	"Encyclopedia of Cancer", Springer Science and Business Media LLC, 2009 Publication	1%
4	cors.archive.org Internet Source	<1%
5	effiloop.com Internet Source	<1%

student publication

Prof. Bramanandam Manavathi, PhD
Department of Biochemistry
School of Life Sciences
University of Hyderabad
Hyderabad-500 046. (TS), INDIA

student publication

Prof. Bramanandam Manavathi, PhD
Department of Biochemistry
School of Life Sciences
University of Hyderabad
Hyderabad-500 046. (TS), INDIA

6	"Engagement, Reception and Breakup: Three Steps of Cell Motility regulated by HPIP signaling", Cancer Cell & Microenvironment, 2015. Publication	<1 %
7	Saratchandra Singh Khumukcham, Bramanandam Manavathi. "Two decades of a protooncogene HPIP/PBXIP1: Uncovering the tale from germ cell to cancer", Biochimica et Biophysica Acta (BBA) - Reviews on Cancer, 2021 Publication	<1 %
8	www.sciencegate.app Internet Source	<1 %
9	Wang, Shun-chang, Da-sen Chai, Chuan-bo Chen, Zheng-ye Wang, and Lei Wang. "HPIP promotes thyroid cancer cell growth, migration and EMT through activating PI3K/AKT signaling pathway", Biomedicine & Pharmacotherapy, 2015. Publication	<1 %
10	Yingying Feng, Xiaojie Xu, Yunjing Zhang, Jianhua Ding et al. "HPIP is upregulated in colorectal cancer and regulates colorectal cancer cell proliferation, apoptosis and invasion", Scientific Reports, 2015 Publication	<1 %

11	Shuo Zhang, Jingtao Gao, Shibo Liu, Lu Yu, Wen Zhang, Yinming Liang, Hui Wang. "Transcription Coactivator BCL3 Acts as a Potential Regulator of Lipid Metabolism Through the Effects on Inflammation", Journal of Inflammation Research, 2021 Publication	<1 %
12	zdzlab.einsteinmed.org Internet Source	<1 %
13	Alice Marino, Derek J. Hausenloy, Ioanna Andreadou, Sandrine Horman, Luc Bertrand, Christophe Beauloye. "AMP-activated protein kinase: A remarkable contributor to preserve a healthy heart against ROS injury", Free Radical Biology and Medicine, 2021 Publication	<1 %
14	pubmed.ncbi.nlm.nih.gov Internet Source	<1 %
15	sabcs.org Internet Source	<1 %
16	www.spandidos-publications.com Internet Source	<1 %
17	Xiaojie Xu, Chengying Jiang, Shibin Wang, Yanhong Tai et al. "HPIP is upregulated in liver cancer and promotes hepatoma cell	<1 %

proliferation via activation of G2/M transition", IUBMB Life, 2013
Publication

18	academic.oup.com Internet Source	<1%
19	tud.qucosa.de Internet Source	<1%
20	www.hindawi.com Internet Source	<1%
21	Submitted to Monroe College Student Paper	<1%
22	Shou, Zhang-Xuan, Xue Jin, and Zhong-Sheng Zhao. "Upregulated Expression of ADAM17 Is a Prognostic Marker for Patients With Gastric Cancer :", Annals of Surgery, 2012. Publication	<1%
23	Submitted to University of Liverpool Student Paper	<1%
24	repositori.upf.edu Internet Source	<1%

Exclude quotes	On	Exclude matches	< 14 words
Exclude bibliography	On		